University of Warsaw

Heavy Ion Laboratory

Annual Report

2016



Warszawa, czerwiec 2017

Various information concerning the Laboratory is distributed via the HIL mailing list.
In order to subscribe to the list please visit the page
`http://mail.slcj.uw.edu.pl/mailman`

Annual Report of the
Heavy Ion Laboratory, University of Warsaw
ul. Pasteura 5a, 02-093 Warszawa, Poland
phone (+48)22-8222123, (+48)22-5546000
fax (+48)22-6592714
`http://www.slcj.uw.edu.pl`

The photo on the title page was taken
in front of the HIL building on 11 May 2017
by Michalina Komorowska

The editors thank Michalina Komorowska and Tomasz Marchlewski for their help in collecting and formatting information presented in the Appendices to the Report

Editors:
Marcin Palacz, Nicholas Keeley, Andrzej Tucholski, Marzena Wolińska-Cichocka
e-mail: raport@slcj.uw.edu.pl
ISSN 1895-6726

Contents

Introduction 5

A Laboratory overview and technical developments **7**
A.1 General information 9
A.2 Cyclotron operation in 2016 and tasks carried out in order to improve the cyclotron infrastructure and efficiency 10
A.3 Polish Workshop on the Acceleration and Applications of Heavy Ions . . . 15
A.4 Arrival and service of Gammapool HPGe detectors 17
A.5 Water flow interlock system for the Warsaw Cyclotron 19
A.6 New website and IT infrastructure of the Heavy Ion Laboratory 20

B Research for medical and biological applications **23**
B.1 Production of and research into medical radioisotopes at the Heavy Ion Laboratory 25
B.2 Targets for Sc radioisotopes production with internal alpha beam 28
B.3 Ca targets for Sc production by proton or deuteron irradiation 30
B.4 Antioxidant interactions between phenolic acids in a model system 33
B.5 Determination of 3 neurotransmitters in rat brain tissue using liquid chromatography with mass spectrometry detection 34
B.6 Flavonoid content and antioxidant properties in different extracts of heather (Calluna vulgaris L.) 35
B.7 Optimisation of Cu(II)-porphyrin complex synthesis for PET radiopharmaceutical applications 36
B.8 Sorption of Sc(III) ions on solid carbon based materials 38
B.9 The adaptation of an external, well cooled, target holder for the PETtrace cyclotron suitable for irradiation of powder targets 40
B.10 A new project of an internal, well cooled, target station for the U-200P cyclotron suitable for the irradiation of different types of targets 42
B.11 Irradiation of CHO-K1 cells by a mixed ion beam containing carbon and oxygen ions 44
B.12 Experimental nanodosimetry of carbon ions using beam intensity modulation 46

C Nuclear physics **49**
C.1 Angular correlation method applied to spin determination of low lying levels in ^{140}Sm — new results 51
C.2 First measurement of the g-factor in the chiral band: the case of the ^{128}Cs isomeric state 54
C.3 Study of the low lying states of ^{136}Nd 56

C.4 Attempt to assign the delayed γ rays to the respective masses of fission fragments produced in the ^{16}O + ^{208}Pb induced fission reaction 59
C.5 The barrier height distributions of the ^{24}Mg + ^{90,92}Zr systems 62
C.6 Influence of non-collective excitations on barrier distributions 65
C.7 Coulomb excitation of ^{45}Sc 68
C.8 Momentum distribution of the spectator α observed in the ^{16}O(^{20}Ne,αα)^{28}Si reaction for a study of the ^{16}O-burning process 71
C.9 Asymptotic normalisation coefficient for the 6.356 MeV subthreshold state in ^{17}O from α-transfer studies 73
C.10 O_h invariant intrinsic coordinate frame for the octupole collective Hamiltonian 75
C.11 Ultra-thin silicon epitaxial strip detectors with very narrow strips produced by a low-temperature technique. 77
C.12 Preparations for the investigations of proton-rich nuclei using the AGATA-NEDA setup at GANIL 79
C.13 Sn targets for lifetime measurements 81
C.14 ^{132}Ba targets for nuclear shell structure studies 84

D Appendices **87**
D.1 List of experiments performed at HIL in 2016 89
D.2 Degrees and theses completed in 2016 or in progress 92
D.2.1 PhD theses of students affiliated to HIL, of HIL staff members, and supervised by HIL staff 92
D.2.2 Other PhD theses based on experiments performed at HIL 92
D.2.3 MSc and BSc theses supervised by HIL staff members 93
D.3 Publications 94
D.3.1 Publications in journals of the Journal Citation Reports (JCR) list 94
D.3.2 Other publications in journals and conference proceedings not included in the JCR list 100
D.4 Seminars 103
D.4.1 Seminars co-organised by HIL 103
D.4.2 Other seminars organised at HIL 105
D.4.3 External seminars given by the HIL staff 106
D.4.4 Poster presentations 109
D.4.5 Lectures for students and student laboratories 110
D.4.6 Science popularisation lectures 111
D.5 Honours and Awards 112
D.6 Laboratory staff 113
D.7 Laboratory Council 114
D.8 Programme Advisory Committee 115
D.9 External participants in HIL experiments and HIL guests 116

Introduction

This year was a historical year for our laboratory. From the 1st of March 2016 the Heavy Ion Laboratory (HIL), together with our consortium partner, Cyclotron Centre Bronowice of IFJ PAN in Kraków, we are among twelve European Laboratories (GANIL, INFN Legnaro and Catania, CERN-ISOLDE, University of Jyväskylä, CNRS-ALTO, GSI, KVI, IFIN-HH and ECT*) with Transnational Access granted by the European Union trough the ENSAR2 (European Nuclear Science and Application Research 2) project within the HORIZON 2020 framework. This means that we can support our visitors by covering their research costs (accommodation and travel) for a period of four years. A few experiments performed in the first half of the year were already supported in this way. The others, accepted by the Programme Advisory Committee and by a Selection Panel of ENSAR2, will be performed next year. Among them are the experiments of the EAGLE-GAMMAPOOL project related to nuclear spectroscopy. A Memorandum of Understanding between HIL and the Owner's Committee of the European Gamma-Ray Spectroscopy Pool (EGP) outlines the project of hosting some of the EGP detectors and associated equipment by HIL and its use in experiments till December 2021.

Noblesse oblige, following increasing international recognition, we have changed our website that is presently operated by an easy-to-use content management system and has a more attractive and consistent design. The design of the HIL logo was also modernised.

According to the work-plan, cyclotron operation in 2016 was focused on the development of new metallic ion beams (like ^{24}Mg) and on preparation of the installation of the new RF system. Consequently, the amount of beam-time delivered to users was relatively small. The final upgrade of the RF system, due to a delay in supplying components by the manufacturers, was shifted to the autumn of 2017. Nevertheless, several experiments were successfully performed, among them a series devoted to a study of the properties of nuclei using the method of Coulomb excitation.

From many papers published this year I would like to mention just one — devoted to a study of superdeformed and triaxial states in ^{42}Ca (Physical Review Letters 117, 062501). Apart from its scientific value it shows how important is a synergy between larger and smaller nuclear physics laboratories. The main experiment was performed at the Laboratori Nazionali di Legnaro but some results were re-measured at HIL. The GOSIA code, developed at HIL, was used to extract the electromagnetic properties of various states in ^{42}Ca. Experimental evidence for superdeformation of the band build on the 0_2^+ state was obtained and the importance of the Coulomb excitation method as a tool to study superdeformation was clearly demonstrated. This method, introduced at HIL by Tomek Czosnyka many years ago, became our *specialité de la maison*.

Finally, I would like to welcome dr Mansi Saxena from the University of Delhi, India, who joined us in the autumn as a scholar of the POLONEZ funding programme of the National Science Centre of Poland. She will say with us for two years. For the last call of this programme we received three applications and the results will be announced in mid-2017. We are crossing our fingers for their success.

Prof. Krzysztof Rusek, Director of HIL

Part A

Laboratory overview and technical developments

A.1 General information

J. Choiński, P. Napiorkowski and K. Rusek

Heavy Ion Laboratory, University of Warsaw, Warszawa, Poland

The Heavy Ion Laboratory (HIL) is a unit of the University of Warsaw, the largest university in Poland. HIL was founded jointly by the Ministry of Education, the Polish Academy of Sciences and the Polish Atomic Energy Agency. It is the largest experimental nuclear physics laboratory in the country, equipped with two cyclotrons — a $K = 160$ heavy-ion U-200P cyclotron and a GE PETtrace, $K = 16.5$ commercial cyclotron delivering high intensity proton and deuteron beams.

The first heavy-ion beam was extracted from the U200P in 1994 and since that time HIL has been an effective "user facility", serving up to the present time several hundred scientists from Poland and abroad and has become a recognised element of the European Research Community. From the 1st of March 2016, HIL has formed part of ten European laboratories with Transnational Access granted by the European Union by through the ENSAR2 (European Nuclear Science and Application Research 2) project within the HORIZON 2020 framework. Beam time is allocated by the Director based on the recommendations of the international Programme Advisory Committee. The only criteria are the scientific merit of the project and its technical feasibility. The research programme is mostly focused on nuclear physics and medical applications including the production of radio-isotopes.

Experimental teams may take advantage of permanent set-ups installed on the beam lines or use their own dedicated equipment. Available apparatus includes IGISOL — a Scandinavian type on-line separator, CUDAC — a PIN-diode array particle detection system, JANOSIK — a multi-detector system consisting of a large NaI(Tl) crystal with passive and active shields and a 32-element multiplicity filter and ICARE, a charged particle detector system used for particle identification and energy measurements, moved to HIL from IReS Strasbourg. The most recent experimental tool, still being developed and improved, is the EAGLE array — a multi-detector γ-ray spectrometer, equipped with 16 HP germanium detectors with anti-Compton shields and up to 14 HP germanium detectors from the GAMMAPOOL consortium. It can be easily coupled to ancillary detectors such as the internal conversion electron spectrometer built by the University of Lodz, a charged particle 4 π multiplicity filter (Si-ball), a scattering chamber equipped with 100 PIN-diode detectors, a 60-element BaF_2 gamma-ray multiplicity filter, a sectored HPGe polarimeter and a plunger.

Since 2012 the Radiopharmaceuticals Production and Research Centre has formed an important part of the HIL, focused on the production of and research into Positron Emission Tomography radiopharmaceuticals. The production of longer-lived radioisotopes for life-sciences applications is also carried out.

Being a university unit, HIL is in a natural way involved in teaching. On average about 15 students/year (Bachelors, Masters, PhD, ERASMUS), from Poland and abroad, work at HIL supervised by its staff members. As part of its broader educational mission, the HIL staff organise an annual one-week workshop on "Acceleration and applications of heavy-ions" for about 20 students from various Polish universities.

A.2 Cyclotron operation in 2016 and tasks carried out in order to improve the cyclotron infrastructure and efficiency

J. Choiński, P. Gmaj, A. Bednarek, T. Bracha, A. Górecki, A. Jakubowski, P. Jasiński, W. Kalisiewicz, M. Kopka, W. Kozaczka, P. Krysiak, K. Łabęda, K. Makowski, I. Mazur, J. Miszczak, Z. Morozowicz, O. Saeed Mohamed Nassar, B. Paprzycki, K. Pietrzak, B. Radomyski, K. Sosnowski, Ł. Standyło, K. Sudlitz, J. Sura

Heavy Ion Laboratory, University of Warsaw, Warszawa, Poland

Operation

In 2016 cyclotron operation was focused mainly on the development of the new ion beams required by users and preparation of the installation of the new RF system. Therefore, the availability of the accelerator was kept at a reduced level (see Fig. 1). The final upgrade of the RF system, due a further delay in supplying the necessary components, is planned for 2017. The changes resulting from the beam development will result in a qualitative change in the attractiveness of the U200P cyclotron in the eyes of the nuclear physics research community by 2017, placing our centre much higher in the European research centres ranking.

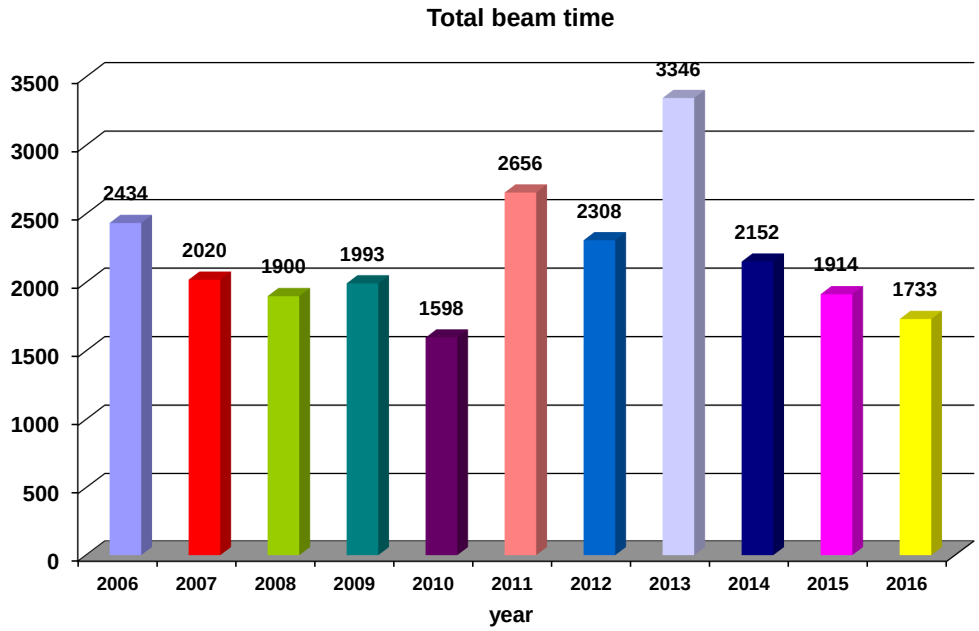


Figure 1: Total cyclotron beam time in the years 2005–2016.

The monthly distribution of beam time in 2016 is presented in Fig. 2. The cyclotron regained normal availability only in the last quarter of the year.

As in the previous few years, the main topics of the experiments were related to nuclear physics research, and biological and medical research. The latter also includes medical radioisotope production (examples: ^{211}At, ^{43}Sc, ^{44}Sc, ^{72}Se or ^{72}As) and chemical specimen production in collaboration with the Institute of Nuclear Chemistry and Technology, the

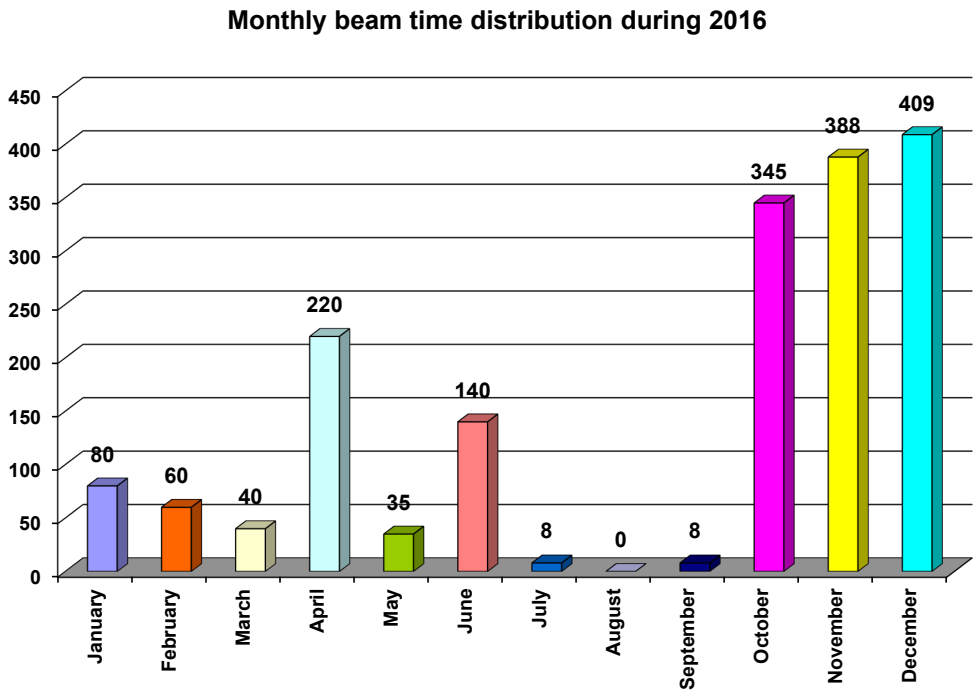


Figure 2: Beam time distribution (hours) in 2016 per month.

Henryk Niewodniczański Institute of Nuclear Physics of the Polish Academy of Sciences, and POLATOM National Centre for Nuclear Research.

As a result of growing interest in experiments using metallic ion beams (see above), the possibility of producing magnesium, calcium and nickel beams was investigated. After a series of tests of different techniques for magnesium beam production, in cooperation with FLNR-Dubna, a method was chosen based on the evaporation of metallic magnesium using plasma thermal energy. This technique will be used for experiments planned in April 2017.

As the production of medical isotopes requires higher beam intensities than currently available at the U-200P, it is planned to adjust the magnetic field distribution in the cyclotron. For the same reason, a large part of the beam time was devoted to work on the development of the structure of the cyclotron and beam tests. Despite the reduced availability of the accelerator, the annual student workshop did take place students workshop took place in the usual autumn time.

The diversity of the experiments performed during 2016 is illustrated in Fig. 3.

Figure 4 illustrates the number of scientists using specific experimental frameworks. Detailed descriptions of the experimental setups available at HIL can be found on the laboratory web page: `www.slcj.uw.edu.pl`.

A list of experiments performed in 2016 is presented in Appendix D.1 of this Annual Report.

Maintenance and development

ECR Source

Due to the user demand, the cyclotron team worked on expanding the list of available beams, in particular on the preparation of metallic beams as mentioned above. This type of ions are obtained in an ECR type ion source using special methods and devices, like a

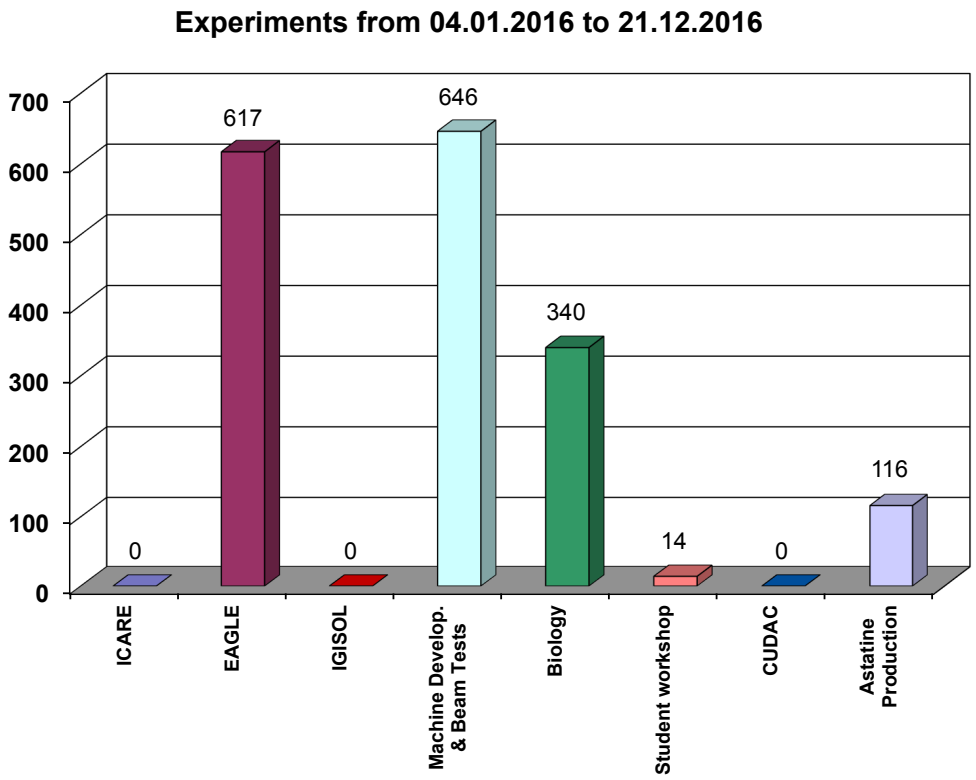


Figure 3: Distribution of beam-time (in hours) among different experimental setups.

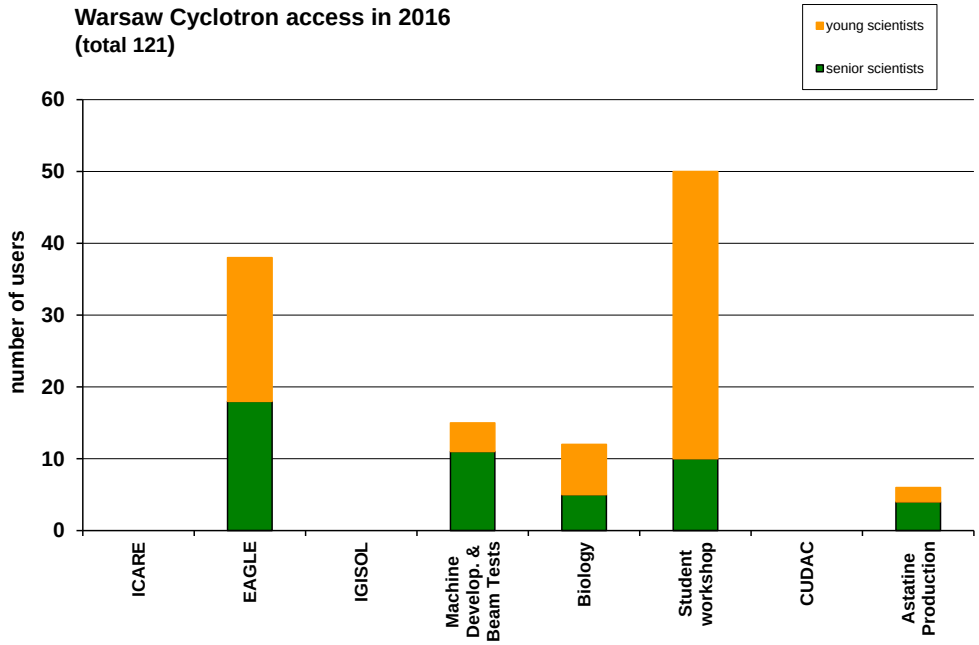


Figure 4: Number of users of the Warsaw cyclotron beams in 2016.

vapourising oven, sputtering system or the MIVOC method, all of them usually combined with a thin liner in the plasma chamber. In 2016 efforts were continued to optimise the operation of ECR sources based on the special test bench which was designed and installed in HIL in 2015. This bench was partially financed by NCBiR within the scope of the EMILI-EURISOL project, grant no. ERA-NET-NUPNET/02/12, and its purpose is

to achieve the higher ion currents and longer uninterrupted operation of the source which is necessary for experiments.

RF system

The currently used RF amplifiers have come to the end of their useful lives as they are already more than 30 years old. Spare parts are no longer available in the world market place. This mainly concerns such important components as power tubes GK-11A, thyristors T-160 etc. In 2015 the winners of three tenders for the components of the new RF system were selected and the first two stages of the system were delivered and tested in December 2016. The commissioning of the whole system was, however, postponed to next year (2017) due to the delay of the manufacturer of the power stage of the system. The delays in commissioning the new RF system intriduce a large disturbance to the cycle of cyclotron work and, as a result, its availability for experiments.

Power infrastructure

In addition to the normal maintenance resulting from wear and tear, the power infrastructure is constantly being refitteded and modernised (new optical elements for beam lines, PS system control updating etc.). A series of infrastructure modernisation was conducted as an adaptation to the new RF system installation.

Projects

Focusing spiral inflector (postponed to 2017)

In the next year we plan to replace the cyclotron inflector with a focusing one. Since the inflector affects the total beam transmission, we expect some improvement of the beam intensity at the level of 15%.

ECR and ICBT (Innovative Charge Breeding Techniques)

At the end of 2015, the European ERANET NUPNET EMILIE project was completed with commissioning of the ECR test bench. This bench was built for the purpose of increasing knowledge and and improving practices concerning ion sources of the ECR type. The work focused on optimisation of charge breeding efficiency and ECR optimisation was continued within the scope of ICBT (EURISOL – JRA Joint Research Activity).

New power supplies (beam line active elements)

The strategy of changing all the control system interfaces to one platform (LabView) was continued in 2016 by integrating consecutive amplifiers in use. The aim is to make a homogeneous control environment.

This strategy will continue in the next few years by adopting the LabView platform where possible. This approach is improving significantly and will further improve the reliability of the cyclotron operation.

RF system (postponed to 2017)

Up to the end of 2017 it is planned to replace the outdated amplifiers supplying the accelerating structure of the U-200P cyclotron with new ones. The new RF system will now be commissioned by the end of 2017 due to the above mentioned manufacturer delay. This means a two years shift compared to previous predictions.

Power infrastructure

The power infrastructure will continue to be developed to adapt it to the new requirements resulting from the renewal of the power supply and control system, development of the ECR research bench and the replacement of the RF amplifiers.

Magnetic structure of the U-200P cyclotron (postponed)

In 2016 new collaboration arrangements with JINR FLNR were drawn up and approved which will lead to general reconstruction of the magnetic field. The project will begin in 2017 with the design of a magnetic measurement system.

Vacuum system

The vacuum system of the cyclotron was gradually renewed in 2016 by replacement of two old vacuum pumps with two new cryogenic pumps and one on the beam line. The last (fourth) old cryogenic pump of the accelerator will be replaced in 2017.

A.3 Polish Workshop on the Acceleration and Applications of Heavy Ions

P.J. Napiorkowski[1], A. Trzcińska[1], T. Abraham[1], P. Gmaj[1], M. Komorowska[1,2], M. Kowalczyk[1], K. Kilian[1], T. Marchlewski[1,3] M. Matejska-Minda[1] M. Palacz[1], K. Rusek[1], O. Saeed Mohamed Nassar[1], M. Sitarz[1] A. Stolarz[1], K. Szkliniarz[4] R. Tańczyk[1], M. Wolińska-Cichocka[1]

1) Heavy Ion Laboratory, University of Warsaw, Warszawa, Poland
2) IRFU/SPhN, CEA Saclay, Gif-sur-Yvette, France
3) AGH University of Science and Technology, Kraków, Poland
4) Institute of Physics, University of Silesia, Katowice, Poland

The 12th edition of the Polish Workshop on the Acceleration and Applications of Heavy Ions was organised at HIL in October 2016. It was addressed to students of first cycle studies interested in nuclear physics, and offered them a unique opportunity to gain experience in methods of data acquisition and analysis, in operating the cyclotron including beam diagnostics measurements, and in charged particle and gamma-ray detection techniques. Medical applications of nuclear physics were also included in the programme of the Workshop.

In 2016 19 students attended the lectures and the practical training. The biggest group of 7 persons came from the University of Warsaw. There were 3 students from each of the Poznań University of Technology, the Warsaw University of Technology and the Silesian University. Also students from the University of Białystok, the University of Wrocław and the Academy of Mining and Metallurgy participated in the Workshop.

In 2016, the programme of lectures was as follows:

- HIL in a nutshell (K. Rusek);
- Radioprotection at HIL (R. Tańczyk);
- Introduction to heavy ion acceleration and elements of ion optics (O. Saeed Mohamed Nassar);
- Detection of gamma radiation, charged particles and neutrons (M. Palacz);
- In-beam gamma spectroscopy (P. Napiorkowski);
- Nuclear reactions (K. Rusek);
- Medical radiosotope production (K. Szkliniarz);
- Radiopharmaceuticals for Positron Emission Tomography (K. Kilian);
- Targets for nuclear physics (A. Stolarz);

Students took part in the following experimental tasks:

- Beam focusing in heavy ion acceleration;
- Rutherford Scattering.

- Identification of excited bands in gamma-gamma coincidences — gamma spectroscopy with the EAGLE setup;
- Target production and measurement of their thickness;
- Measurement of ^{137}Cs activity in environmental samples.

As usual, the Workshop was completed by a session of student presentations.



A.4 Arrival and service of Gammapool HPGe detectors

T. Abraham, M. Kisieliński, J. Srebrny, M. Kowalczyk, A. Pietrzak, A. Jakubowski, M. Antczak

Heavy Ion Laboratory, University of Warsaw, Warszawa, Poland

The European Array for Gamma Levels Evaluations (EAGLE) [1, 2] is an array of High Purity Germanium (HPGe) detectors used for γ-ray spectroscopy experiments at HIL. Laboratory owns 19 HPGe detectors and 16 Anti Compton Shields (ACS). One of the HPGe detectors remains at the Institute of Nuclear Physics of the Polish Academy of Science in Krakow as part of a collaboration. The number of complete sets including a detector and ACS available for experiments is thus 16, the remaining HPGe detectors forming a reserve.

On October 6 2015 the European Gammapool Owners Committee decided to lend its resources (21 HPGe detectors and 15 ACS) to HIL in 2017. The state of this equipment was uncertain and we decided to check it before shipment to Warsaw. In September 2016 our expert visited IPN Orsay and tested 19 out of 21 detectors (the two remaining detectors were sent for repairs before this visit). The outcome of this assessment is shown in Table 1. After testing, we decided to bring to HIL 14 detectors. Seven of them were in good condition and the remaining 7 detectors were broken and needed to be repaired at HIL. The 5 detectors which were left at Orsay were to be sent to Canberra service for repairs and then shipped to HIL.

By the end of 2016 there were 8 Gammapool detectors in use in the EAGLE frame and the remaining 6 detectors were under repair. Combining the Gammapool and HIL detectors allowed a total number of 24 detectors with ACS to install in EAGLE in Autumn 2016.

Bibliography

[1] J. Mierzejewski *et al.*, Nucl. Inst. and Meth. **A659** (2011) 84

[2] J. Mierzejewski *et al.*, HIL Annual Report 2010, page 24

Table 1: State of the Gammapool HPGe detectors on 14 September 2016.

Orsay id	FWHM 1173 keV	FWHM 1333 keV	Applied voltage	Remarks	At HIL
GUOC 14	2.16 keV	2.3 keV	-3 kV	OK	Yes
GFOC 31	2.35 keV	2.5 keV	-4 kV	OK	Yes
GUOC 8	2.5 keV	2.6 keV	-3.7 kV	OK	Yes
GFOC 50	2.45 keV	2.55 keV	-3 kV	OK	Yes
GUIC 35	2.33 keV	2.56 keV	-3.6 kV	OK	Yes
GFOC 18	2.7 keV	2.9 keV	-3.5 kV	OK	Yes
GUOC 12	2.6 keV	2.75 keV	-3.5 kV	OK	Yes
GFOC 49	3.05 keV	3.16 keV	-3 kV	Oscillations in the signal	Yes
GUOC 1	3.2 keV	3.4 keV	-3.2 kV	Base line of the signal unstable	Yes
GUOC 16	4.9 keV	4.9 keV	-4 kV	Noisy	Yes
GUIC 34		7 keV	-3kV	Very noisy, possible vacuum problem	Yes
GFOC 21		20 keV	-4 kV	Very noisy	Yes
GFOC 33		30 keV	-4 kV	Very noisy	Yes
GUIC 36				No signal, preamplifier transistor burned out. Can be repaired in Warsaw, but other defects possible.	Yes
GUOC 13				Signal shape problem	No
GUOC 32				Vacuum leak inside the dewar	No
GUOC 30				High detector current	No
GFOC 26				High detector current	No
GUOC 6				Vacuum leak on top of the end-cup, unknown if the crystal is OK.	No
GUIC 3				At Canberra for repairs, crystal damaged by a screw flying loose in the cryostat	No
GFOC 28				At GSI for repairs	No

A.5 Water flow interlock system for the Warsaw Cyclotron

J.Miszczak, M.Sobolewski, Z.Kruszynski

Heavy Ion Laboratory, University of Warsaw, Warszawa, Poland

In the HIL Annual Report for 2001 we described a water interlock system for the main and trim coils of the cyclotron based on commercial flow meters made by the Metron company [1]. The interlock system worked reliably for several years, but around 2007 the flow meters gradually started to fail. Even when the flow of water was OK, the meters started to show low flow, triggering the interlocks. Unfortunately the meters are not serviceable and have to be replaced. In 2016 it was decided to scrap the existing flow meters and go with the idea of a rotameter based design. This is a return to the system that was used before 2001, but this time made entirely of stainless steel and with non-contact inductive sensing of the position of the float. The design has its challenges, but it is felt that due to its simplicity it will last for many years with minimum maintenance. The work will be continued in 2017.

Bibliography

[1] J.Miszczak, M.Sobolewski, Z.Kruszynski, HIL Annual Report 2001, page 14.

A.6 New website and IT infrastructure of the Heavy Ion Laboratory

Ł. Świątek, W. Piątek, P.J. Napiorkowski J. Miszczak

Heavy Ion Laboratory, University of Warsaw, Warszawa, Poland

In 2016 the Heavy Ion Laboratory changed its website. The new website uses a convenient and easy-to-use content management system. The website has an attractive and consistent design. Easy handling allows for parallel publishing of content by various scientific teams. The front page of the new site is shown in Fig. 1.

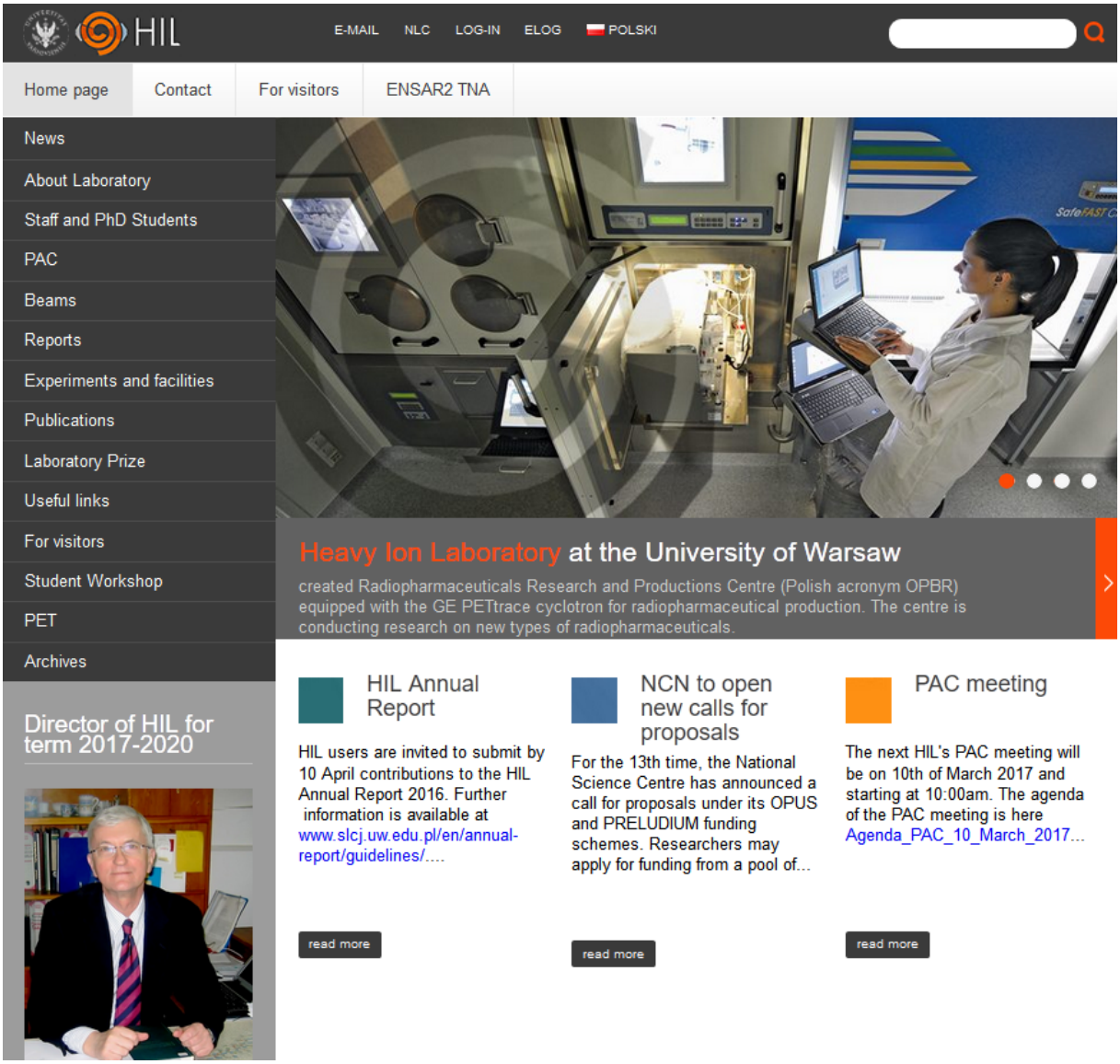


Figure 1: The front page of the new HIL website.

Along with the website the laboratory changed its logo. The new one was designed with a better appearance on mobile devices in mind.

In the last quarter of 2016 two server machines were purchased for deploying and serving virtual infrastructure. For this purpose the VMware ESXi supervisor was used as a virtualization tool. The aim of this develompment is to facilitate management of the services provided by the HIL servers, updating of their software, and to reduce the time it takes to restore services in the event of a failure. By the end of the year, some services were moved from physical servers to virtual machines, such as the DNS server and the secondary NIS server.

In 2017 the mail server will be moved to virtual machine, its operating system will be updated and the mail web interface will be changed. It is also planned to create fallback servers offering e-mail and www services.

Several mechanisms have been deployed on the mail server that work in close cooperation with a firewall to block connections to individual IP addresses from which attempts are made to break into users' e-mail accounts or to send out spam.

Part B

Research for medical and biological applications

B.1 Production of and research into medical radioisotopes at the Heavy Ion Laboratory

J. Jastrzębski[1], J. Choiński[1], A. Jakubowski[1], K. Kapinos[1], M. Kisieliński[1], M. Sitarz[1,2], A. Stolarz[1], K. Szkliniarz[3], A. Trzcińska[1], J. Wojtkowska[4], W. Zipper[3]

1) Heavy Ion Laboratory, University of Warsaw, Warszawa, Poland
2) Faculty of Physics, University of Warsaw, Warszawa, Poland
3) Institute of Physics, University of Silesia, Katowice, Poland
4) National Centre for Nuclear Research, Świerk, Poland

The previously reported [1] research on the production efficiency and isotopic purity of medical radioisotopes investigated at HIL was continued during 2016. Three accelerators were used: a $K = 160$ isochronous cyclotron accelerating gaseous ions from He to Ar to energies from 2 to 10 MeV/nucleon, a high current medical p/d cyclotron, accelerating protons to an energy of 16 MeV and deuterons to an energy of 8 MeV, equipped with an external beam line for the irradiation of solid samples [2] and the home made C30 proton cyclotron at the National Centre for Nuclear Research, Świerk, with a proton beam energy of 28 MeV.

This year we conducted the following studies:

- we made the final measurements of ^{99m}Tc production efficiency and radioisotopic purity via the ^{100}Mo(p,2n)^{99m}Tc reaction using a highly enriched ^{100}Mo target and the proton beam at Świerk,
- the production efficiencies of the ^{44}Ca(p,n)^{44}Sc and ^{44}Ca(p,n)^{44m}Sc reactions were investigated with enriched $^{44}CaCO_3$ targets and proton beams of two different energies (12 MeV and 22 MeV), reflecting the behaviour of theoretical curve (see Fig. 1),
- the production of ^{47}Sc (theranostic match to the ^{43}Sc and ^{44}Sc positron emitters) was measured using the ^{48}Ca(p,2n)^{47}Sc and ^{48}Ti(p,2p)^{47}Sc reactions with $^{48}CaCO_3$ and $^{48}TiO_2$ targets respectively,
- we also studied the production efficiency and the radioisotopic purity of the ^{43}Sc medical radioisotope using the ^{43}Ca(p,n)^{43}Sc reaction and $^{43}CaCO_3$ targets.

Figures 1, 2 and 3 illustrate this research. The results of this work were published in Refs. [3, 4]. A PhD report of Katarzyna Szkliniarz based on the same results was defended in May 2017. This work was supported by the Polish Funding Agency NCBiR under the grants "ALTECH" (PBS1/A9/2/2012), "PET-SKAND", PBS3/A9/28/2015) and the ENSAR2, WP15 H2020 European grant. Discussions with Aleksander Bilewicz are also greatly appreciated.

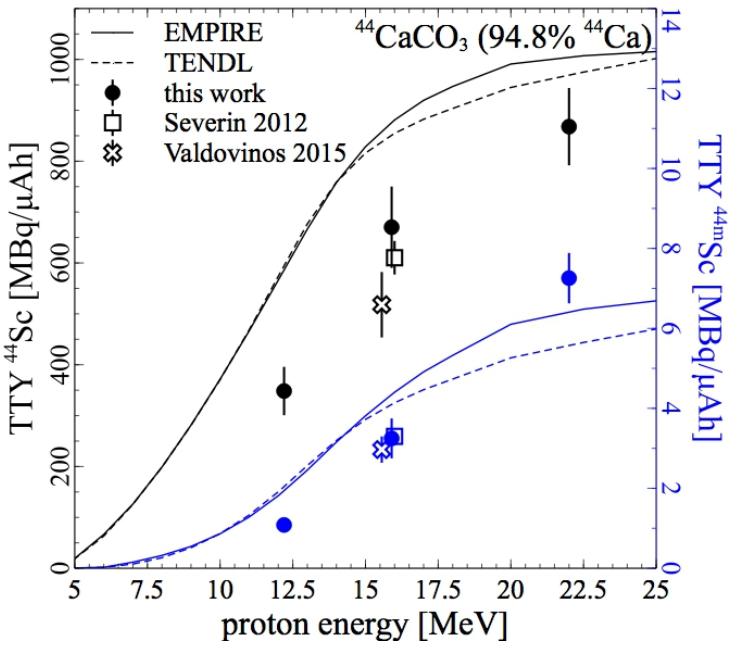


Figure 1: Measured Thick Target Yields of ^{44}Sc and ^{44m}Sc radioisotopes produced in the ^{44}Ca(p,n) reaction compared with the theoretical predictions based on EMPIRE evaporation code calculations. The data from Refs. [4,5] measured with a metallic target and converted to the $^{44}CaCO_3$ equivalents are also shown.

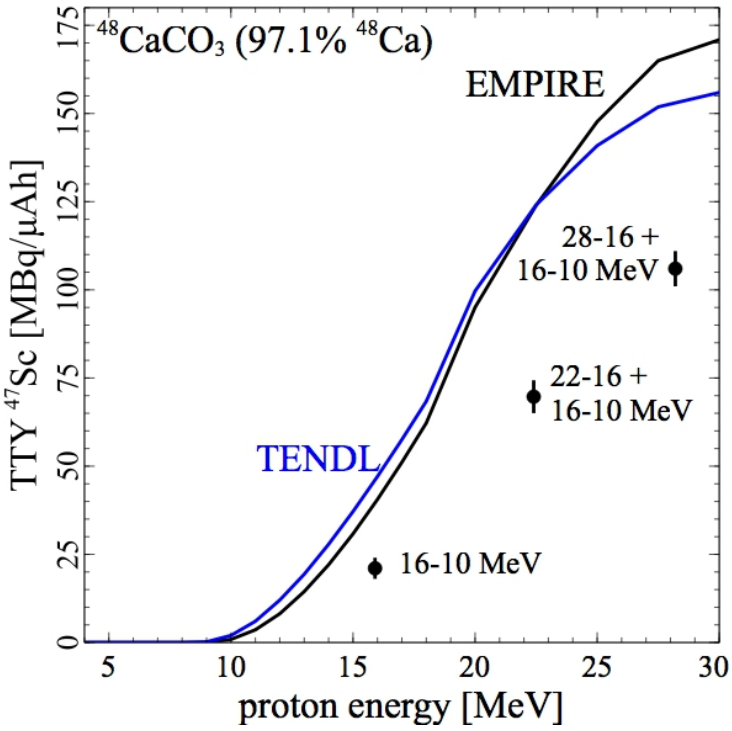


Figure 2: Measured Thick Target Yield of ^{47}Sc obtained using the ^{48}Sc(p,2n) reaction with theoretical predictions based on EMPIRE evaporation code calculations and TENDL tabulations. The experimental data are converted to 97.1% $^{48}CaCO_3$ target enrichment.

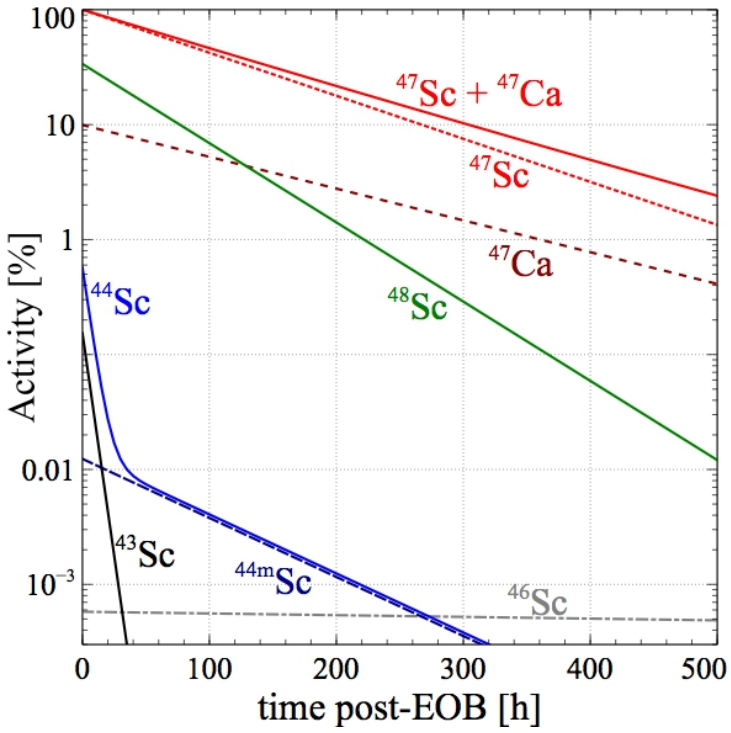


Figure 3: Evolution with time of the relative intensities of radioisotopes produced on Ca during a 10 h irradiation of a $^{48}CaCO_3$ target with a 22.4–16.6 MeV proton beam. The experimental data are converted to 97.1% $^{48}CaCO_3$ target enrichment.

Bibliography

[1] J. Jastrzębski *et al.*, HIL Annual Report 2015, page 25

[2] J. Choiński *et al.*, this Report, page 40

[3] K. Szkliniarz *et al.*, Applied Radiation and Isotopes **118** (2016) 182

[4] K. Szkliniarz *et al.*, Modern Phys. Lett. **A32** (2017) 1740012

[5] G.W. Severin *et al.*, Applied Radiation and Isotopes **70** (2012) 1526

[6] F.Valdovinos *et al.*, Applied Radiation and Isotopes **95** (2015) 23

B.2 Targets for Sc radioisotopes production with internal alpha beam

A. Stolarz[1], J.A. Kowalska[1], J. Jastrzębski[1], J. Choiński[1], M. Sitarz[1,2], A. Jakubowski[1], K. Szkliniarz[3], A. Trzcińska[1], W. Zipper[3]

1) Heavy Ion Laboratory, University of Warsaw, Warszawa, Poland
2) Faculty of Physics, University of Warsaw, Warszawa, Poland
3) Institute of Physics, University of Silesia, Katowice, Poland

The production of scandium medical radioisotopes by alpha particles incident on calcium [1–3] is carried out using calcium carbonate ($CaCO_3$) powder, natural and isotopically enriched, as target material. The chemical properties of calcium (Ca) and the commercial availability of the isotopically enriched material only in the form of $CaCO_3$ were arguments for working with targets made directly from the carbonate powder. This allows one to avoid the time-consuming two-step $CaCO_3$ conversion into metal. Such a conversion can be done in vacuum in the pyrometallurgical process by carbonate decomposition to oxide, followed by the oxide reduction into Ca using e.g. zirconium (Zr) or tantalum (Ta) [4] as reductant:

$$CaCO_3 \rightarrow CaO + CO_2 \quad \text{(heating at a temperature above 700° C, first step)}$$
$$2CaO + Zr \rightarrow Ca + ZrO_2 \quad \text{(second step)}$$

The process is not only time-consuming but may also introduce new contaminants to the target. In addition, working with metallic Ca would require the construction of special vacuum containers and a transfer vacuum line to the cyclotron to prevent contact of the Ca with air.

The availability of alpha projectiles from the Warsaw Cyclotron only as an internal beam imposes constraints on the target set-up shape, i.e. the holder and the target frames have to be frame-less on one side so as not to lose the beam. This is an essential for cyclotrons with dense ion beam trajectories as in our U-200P. The target unit used in our cyclotron is composed of a water cooled target holder (copper block), to which the target is fixed by a "fork" made of aluminium and two screws, both components meant to ensure the proper alignment of the target and to improve its contact with the surface of the water cooled holder. The "fork" aperture and the target size are designed with safety margins considering the possible beam beta oscillations. To protect the cyclotron against a possible contamination in case of any target failure (peeling off, evaporation), the target together with the copper holder is wrapped in aluminium (Al) foil. At the front of the target a thin copper (Cu) foil is mounted for monitoring the beam current. A typical target configuration and a target ready for irradiation are shown in Fig. 1.

To comply with the frame-less requirement, targets with thickness of 40–70 mg/cm^2 (depending on the Sc isotope produced, i.e. the alpha particle energy corresponding to the desired reaction) were produced by compacting the $CaCO_3$ powder into a wafer wrapped in a thin Al foil, which mechanically reinforces the fragile thin wafer (Fig. 2, left). To produce such wafer, $CaCO_3$ powder, evenly distributed on the surface of a pre-formed Al foil (20 µm), was wrapped in this foil, forming a rectangular "candy" (Fig 2, right). The powder inside the "candy" was then compacted with a force of 38.5 kN using a hydraulic press.

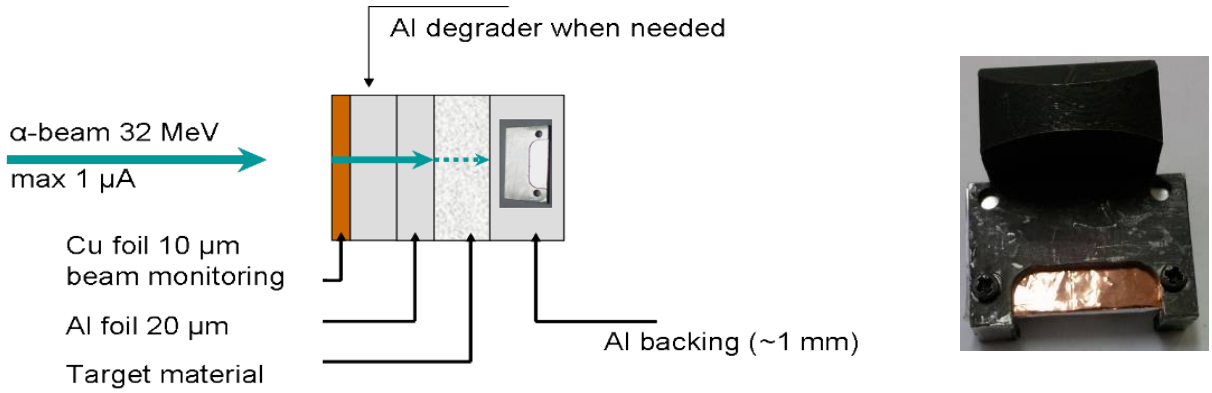


Figure 1: The composition of the target used for alpha beam irradiation (left) and a target mounted in the holder ready for irradiation.



Figure 2: Wafer of $CaCO_3$ and the packed target in the form of a "candy".

Such a procedure ensures an efficient (practically with no material loss) production of a thin target. The thickness of the whole bundle was checked with two different tools: a micrometer and an induction thickness gauge. The devices showed the thickness variation across the target area to be not larger than 20 μm. It is presumed that these thickness variations resulted from variations in the thickness of the carbonate wafer and were calculated to correspond to an areal density of 3 mg/cm^2 (as the density of the carbonate, compacted with applied force, is about (60–70)% of the gravimetric density). This corresponds to a thickness inhomogenity of 5–6%.

This work was supported by a grant awarded by the Polish National Centre for Research and Development, *PET-SKAND — Production of radiopharmaceuticals for PET diagnostic*, PBS3/2319/2014.

Bibliography

[1] K. Szklinarz *et al.*, HIL Annual Report 2015, page 30

[2] K. Szklinarz *et al.*, HIL Annual Report 2015, page 33

[3] K. Szkliniarz *et al.* Applied Radiation and Isotopes **118** (2016) 182

[4] J.D. Stinson, Proceedings of the 1974 Annual Conference (INTDS) (1974) 100

B.3 Ca targets for Sc production by proton or deuteron irradiation

A. Stolarz[1], J.A. Kowalska[1], J. Jastrzębski[1], J. Choiński[1], M. Sitarz[1,2], K. Szkliniarz[3], A. Trzcińska[1], W. Zipper[1]

1) Heavy Ion Laboratory, University of Warsaw, Warszawa, Poland
2) Faculty of Physics, University of Warsaw, Warszawa, Poland
3) Institute of Physics, University of Silesia, Katowice, Poland

Targets for Sc radioisotope production by bombardment of Ca with protons or deuterons and studies of the reaction parameters as a function of projectile energy [1], were prepared using calcium carbonate ($CaCO_3$), natural or isotopically enriched, as the target material. The reasons for working with $CaCO_3$ are explained in another contribution [2] where targets for Sc radioisotope production in reactions of Ca with alpha particles are described.

Irradiation in our PETtrace machine requires circular targets to fit into the target holder. The same shape was also used for targets irradiated with protons delivered by the C-30 cyclotron. The targets, as mentioned above, were prepared from $CaCO_3$ powder. Unfortunately, it is not easy to produce self-supporting mechanically stable pellets of $CaCO_3$, especially thin ones. Therefore, Sc isotopes for radiochemical or biomedical studies are produced using targets where target material is supported by a backing, which is not activated by protons or deuterons, e.g. carbon, and encapsulated. Such targets were prepared by N.P. van der Meulen et al. [3] and C. Müller et al. [4] by pressing together the $CaCO_3$ placed on top of graphite powder or on top of a pre-pressed graphite disk. However, these methods are not suitable for studies where targets with determined uniform thickness are essential (e.g. determination of target yield or quantitative investigation of produced impurities). Both methods result in a blob of target material of irregular shape and inhomogeneous thickness, in the graphite backing (Fig. 1).

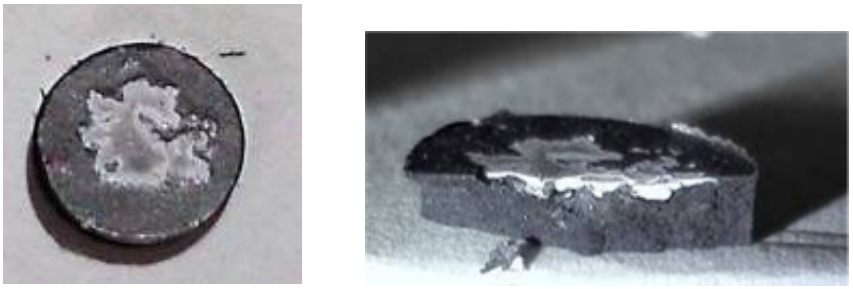


Figure 1: Calcium carbonate target prepared by pressing a 15 mg "pinch" of $CaCO_3$ powder placed on top of graphite powder.

In studies of the isotope production parameters as a function of projectile energy relatively thick targets are also needed. Targets with a thickness of about 300 mg/cm^2 or about 55 mg/cm^2 are needed to cover the reaction cross section for the proton energy range of 16 to 4 MeV, and for deuterons of 8 to 0 MeV respectively. These thicknesses made target preparation as a pure $CaCO_3$ pellet very costly in the case of isotopically enriched material. To economise, the usually very expensive enriched Ca isotopes, targets for our studies were designed as a mixture of $CaCO_3$ with a diluter mixed thoroughly in various proportions and then pressed into a pellet. This method allows production

of targets with low content of the target material, i.e. $CaCO_3$, but with sufficient total thickness to give the required decrease in the projectile energy. Considering the diluter material, two aspects were taken into account: the activation of the added material in reactions with protons or deuterons and its contribution to the heat transfer from the target material, since $CaCO_3$ is an insulator. For the latter aspect the best choice would be a metallic powder with a high thermal conductivity coefficient. However, because of the activation by protons or deuterons only Al with 250 W/(m×K) can be considered, as in the (p,n) reaction only very short lived (4.16 s) ^{27}Si is produced or in the (d,p) reaction only ^{28}Al with $t_{1/2} = 2.24$ min. The other considered diluter was graphite, as with regard to activation by protons or deuterons it has no competitors. In reactions with p or d only very short lived or stable isotopes of carbon (^{11}C), nitrogen (^{13}N, ^{14}N, ^{15}N), boron (^{9}B, ^{10}B) or beryllium (^{7}Be) are produced [3]. However, the possible enhancement of the heat transfer by the graphite was difficult to appraise, since its thermal conductivity reported in the literature ranges from 140 W/(m×K) up to 500 W/(m×K) or even higher when the heat is distributed parallel to the layer planes (hexagonally arranged carbon atoms) and from 3 W/(m×K) to 10 W/(m×K) when perpendicularly to the planes (randomly oriented atoms) [4–6]. In the case of powder it is practically impossible to predict which plane orientation dominates, if any. The impact of graphite and Al on the heat transfer from the target material was assessed by comparing the time needed for temperature increase across pellets made of Al, graphite, $CaCO_3$ and two-component mixtures of equal amounts of $CaCO_3$ and either graphite or Al.

Diamond powder was also included in our tests as the information about its thermal conductivity is ambiguous. Although the very high thermal conductivity of bulk diamond is not preserved in powder form [3], it is often used as a filler in materials used as heat conductors to enhance the heat dissipation. Our measurements [4] showed that graphite powder transports the heat significantly better (about twice as fast) than Al powder and in this respect is far better than diamond powder. The test showed that conductivity of diamond powder is much worse than that of pure $CaCO_3$ so it is not worth consideration as a diluter for $CaCO_3$ targets.

Bearing in mind the results obtained for the heat transfer and the negligible activation of carbon under proton or deuteron bombardment, targets for our studies were made from a graphite and $CaCO_3$ mixture. Both components thoroughly mixed in various proportions, depending mainly on the price of the target isotope, were compacted into about 300 mg/cm^2 (in total) thick pellets with a force of about 40 kN.

Unfortunately, targets prepared in this way were not convenient in further treatment i.e. extraction of the produced Sc isotopes. The inner part of the pellet was very hard, limiting the access of the acid used to dissolve the target. Mechanical smashing was necessary to achieve a quick complete dissolution of the active material. To overcome this problem a new method of Ca target preparation was developed. In the first step the $CaCO_3$ pellet and graphite bed with a pocket corresponding to the $CaCO_3$ pellet size are prepared separately. In the second step the $CaCO_3$ is inserted into the pocket and both elements are pressed again with a force of about 46 kN, creating a stable integrated pellet (Fig. 2).

Target material prepared in this way, even as a thin target, has a uniform thickness and a well defined area. Additionally, the open access to the target material ensures its quick dissolution after irradiation.

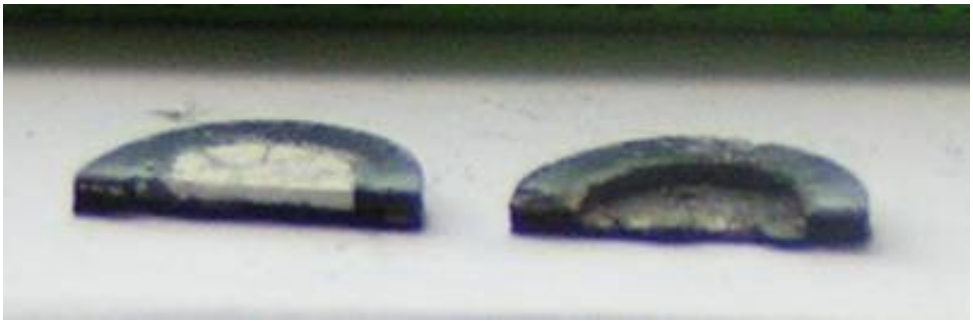


Figure 2: Cut through a 100 mg/cm^2 $CaCO_3$ target in graphite bed.

This work was supported by a grant awarded by the Polish National Centre for Research and Development: PET-SKAND-Production of Sc-based radiopharmaceuticals for PET diagnostics, PBS3/2319/2014.

Bibliography

[1] K. Szkliniarz *et al.*, HIL Annual Report 2015, page 30 and 33

[2] A. Stolarz *et al.*, this Report, page 28

[3] N.P. van der Meulen *et al.*, Nucl. Med. and Biol. **42** (2015) 745

[4] C. Müller *et al.*, J. Nucl. Med. **54** (2013) 2168

[5] N. Soppera, E. Dupont, M. Bossant, JANIS Book of proton-induced cross-sections, Comparison of evaluated and experimental data from ENDF/B-VII.1, JENDL/HE-2007, PADF-2007, TENDL-2011 and EXFOR, OECD NEA Data Bank, June 2012

[6] M. Smalc *et al.*, Proceedings of IPACK 2005, San Francisco, July 2005

[7] J. Rantala, Electronic Cooling **8** (2002), `https://www.electronics-cooling.com/`

[8] Introduction to Materials Science, Chapter 19, Thermal Properties, Dep. Material Science & Engineering, MSE 2090, University of Virgia, 2010

[9] C.P. Wong, Kyoung-Sik Moon, Yi Li, (Eds.), Nano-Bio- Electronic, Photonic and MEMS Packaging, Springer 2010; J. Felba, page 277

[10] A. Stolarz *et al.*, World Conference of the INTDS, Cape Town, 2016, submitted to Physics Procedia

B.4 Antioxidant interactions between phenolic acids in a model system

A. Sentkowska[1], K. Pyrzyńska[2], K. Kilian[1]

1) Heavy Ion Laboratory, University of Warsaw, Warszawa, Poland
2) Faculty of Chemistry, University of Warsaw, Warszawa, Poland

Polyphenolic acids are well known for their antioxidant properties. They are associated with many health benefits such as preventing and treating numbers of disease, such as flu and colds, diabetes or even cancer. In foodstuffs the composition of these compounds is complex. In the literature there is still very little information about the interactions between particular polyphenolic acids. However, interactions between polyphenolic compounds as well as other antioxidants can occur and can be synergistic, additive or antagonistic.

In this study the individual antioxidant capacity of four major phenolic acids often found in food (protocatechuic, caffeic, ferrulic and gallic acids) were tested using two different in vitro assays: $DPPH^{\bullet}$ radical scavenging activity and cupric reducing antioxidant capacity (CUPRAC). Additionally, the presence of vitamin C and some vitamins from the B group (niacinamide-B3, panthothenic acid-B5) were evaluated.

The measurements were carried out using a Perkin Elmer Lambda 25 UV/VIS spectrophotometer. For the cupric reducing antioxidant capacity (CUPRAC), the procedure was as follows: 1 mL of $CuCl_2$ solution (0.01 mol/L) was mixed with 1 mL of neocuproine alcoholic solution ($7.5 \cdot 10^{-3}$) mol/L) and 1 mL of 1 mol/L acetate buffer (pH 7), followed by adding 0.5 mL of polyphenolic acid solution and 0.6 mL of water. The tube containing the sample and reagents was incubated in a water bath at a temperature of 50°C for 20 min., after which it was cooled under running water. Absorbance against the blank reagent was measured at 450 nm. The calibration curve was drawn with trolox (TR) and the antioxidant activity of the individual polyphenolic acids and their mixtures was expressed as trolox equivalent (mmol/L TR). For the DPPH assay 0.1 ml of sample was added to 2.4 ml of DPPH solution ($3.0 \cdot 10^{-5}$ mol/L) in methanol. After 30 min. the absorbance was measured at 539 nm. Trolox solution in concentration up to 1000 µmol/L was used for the calibration curve and the results were expressed in trolox equivalent (mmol/L TR).

The results generally indicate that the majority of mixtures showed a loss of antioxidant activity compared with the theoretical values. This is particularly apparent for the results obtained from the DPPH assay. Using the other assay (CUPRAC) all types of interactions can be found. The addition of ascorbic acid (vitamin C) to the solutions containing individual polyphenolic acids influenced their antioxidant capacity. The interactions found in the DPPH assay were antagonistic. On the other hand, the type of interaction found using the CUPRAC assay strictly depend on the individual polyphenolic acid. The addition of vitamin B3 or B5 caused a decrease in the antioxidant activity measured with the DPPH method. For the same composition in CUPRAC the decrease in antioxidant activity was not so dramatic. A lower difference in antioxidant activity was observed for ferulic acid. This polyphenolic acid showed the lowest antioxidant properties in both assays.

B.5 Determination of 3 neurotransmitters in rat brain tissue using liquid chromatography with mass spectrometry detection

A. Sentkowska, K. Kilian

Heavy Ion Laboratory, University of Warsaw, Warszawa, Poland

Analysis of neurotransmitters and their metabolites is useful for the diagnosis of central nervous system diseases. A liquid chromatography tandem mass spectrometry (LC-MS/MS) method was developed and optimised to monitor the level of 5-hydroxytryptamine (5-HT), 5-hydroxyindole acetic acid (5-HIAA) and γ-aminobutyric acid (GABA) in rat brain tissue.

Chromatographic analysis was performed using a Shimadzu high performance liquid chromatography system with a binary pump, degasser, autosampler and connected to 8030 Triple Q Mass spectrometer. A MS system was equipped with an electrospray ionisation source (ESI) operated in negative-ion mode and a quadrupole mass analyser in scan mode from 50 to 1500 m/z. Nitrogen was used as curtain and auxiliary gas at 0.3 MPa.

Separations were obtained using a Zorbax Eclipse Plus C18 column (150 × 4.6 mm, 5 µm). Isocratic elution was used: 0.1% formic acid and acetonitrile (90/10 v/v). Compounds were identified by comparing retention time and m/z values obtained by MS and MS^2 with the mass spectra from standards tested under the same conditions. Quantification of compounds was made from the calibration curves obtained in Multiple Reaction Mode (MRM).

The reproducibility and repeatability of the method was determined using standard solution. Subsequently, the procedure was applied successfully to the analysis of neurotransmitters in rat brain tissue. Seventy samples differing in the method of extraction were examined. The values were consistent with the literature in terms of the range of concentration.

B.6 Flavonoid content and antioxidant properties in different extracts of heather (Calluna vulgaris L.)

P. Dróżdż[1], A. Sentkowska[2], K. Pyrzyńska[3], K Kilian[2]

1) Forest Research Institute, Sękocin Stary, Raszyn, Poland
2) Heavy Ion Laboratory, University of Warsaw, Warszawa, Poland
3) Faculty of Chemistry, University of Warsaw, Warszawa, Poland

Heather (*Calluna vulgaris* (L.) Hull) a member of the Ericaceae family, can be found in most parts of Europe and Northern America. It grows on acidic soils in open sunny situations and in moderate shade. It is known as an antiseptic, woundhealing, antirheumatic and choleretic remedy. Aerial parts of heather exhibit anti-inflammatory and antioxidant capacity.

In the literature very little data can be found on the antioxidant properties of different extracts of heather. From various extraction studies, it was observed that the choice of solvent for extraction of flavonoids from plant materials was not coherent, which can be explained by the differences in the studied matrices as well as the complexity of flavonoid properties.

This study evaluated the effects of four different solvents, i.e., water, ethanol, a water-ethanol mixture and ethyl acetate, on the antioxidant activities of heather. The cupric reducing antioxidant capacity (CUPRAC) method, scavenging ability on 1,1-diphenyl-2-pirylhydrazyl radicals (DPPH) radicals and chelating activity on Fe^{2+} ions were used for evaluation of the antioxidant activity of the extracts.

The measurements were carried out using a Perkin Elmer Lambda 25 UV/VIS spectrophotometer. For the cupric reducing antioxidant capacity (CUPRAC), the procedure was as follows: 1 mL of $CuCl_2$ solution (0.01 mol/L) was mixed with 1 mL of neocuproine alcoholic solution ($7.5 \cdot 10^{-3}$ mol/L) and 1 mL of 1 mol/L acetate buffer (pH 7), followed by adding 0.5 mL of heather extract and 0.6 mL of water. The tube containing the sample and reagents was incubated in a water bath at a temperature of 50°C for 20 min., after which it was cooled under running water. Absorbance against the blank reagent was measured at 450 nm. The calibration curve was drawn with trolox (TR) and the antioxidant activity of the samples was expressed as trolox equivalent (mmol/L TR). For the DPPH assay 0.1 ml of sample was added to 2.4 ml of DPPH solution ($3.0 \cdot 10^{-5}$) mol/L) in methanol. After 30 min. absorbance was measured at 539 nm. Trolox solution in concentration up to 1000 µmol/L was used for the calibration curve and the results were expressed in trolox equivalent (mmol/L TR). For the chelating activity measurement 1 ml of heather extract was mixed with 3.7 ml of distilled water. Then the mixture was reacted with 0.1 ml, 2 mmol/L $FeCl_2$ and 0.2 ml ferrozine. The absorbance was measured at 562 nm. Chelating activities of the extract (%) were calculated in relation to the absorbance of the control sample.

The results of this research showed that flavonoid content and the resulting antioxidant properties are strictly dependent on the solvent used for the extraction. Ethyl acetate and the ethanol-water mixture were proven to be the best solvents. Extracts of Calluna vulgaris may be considered a good source of compounds with high antioxidant properties. This fact may be explored in pharmaceuticals, foodstuffs, feed additives and cosmetics.

B.7 Optimisation of Cu(II)-porphyrin complex synthesis for PET radiopharmaceutical applications

M. Pęgier[1], K. Kilian[2], M.L. Pęgier[1,2], K. Pyrzyńska[2]

1) Heavy Ion Laboratory, University of Warsaw, Warszawa, Poland
2) Faculty of Chemistry, University of Warsaw, Warszawa, Poland

Porphyrin based photosensitizers are useful agents for photodynamic therapy and fluorescence imaging of cancer. Additionally, porphyrins are excellent metal chelators, forming stable metalo-complexes and the ^{64}Cu isotope can serve as a positron emitter ($T_{1/2}$ = 12.7 h) The other advantage of ^{64}Cu is its decay characteristics that facilitate the use of ^{64}Cu-porphyrin complex as a therapeutic agent. Thus, ^{64}Cu chelation with porphyrin photosensitizer may become a simple and versatile labelling strategy for clinical positron emission tomography. The present study reports the influence of several interferents on the synthesis of Cu complex with tetrakis(4-carboxyphenyl)porphyrin (TCPP) using an optimised method. Interferents such as Ni^{2+}, Zn^{2+}, Al^{3+}, Fe^{3+} and an excess of chlorides added to the reaction environment were mixed with Cu^{2+} ions prior to addition to a mixture of TCPP and ascorbic acid in a borate buffer (pH = 9). The reaction rate was observed with UV-VIS spectrophotometry. Nickel is the target material for ^{64}Cu production and thus can be present in large excess. Zinc is a common contaminant and it also forms easily a complex with TCPP. Iron has a stable oxidation state +II and could possibly form a complex with TCPP according to the SAT mechanism utilising ascorbic acid as a reducing agent similarly as copper. Al is also a common interferent. Chlorides were tested, because HCl is used for dissolution of targets. Copper is known to form anionic chloride complexes which can influence TCPP complex formation. It can also significantly affect the purification step using an anion exchanger due to the same negative charge, which could possibly prevent separation of ^{64}Cu-TCPP complex from free copper. Results for nickel and zinc — the most important form the experimental point of view — are presented in Fig. 1. A 3-fold excess of nickel and zinc does not influence the reaction rate. A 5-fold and 10-fold excess of Zn^{2+} causes a decrease of absorbance at 542 nm compared to synthesis without zinc, but the Cu-TCPP complex is still formed. A 100-fold excess of chlorides, a 10-fold excess of Al^{3+} and a 10-fold excess of Fe^{3+} do not change the reaction yield and kinetics.

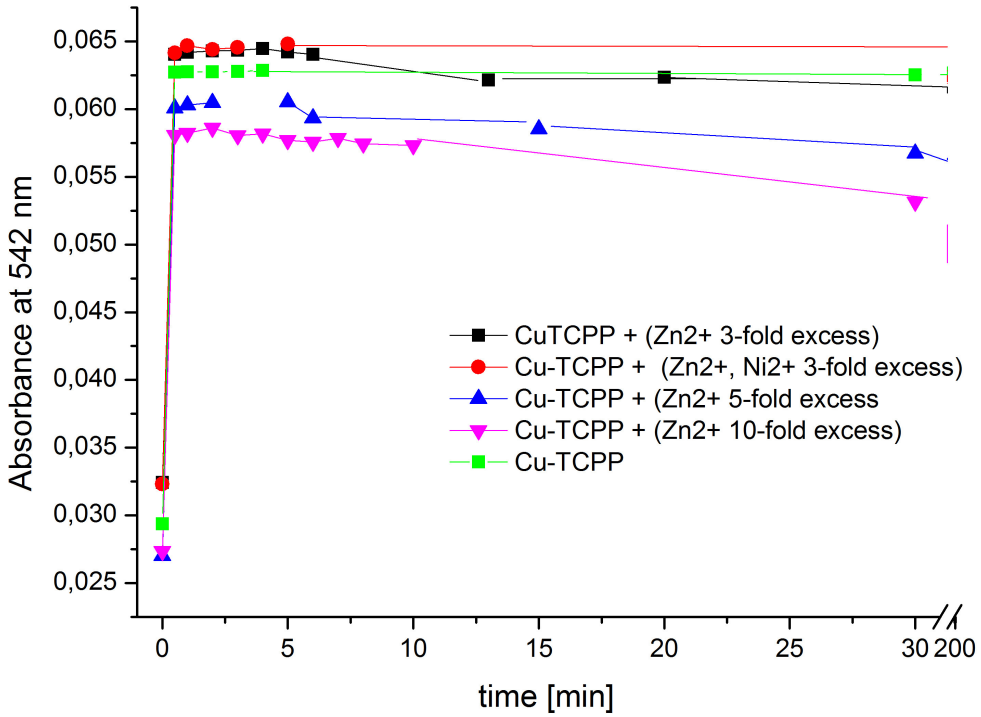


Figure 1: Changes in absorbance at λ_{max} over time for the reaction of Cu(II) and TCPP in the presence of Zn^{2+} and Ni^{2+}. $[Cu^{2+}] = [TCCP] = 5 \cdot 10^{-6}$ M.

B.8 Sorption of Sc(III) ions on solid carbon based materials

M. Pęgier[1,2] K. Kilian[1], K. Pyrzyńska[2]

1) Faculty of Chemistry, University of Warsaw, Warszawa, Poland
2) Heavy Ion Laboratory, University of Warsaw, Warszawa, Poland

The ^{43}Sc and ^{44}Sc nuclides with their relatively long half-lives are promising for clinical Positron Emission Tomography. Both isotopes can be produced form calcium based target materials. Prior to radiolabelling of the precursor, the target material should be separated from the desired radionuclide. For this purpose solid phase extraction (SPE) on different sorbents is often used. The aim of this study was to check the sorption parameters of scandium(III) ions on various carbon-based materials. The tested materials were: activated carbon (AC), multiwalled carbon nanotubes (CNT), multiwalled carbon nanotubes functionalized with carboxylic groups (CNT-COOH), graphene oxide (GO). Chelex 100 was used as a reference material.

Carbon materials can potentially be used in the separation of radioactive scandium isotopes from calcium matrix. The other application can be environmental analysis (preconcentration of scandium from water). AC is a common sorbent used for the removal of various substances from a sample. CNT is a relatively new material and its properties like large surface area, small size, good chemical stability made it popular as a sorbent. Additional functionalization of CNT with carboxylic groups should offer better parameters for sorption of metal ions through ion exchange and chelation and thus CNT-COOH has been used for experiments. Chelex 100 is a popular chelating resin utilized in metal preconcentration. It offers good performance but lacks selectivity. The other disadvantage of this material is the change of size with pH-change, which can cause flow resistance. Static experiments were performed in which a certain amount of sorbent was shaken with a scandium(III) ion solution for 24 h. Different pH conditions were checked.

Sorption curves (Fig. 1) show that sorption of scandium rises with rising pH, in agreement with theory, that deprotonation of carboxylic groups makes them accessible for metal ions. Also above pH = 4.5 precipitiation of $Sc(OH)_3$ can occur, which gives a contribution to total retention on the sorbent. CNT without functionalization show generally low sorption and reaches 50% in the highest pH. Sorption is probably associated to some extent with the formation of $Sc(OH)_3$. AC show moderate properties towards sorption of Sc. The relatively high values obtained for high pH are not optimal, because in this range many matrix components including calcium can also be retained and released with the eluate together with the scandium ions. The best characteristics were shown by GO and CNT-COOH. Practically quantitative sorption in pH = 2 offers much better conditions for separation of scandium from the matrix and preconcentration in the sample. In dynamic experiments GO exhibits high flow resistance (probably due to low particle size). Thus CNT-COOH was tested for performance. In dynamic mode sorption of Sc in pH = 2 is still more than 98%. Additional rinsing with buffer (pH = 2) prior to elution causes removal of 95% of calcium and offers good properties for radiochemical separation of ^{43,44}Sc from the target material ($Ca(CO)_3$).

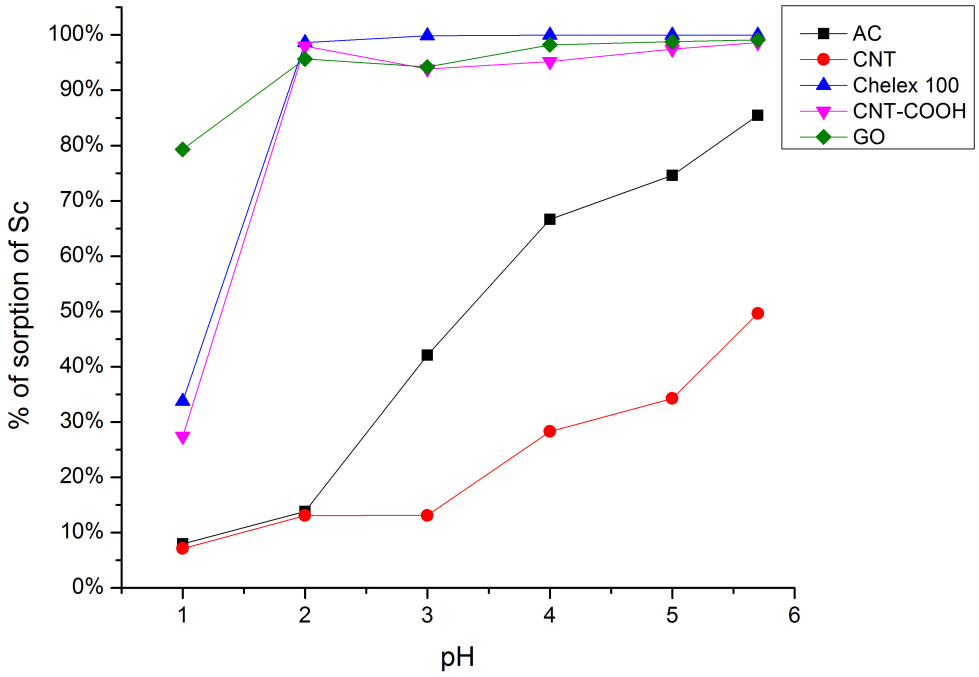


Figure 1: Sorption of scandium(III) on carbon-based materials and Chelex 100 at different pH values.

B.9 The adaptation of an external, well cooled, target holder for the PETtrace cyclotron suitable for irradiation of powder targets

J. Choiński, T. Bracha, B. Radomyski, Ł. Świątek, M. Antczak, A. Jakubowski, P. Jasiński, J. Jastrzębski, R. Kopik, M. Kopka, K. Łabęda, A. Pietrzak, A. Stolarz, K. Sosnowski, R. Tańczyk

Heavy Ion Laboratory, University of Warsaw, Warszawa, Poland

In 2016 the execution of objective no. 3 of the grant "PET-SKAND", agreement no. PBS3/A9/28/2015 awarded to a consortium of three institutions and financed by the National Centre for Research and Development, was continued. Our PETtrace cyclotron is additionally equipped with a standalone external target system originally designed to irradiate metallic targets, particularly molybdenum. The realisation of the "PET-SKAND" project has given us the opportunity to upgrade some parts of the station including the safety conditions for the operational staff and to adapt it to the specific requirements of calcium powder targets.

The dual beam proton/deuteron cyclotron is regularly used for commercial production of fluorine F-18. This means that the targets for F-18 are highly radioactive which dramatically restricts a "free-entry" to the cyclotron cave in order to maintain or prepare a standalone external target system. In 2015, the station was situated very close to the cyclotron. During 2016 we designed and manufactured a completely new beam line. Currently, it consists of: a drift tube length of a total of 3.4 m, two sets of steering magnets made of permanent magnets, one quadrupole doublet and an upgraded, four-sector collimator. This new beam line allows additional shielding to be installed — a concrete wall of thickness 0.25 m, between the cyclotron and the diagnostic box of the target holder system. The beam line was temporarily assembled in the experimental hall area and tested. After passing all tests it was dismounted, transferred to and reassembled in its final location in the PETtrace cave. The old collimator in the diagnostic box was also replaced with a new one. At the end of 2016 the concrete wall shielding was assembled. Its specific weight is 3300 kg/m^3. It considerable reduces the radiation exposure of the staff coming from the cyclotron F-18 targets during station preparation and maintenance. The new beam line gives us the opportunity to tune a proton or deuteron beam to the surface of the targets. Beam transport efficiency to a target size of 12 mm thereby reaches above 96%, significantly improved compared to the previous values which were below 30%. By adding the beam line we have redesigned the diagnostic box. It is now much bigger and contains the new collimator, the Faraday cup, a beam monitor and a new, bigger turbo pump which is much more efficient. With this pumping system the static vacuum reaches a value of $5 \cdot 10^{-7}$ mbar. Figure 1 and Figure 2 show photographs of the modified beam line with the shielding wall and the new diagnostic box.

The new system was checked and passed all tests excluding the beam monitor. It was decided to redesign its electronics. Last year we also made several irradiations of targets for our collaboration groups within the framework of the "PET-SKAND" grant.

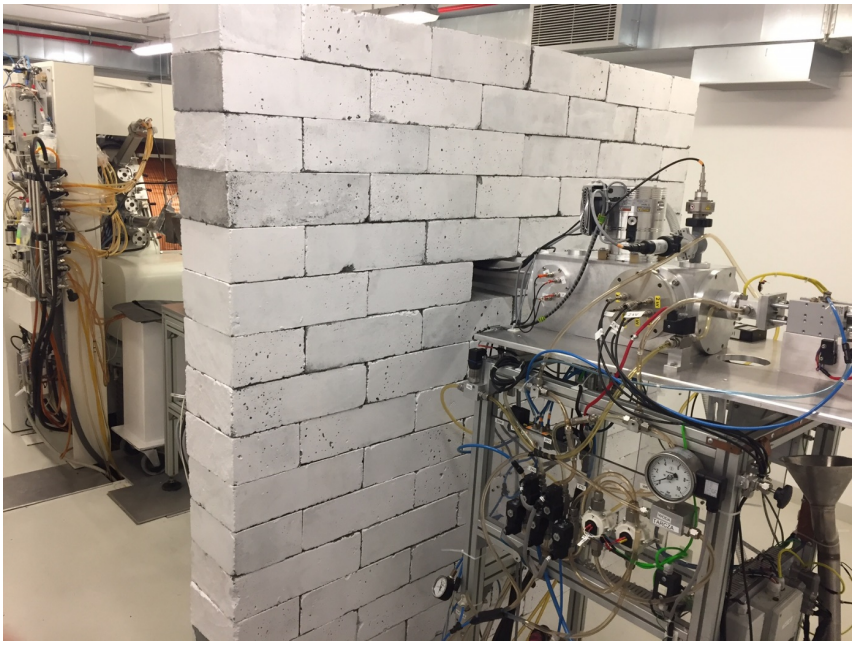


Figure 1: The shielding wall and modified target system.



Figure 2: The modified beam line with shielding wall.

B.10 A new project of an internal, well cooled, target station for the U-200P cyclotron suitable for the irradiation of different types of targets

J. Choiński, B. Radomyski, A. Pietrzak, A. Jakubowski, M. Antczak, T. Bracha, P. Jasiński, R. Kopik, K. Łabęda, Ł. Świątek

Heavy Ion Laboratory, University of Warsaw, Warszawa, Poland

For several years the Heavy Ion Laboratory has been involved in medical radioisotope production, mostly Astatine-211 utilising the α-particle beam from the U-200P cyclotron [1]. We use very simple station which was designed for completely different purposes. This station allows a target material to be irradiated with theinternal beam of the cyclotron. The range of available beam energies may be changed from the initial up to maximum. Unfortunately, this station also has several shortcomings. The most important are: a very weak water cooling system and all preparations must be made manually. Since we have noticed a need for higher beam intensities it was decided to design and construct a new internal, well cooled target station for the U-200P cyclotron. A small team for this project has been constituted. During the past year we designed most parts of the station and some of them are being manufactured now, see Fig. 1. Currently, the final version consists of a vacuum chamber, a target holder, a drive system for the target holder, and a drive system for the target station. We have also bought vacuum system components. A target can be clamped in the target holder with the help of a remotely controlled drive system. The target holder can be positioned inside the cyclotron valley with the help of a remotely controlled drive system. Before we found a final solution for the target holder with its drive system we constructed several target holders and drive systems for test purposes. The construction of the current version of the target holder with a metallic target should be strong enough to withstand about 500 W. Typically we use a beam of α particles with an energy about of 33 MeV.

In the coming year we plan to finish the design work, software and hardware preparation of the remotely controlled systems and to assemble all the parts together on a temporary stand. This will allow to carry out: mechanical, vacuum anf water cooling tests and also to test remote control systems. When all tests have been passed the old station will be dismounted and the new one will be assembled in its place. It is assumed that during target irradiation the beam current will be on-line monitored. After irradiation, the target holder will be moved back to its initial position and the target remotely unlocked from the target holder so that it will drop into the transportation lead pot.

Bibliography

[1] K. Szkliniarz *et al.*, HIL Annual Report 2015, page 27

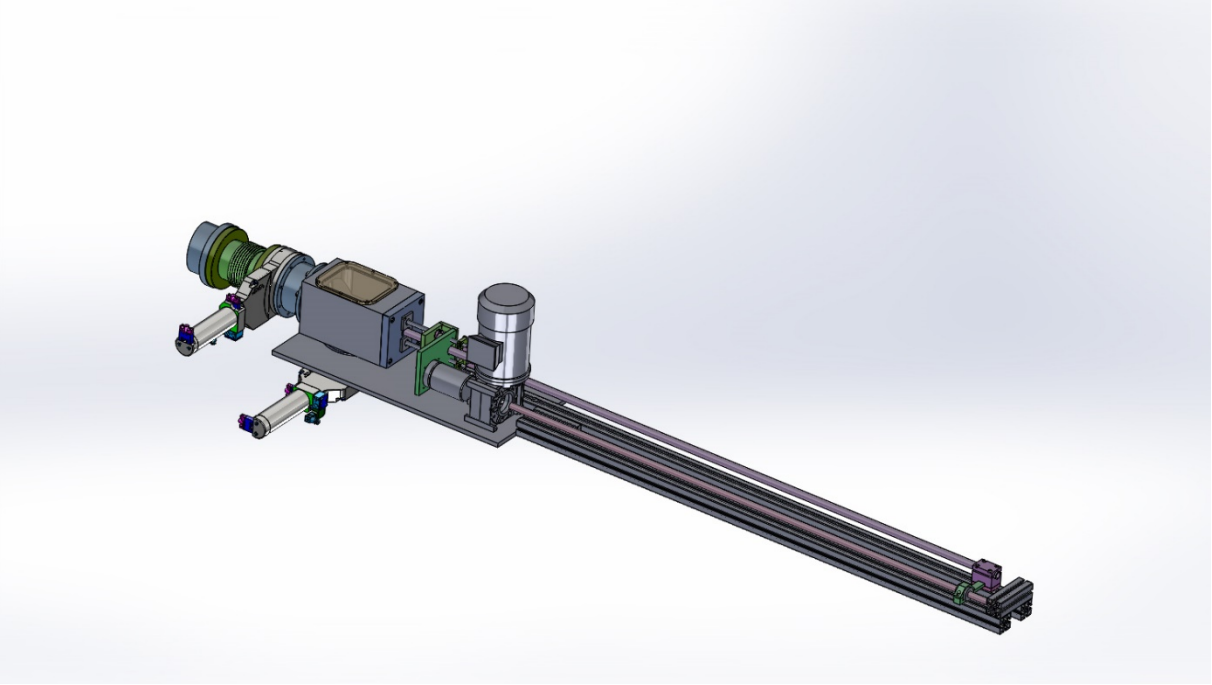


Figure 1: Computer visualisation of the internal, well cooled, target station.

B.11 Irradiation of CHO-K1 cells by a mixed ion beam containing carbon and oxygen ions

J. Czub[1], D. Banaś[1,2], J. Braziewicz[1,2], I. Buraczewska[3], M. Jaskóła[4], U. Kaźmierczak[5], A. Korman[4], A. Lankoff[7,3], H. Lisowska[7], Z. Szefliński[5], M. Wojewódzka[3], A. Wójcik[6,7]

1) Institute of Physics, Jan Kochanowski University, Kielce, Poland
2) Holycross Cancer Center, Kielce, Poland
3) Institute of Nuclear Chemistry and Technology, Warszawa, Poland
4) National Centre for Nuclear Research, Świerk, Poland
5) Heavy Ion Laboratory, University of Warsaw, Warszawa, Poland
6) The Wenner-Gren Institute, Stockholm University, Stockholm, Sweden
7) Institute of Biology, Jan Kochanowski University, Kielce, Poland

Carbon and oxygen ions were accelerated simultaneously at the Heavy Ion Laboratory to estimate the effect of irradiation of living cells by two different ion beams. Such a mixed ion beam was used for the irradiation of Chinese hamster ovary (CHO-K1) cells. The possibility of accelerating two ions together by a cyclotron is related to an identical q/m ratio, where q is the charge and m is the mass of the ions. The two ions were accelerated at the same time to an energy of 108 MeV for carbon ions and 139 MeV for oxygen ions. The ions then passed through a 20 mg/cm^2 thick gold foil located in the vacuum chamber. This step is necessary to scatter the beam in multiscattering processes inside the gold foil. At a distance of 233 cm from the gold foil the beam was collimated by a square collimator of size 1 cm×1 cm. Next, the beam passed through a Havar foil (2.3 mg/cm^2 thick) which was placed at the end of the beam pipe. After 2.2 cm of air, the beam passed through a Mylar foil (12 µm thick) and then through 2.1 mm of air. After that, the beam passed through a Mylar foil (6 µm thick) that forms the bottom of a special design of Petri dish. The live cells were seeded on this Mylar foil. The Petri dish with cells was fully filled by a suitable medium for these cells and closed by a 3D lid. In this experimental setup the Petri dish was placed perpendicular to the beam axis. Additionally, inside the scatterring chamber a detector was placed at an angle 20 degrees to the primary direction of the beam. This detector was used in dosimetry. The experimental setup with the irradiation procedure and the manner of measuring the ion beam intensity distribution, and the construction of the special design of Petri dish were described in detail in Refs. [1] and [2]. The beam size emitted in air was 1 cm×1 cm and the Petri dish had a diameter of 4.8 cm. To irradiate the entire surface of the Petri dish with a process of moving of the Petri dish with a step of 1 cm was introduced. The start of this procedure was initiated after collecting an appropriate number of ions by the 20° detector. These registered values corresponded to the required absorbed dose. The electric impulse emitted from the electronics system connected to the 20° detector was transmitted to a special signal converter and next to a sliding machine. After that, the position of the Petri dish was changed. The course of action was controlled by a self-developed computer program connected to the sliding device.

To perform the survival test, a proper number of the CHO-K1 cells in was placed in a special Petri dish. The number of cells was counted using an automatic cell counter (Countess® Automated Cell Counter). The next step was the irradiation of cells at the Heavy Ion Laboratory. After that, the Petri dish with cells was transported to the

Institute of Nuclear Chemistry and Technology to change the medium and incubate the cells in conditions of 37°C with 5% CO_2 for 7 days. After this time, the colonies in the Petri dishes were fixed using methanol and stained using Giemsa solution (10%), and the survival fraction was estimated. For one absorbed dose, three Petri dishes were used. The experimental data of cell survival were fitted by a linear-quadratic equation: $SF = \exp(-aD - bD^2)$, where SF — survival fraction, D — absorbed dose, a, b — fitting coefficients [3].

The fitting process was done using the Matlab R2009b program with the curve fitting toolbox. Figure 1 shows the survival fraction for CHO-K1 cells after irradiation by a mixed beam containing carbon and oxygen ions and single beams of carbon or oxygen.

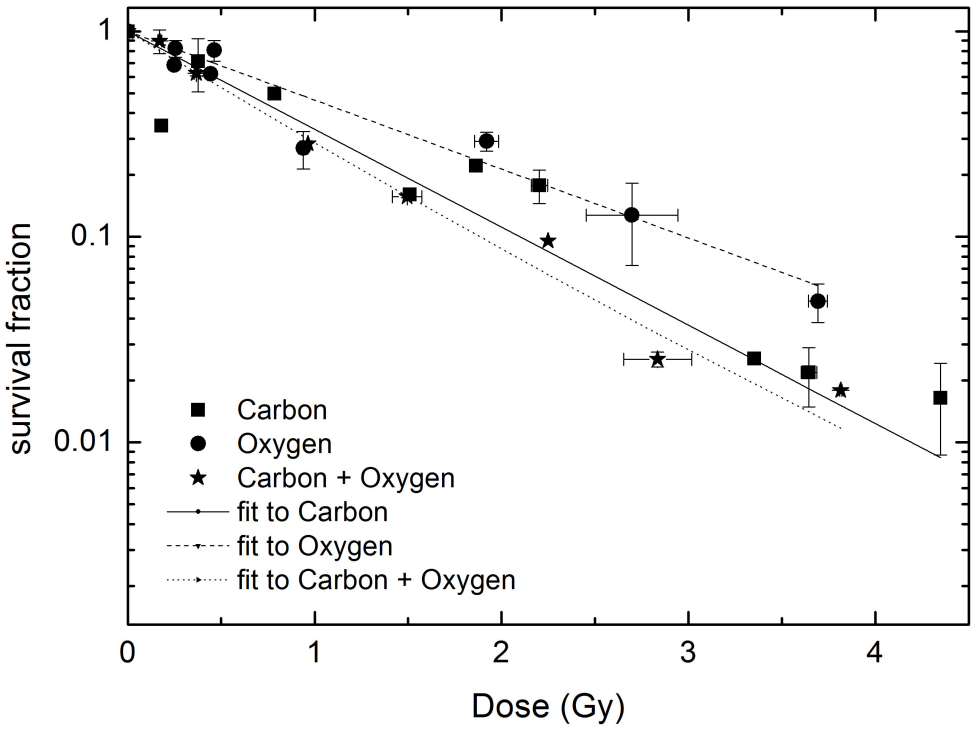


Figure 1: Survival fraction after irradiating by a mixed beam including carbon and oxygen ions and single beams of carbon or oxygen. Error bars are standard deviations. Linear-quadratic equations were fitted to the experimental data

After irradiation a survival test was done showing survival curves. Using the isobologram method, we concluded that the ions of the two types affect the cells in an additive way. A synergistic effect is observed for high values of survival curves equal to 0.6 and 0.9. This effect is probably related with to low fluence values but it needs further study.

This work was supported by the statutory research of prof. Janusz Braziewicz (no. 612 424) at the Jan Kochanowski University, Kielce, Poland.

Bibliography

[1] J. Czub *et al.*, Applied Radiation and Isotopes **67** (2009) 447

[2] J. Czub *et al.*, Rad. Prot. Dosim. **122** (2006) 207

[3] W.K. Weyrather, *et al.*, Int. J. Radiat. Biol. **75** (1999) 1357

B.12 Experimental nanodosimetry of carbon ions using beam intensity modulation

M. Pietrzak[1,2], A. Bantsar[2], S. Pszona[2], Z. Szefliński[3]

1) Faculty of Physics, Warsaw University of Technology, Warszawa, Poland
2) National Centre for Nuclear Research, Świerk, Poland
3) Heavy Ion Laboratory, University of Warsaw, Warszawa, Poland

Carbon ion therapy is the therapy of choice for tumours because of the well-defined carbon ion range. A further benefit of carbon ions is that their biological effect is most pronounced in the Bragg peak and in the distal edge close to the Bragg peak. This enhanced biological effectiveness is related to the ionisation structure of the carbon ion track at the nanometre level. In view of the upcoming radiation therapy with carbon ions, the ionisation structure of the carbon ion track at the nanometre scale is of particular interest.

The ion counting nanodosimeter Jet Counter described in detail elsewhere [1, 2] is a unique device capable of measuring the track structure of ionising particles in a gaseous target equivalent to a nanometric site in condensed matter. The Jet Counter consists of an interaction chamber, where a sensitive volume with a simulated nanometre-sized dimension (target) is obtained by nitrogen expansion from a reservoir by a pulse operating piezoelectric valve with a repetition rate of 1–10 Hz. The target is created dynamically at each gas injection and exists during a 350 µs plateau of gas density. The interaction chamber has a cylindrical form (10 mm in diameter and 10 mm in height) with walls of 1 mg/cm^2 Mylar (Al covered on both sides). A single event is measured when during the 350 µs window a single ionising particle appears.

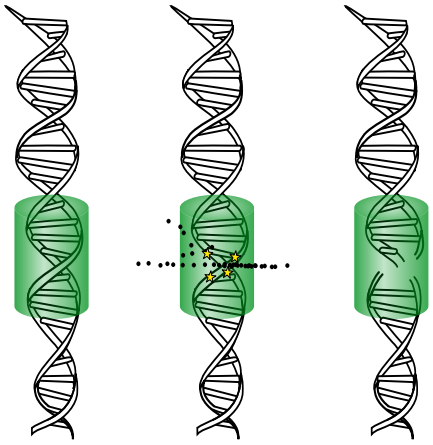


Figure 1: Short DNA segment destroyed by a heavy charged particle. The green area is a nanometric volume simulated in the experiment.

Nanodosimetric experiments were carried out with single carbon ions crossing centrally the nitrogen gas target. The equivalent nanometric volume of the nitrogen target was equal to 1.8 nm (at unit density). We used two beams of energy 92 MeV and 36 MeV, which were scattered by 50 mg/cm^2 and 9 mg/cm^2 gold foils respectively. Therefore, the mean energy inside the interaction chamber was reduced to 52 MeV and 21 MeV respectively. The beam-line arrangement is shown in Figure 2.

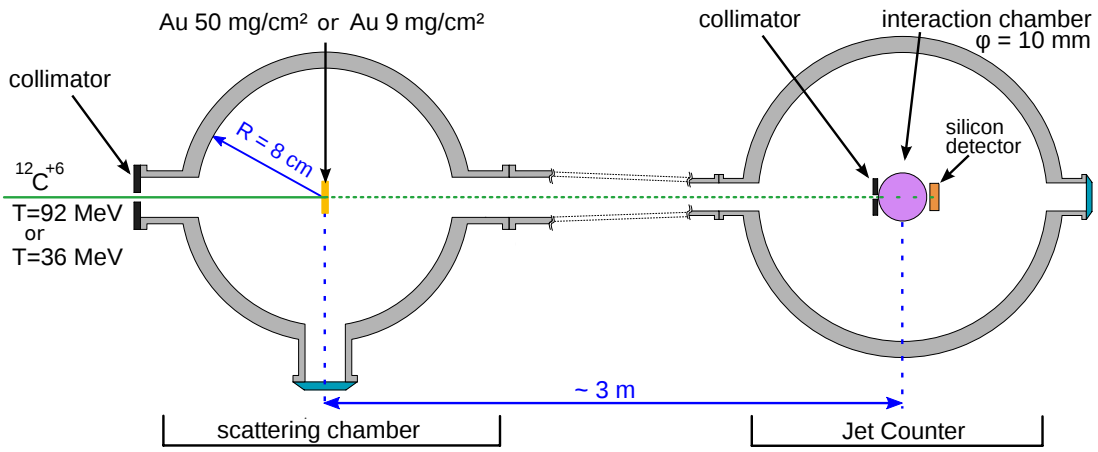


Figure 2: Schematic view of the nanodosimetric set-up on beam-line A at HIL.

A key issue in obtaining good quality results was to avoid multiple coincidences i.e. a number of ionising particles appearing during an ion acquisition window triggered by the first particle. As the acquisition window lasts for 180 µs no other ionising particle may appear before or after its beginning. One possible approach is to reduce the beam intensity, but this also reduces the probability of a single coincidence. To maintain a high rate of data acquisition an active beam intensity modulation system was used. The system consists of a capacitor placed between the cyclotron ion source and the cyclotron itself and is controlled by the Jet Counter coincidence system. The beam is turned off before the coincidence window and about 30 µs after the first coincidence (see Fig. 3). Using this system the probability of multiple coincidence (pile-up) was reduced by a factor of ten. Thus, it was possible to increase the beam intensity and event ratio by the same factor keeping the pile-up contribution at an acceptable level.

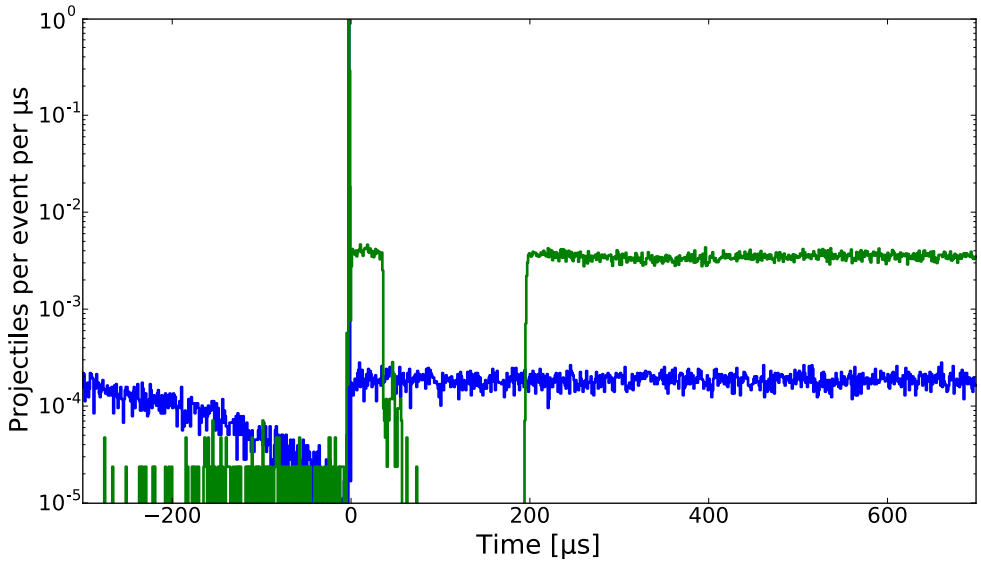


Figure 3: Projectile time of arrival relative to the first coincidence projectile (time zero). Green and blue lines represent results with and without beam modulation respectively. Any additional projectile in the range -200 µs to 180 µs causes pile-up events. The ratio of pile-up events limits the maximum beam rate.

Some of the results obtained in these measurements are presented in Fig. 4. The Ionisation Cluster-Size Distribution (ICSD) was measured with previously inaccessible accuracy thanks to the increased event ratio for the higher beam intensity. The data obtained contain several other interesting pieces of information e.g. primary particle energies for each event and the drift time of created ions, which will be used in the following research phase for comparison with Monte Carlo and ion optics simulations.

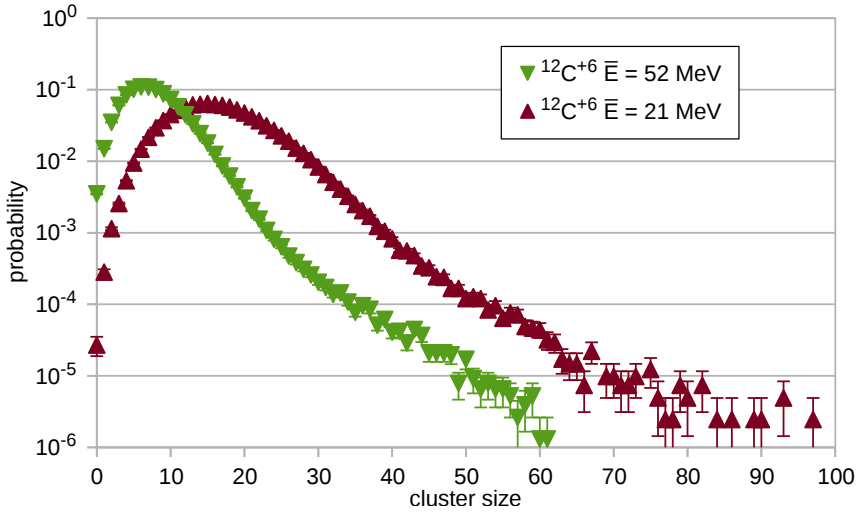


Figure 4: Experimental ionisation cluster-size distribution for carbon ions of different energies. The mean cluster size is equal to 7.9 for 52 MeV carbon ions and 16.8 for 21 MeV carbon ions.

Bibliography

[1] S. Pszona, J. Kula and S. Marjańska, Nucl. Inst. and Meth. **A447** (2000) 601

[2] A. Bantsar, Ph.D. Thesis, 2011, e-Print: arXiv:1207.6893

Part C

Nuclear physics

C.1 Angular correlation method applied to spin determination of low lying levels in ^{140}Sm — new results

J. Samorajczyk-Pyśk[1], Ch. Droste[2], J. Srebrny[1], T. Marchlewski[1,2], R. Szenborn[2], T. Abraham[1], J. Andrzejewski[3], S. Dutt[4], A. Gawlik[3], K. Hadyńska-Klęk [5], Ł. Janiak[2], M. Kisieliński[1,6], M. Klintefjord[5], M. Komorowska[1,2], A. Korman[6], M. Kowalczyk[1,2], J. Kowalska[1], J. Kownacki[1], R. Kumar[7], P. Napiorkowski[1], J. Perkowski[3], W. Piątek[3], M. Piersa[2], T. Rogiński[2], M. Saxena[8], A. Stolarz[1], M. Stryjczyk[2], A. Tucholski[1], W. Wróblewski[1]

1) Heavy Ion Laboratory, University of Warsaw, Warszawa, Poland
2) Faculty of Physics, University of Warsaw, Warszawa, Poland
3) Faculty of Physics and Applied Computer Science, University of Lodz, Łódź, Poland
4) Department of Physics, Aligarh Muslim University, Aligarh, India
5) Department of Physics, University of Oslo, Oslo, Norway
6) National Centre for Nuclear Research, Świerk, Poland
7) Inter University Accelerator Centre, New Delhi, India
8) Department of Physics and Astrophysics, University of Delhi, New Delhi, India

Recently, the properties of the low-lying levels in the ^{140}Sm nucleus were the subject of several studies — see for example Refs. [1–4]. It is planned to continue these studies using the multi-Coulomb excitation of the radioactive ^{140}Sm beam from the HIE-ISOLDE facility. One might expect that the high intensity and high energy beam should result in the population of a larger number of levels in ^{140}Sm (in comparison with the results of Ref. [3]). This was the reason for carrying out new spin measurements of the low-lying states in ^{140}Sm since such information is indispensable for the COULEX experiment analysis.

In this report we present the results of our new, improved experiment where the statistics was about five times larger than in the previous one described in Ref. [2]. The new experiment allowed spins of six excited states in ^{140}Sm to be assigned using method of the γ-γ angular correlations between the 531 keV ($2^+ \rightarrow 0^+$) photon and the 460, 1068, 1098, 1402, 1753 and 2065 keV photons. The results are collected in Figs 1 and 2. Some additional comments are given below.

The low-lying levels of ^{140}Sm were populated in the ^{140}Eu$\rightarrow^{140}$Sm and ^{140}Gd$\rightarrow$ ^{140}Eu$\rightarrow^{140}$Sm decays. The ^{140}Eu and ^{140}Gd nuclei were produced in the ^{104}Pd+^{40}Ar reaction at a beam energy of 187 MeV. The beam was provided by the U-200P cyclotron of the Heavy Ion Laboratory. The EAGLE array with twelve HPGe detectors was used to register the γ-rays. More information about the experiment can be found in Ref. [5].

The γ-γ angular correlations of the 531 keV and 460 keV photons and 531 keV and 1068 keV photons (see Figs. 1and 2) gave the same results as our previous experiment [2], i.e. $I = 2^+$ and 0^+ for the 990 and 1599 keV levels respectively.

For the spin assignment of the 1629 keV level the angular correlation between the 531 keV and 1098 keV photons was measured. The angular correlation coefficients are equal to $A_{22} = 0.25(17)$ and $A_{44} = 1.12(25)$ (open red circle in Fig. 2) and imply that the

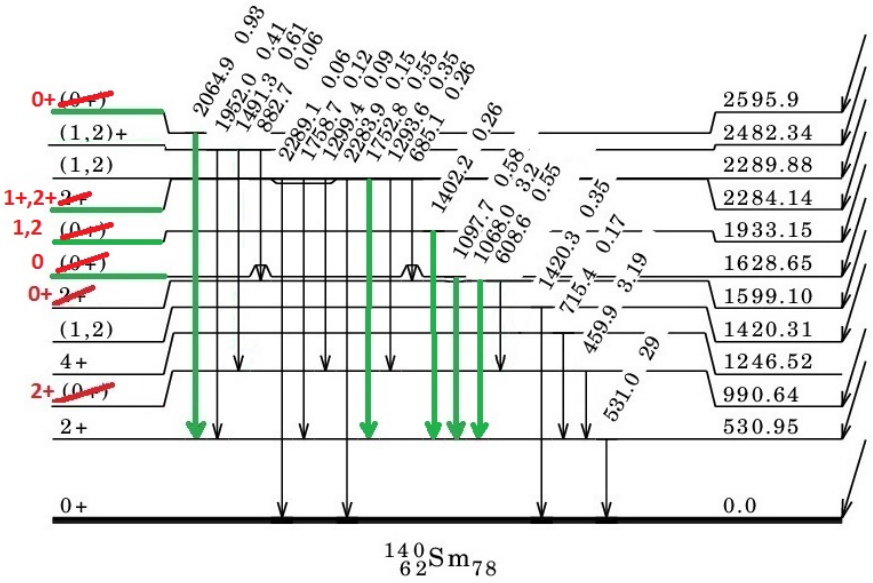


Figure 1: Relevant partial level scheme of ^{140}Sm taken from Refs [2,6,7] and our present results. The spin values marked in red were determined in our measurements. Green arrows and green lines indicate transitions and levels studied in this work.

1629 keV level has spin equal to 0. The parity of this state could not be determined from our data.

The spin of the 1933 keV level was determined by studying angular correlations between the 531 keV and 1402 keV photons. The angular correlation coefficients are equal to $A_{22} = -0.08(16)$ and $A_{44} = -0.14(22)$ (filled red diamond in Fig. 2). Such values of the A_{kk} coefficients clearly show (see Fig. 2) that the spin of the discussed level is not equal to 0 as suggested in Refs [6,7] but equals 1, 2, 3 or 4. The value of log $ft = 6.28$ [7] for population of the 1933 keV level suggests spin $I = 1$ or 2. For $I = 1$ and $I = 2$ the mixing ratios are $\delta = 0.16^{+0.17}_{-0.12}$ (4% quadrupole and 96% dipole transition) and $\delta = 0.39^{+0.23}_{-0.23}$ (13% quadrupole and 87% dipole transition) respectively. The parity of this state was not uniquely determined.

The angular correlation of the 530 keV and 1753 keV photons was used to determine the 2284 keV level spin. The resulting values of the angular correlation coefficients are: $A_{22} = -0.09(12)$ and $A_{44} = -0.06(15)$ (filled red circle in Fig. 2). These values suggest $I = 1$, 2, 3 or 4. The value of log $ft = 5.46$ [7] allows two solutions, namely $I = 1$ or $I = 2$ with parity $\pi = +1$. If the spin value $I = 1$ then the mixing ratio is equal to $\delta = -0.14^{+0.09}_{-0.09}$. This means that the 1753 keV transition is almost pure M1 (98%) with a small (2%) admixture of E2 radiation. If the spin value is $I = 2$ then the mixing ratio equals $\delta = 0.47^{+0.21}_{-0.18}$ which corresponds to a mixture of M1 (82%) with E2 (18%).

For the spin assignment of the 2596 keV level the angular correlation of the 531 keV and 2065 keV photons was measured. As a result we obtained $A_{22} = 0.34(12)$ and $A_{44} = 1.16(20)$ (open red diamond in Fig. 2). This clearly shows that the spin of the 2596 keV level is 0. The parity π=+1 of this state follows from the log ft value of 5.49.

The angular correlation of the 531 keV ($2^+_1 \rightarrow 0^+_1$) photon with the other photons was discussed above. Further analyses with e.g. the 460 keV ($2^+_2 \rightarrow 2^+_1$) photon are in progress.

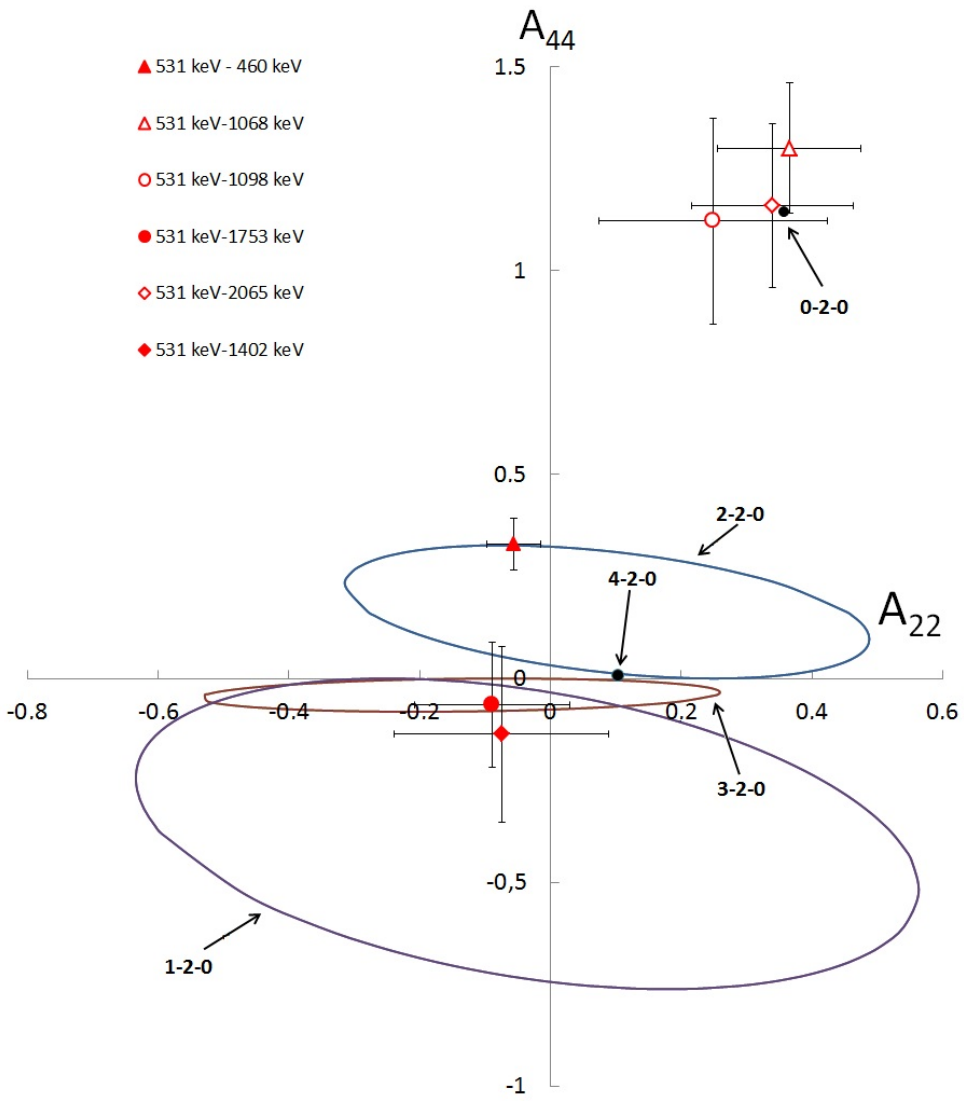


Figure 2: Parametric plot of the $A_{22}(\delta)$ and $A_{44}(\delta)$ angular correlation coefficients for the $I \rightarrow 2 \rightarrow 0$ cascades (for initial spins $I = 0,\ 1,\ 2,\ 3,\ 4$). The experimental results are compared with the theoretical predictions. Filled black circles denote the A_{kk} angular correlation coefficients for pure quadrupole transitions.

Bibliography

[1] M. Klintefjord *et al.*, Acta Phys. Pol. **B46** (2015) 207

[2] J. Samorajczyk *et al.*, Phys. Rev. **C92** (2015) 044322

[3] M. Klintefjord *et al.*, Phys. Rev. **C93** (2016) 024317

[4] F. L. Bello Garrote *et al.*, Phys. Rev. **C92** (2015) 024317

[5] J. Samorajczyk-Pyśk *et al.*, HIL Annual Report **2015**, page 55

[6] R. B. Firestone *et al.*, Phys. Rev. **C43** (1991) 1066

[7] N. Nica, Nucl. Data Sheets **108** (2007) 1287

C.2 First measurement of the g-factor in the chiral band: the case of the ^{128}Cs isomeric state

E. Grodner[1,2], J. Srebrny[3], Ch. Droste[2], L. Próchniak[3], S.G. Rohoziński[2], M. Kowalczyk[3], M. Ionescu-Bujor[4], C. A. Ur[5], M. Kisieliński[3], T. Marchlewski[3], S. Aydin[5,6], F. Recchia[5], G. Georgiev[7], R. Lozeva[7], E. Fiori[7]

1) National Centre for Nuclear Research, Świerk, Poland
2) Faculty of Physics, University of Warsaw, Warszawa, Poland
3) Heavy Ion Laboratory, University of Warsaw, Warszawa, Poland
4) Horia Hulubei National Institute of Physics and Nuclear Engineering, Bucharest, Romania
5) Extreme Light Infrastructure, IFIN-HH, Bucharest, Romania
6) INFN Sezione di Padova, Padova, Italy
7) Aksaray University, Aksaray, Turkey
8) Institut de Physique Nucléaire, Orsay, France

The odd-odd ^{128}Cs isotope is considered as the best example of the manifestation of nuclear chirality thanks to the characteristic patterns of the electromagnetic transitions in the partner bands built on the 56 ns isomeric state [1]. To study in more detail the relative orientation of the angular momentum vectors of unpaired nucleons and the core we performed a measurement of the g-factor of the bandhead of the chiral band, the 56 ns isomeric state. We applied the Time-Differential Perturbed Angular Distribution method (TDPAD) where the interaction between the nuclear magnetic moment and an applied external magnetic field results in a precession of the angular distribution of the γ radiation around the applied magnetic field axis. Thus, an oscillating intensity from the decay of the isomeric state is observed. The sign and magnitude of the g-factor can be extracted from the intensity ratio of two measurements at angles $\theta = \pm 45^\circ$

$$R(t) = \frac{I(-45^\circ, t) - I(+45^\circ, t)}{I(-45^\circ, t) + I(+45^\circ, t)} = \frac{3A_2 \sin(\phi - 2\omega_L t)}{4 + A_2} \qquad (1)$$

with A_2 being the effective angular distribution coefficient and ϕ being a phase depending on the detector position angle and the beam bending in the magnetic field. The factor $\omega_L = gB\mu_N/\hbar$ denotes the Larmor frequency of precession of the angular distribution around the magnetic field axis where μ_N is the nuclear magneton and g the nuclear g-factor of the isomeric state that has to be determined. The ^{128}Cs nucleus was produced in the ^{122}Sn(^{10}B, 4n)^{128}Cs reaction with a beam energy of 55 MeV. A pulsed beam with 1 ns pulses and 400 ns repetition period was provided by the Tandem accelerator of the ALTO facility at IPN Orsay. A self supporting ^{122}Sn target, 22 mg/cm^2 thick, played simultaneously the role of the stopper for the recoils. The target was placed between the pole tips of an electromagnet (in the GAMIPE set-up from LNL Legnaro). A magnetic field of 21450$\pm$10 gauss was applied perpendicular to the beam-detection plane. Two Low-Energy Photon Spectrometer (LEPS) detectors were placed at angles $\pm 45^\circ$ with respect to the beam axis. In total around 10^{10} gamma quanta have been registered during 5 days of the beam-time.

In the Warsaw-Orsay-Legnaro collaboration experiment a modulated intensity was observed for gamma transitions in accordance with the level scheme of the isomeric state decay reconstructed in Ref. [2], see also Ref. [4]. However, due to possible unobserved highly converted transitions below the 64-keV gamma decay, spin assignment is still uncertain. In the following discussion a $I^\pi = 9^+$ spin value of the isomeric state is taken

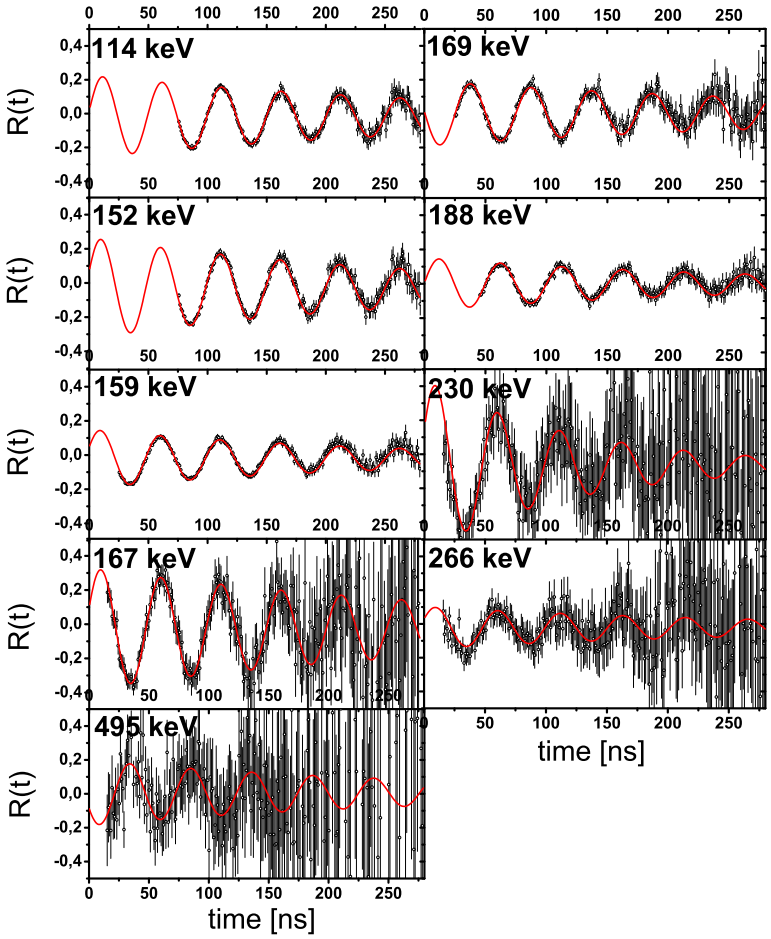


Figure 1: Experimental modulation ratios for the transitions involved in the isomeric decay and least-squares fits (solid red lines).

according to the excitation energy systematics [3] and not $I^\pi = 7^+$ as in [4]. The background subtracted time spectra collected at angles $+45°$ and $-45°$ were used to construct the intensity ratios for transitions from the decay of the isomeric state, see Fig. 1. An attenuation of the $R(t)$ oscillations has been taken into account by time dependence of the $A_2(t) = A_2 \cdot \exp(-\lambda_2 t)$ distribution coefficients reflecting the spin-deorientation process. An average value of $1/\lambda_2 \approx 300$ ns has been determined. According to Ref. [2] the transitions below the isomeric state are fast enough to preserve the original gamma angular distribution of the preceding states. Therefore, in all transitions the same oscillation frequency is observed. Fitted parameters of formula (1), see Fig. 1, give the value $g = +0.59(1)$ of the g-factor of the $\pi h_{11/2} \otimes \nu h^{-1}_{11/2}$ isomeric bandhead.

Bibliography

[1] E. Grodner *et al.*, Phys. Rev. Lett. **97** (2006) 172501

[2] E. Grodner *et al.*, to be published

[3] Y. Liu, J. Lu, Y. Ma, S. Zhou, and H. Zheng, Phys. Rev. **C54** (1996) 719

[4] E. Grodner, M. Kowalczyk and J. Srebrny, HIL Annual Report 2015, page 53

C.3 Study of the low lying states of ^{136}Nd

A. Tucholski[1], J. Srebrny[1], Ch. Droste[1], M. Fila[2], C. Petrache[3], A. Astier[3], B. Lv[3], E. Dupont[3], S. Lalkovski[4,5], E. Grodner[6], T. Marchlewski[1], L. Próchniak[1], P.J. Napiorkowski[1], T. Abraham[1], A. Stolarz[1], J. Samorajczyk[1], M. Kisieliński[1], M. Kowalczyk[1], G. Saworska[2], J. Kownacki[1], A. Kordjasz[1]

1) Heavy Ion Laboratory, University of Warsaw, Warszawa, Poland
2) Faculty of Physics, University of Warsaw, Warszawa, Poland
3) CSNSM, CNRS-IN2P3 and Université Paris-Sud, Orsay, France
4) Sofia University "St. Kliment Ohridski", Sofia, Bulgaria
6) National Centre for Nuclear Research

Measurements of the lifetimes of the low lying excited states of ^{136}Nd using the ^{120}Sn $(^{20}\mathrm{Ne}, 4\mathrm{n})^{136}$Nd reaction were performed at cyclotron at the Heavy Ion Laboratory, of the University of Warsaw. The EAGLE facility was used together with the new plunger device centred in the EAGLE array, Fig. 1.

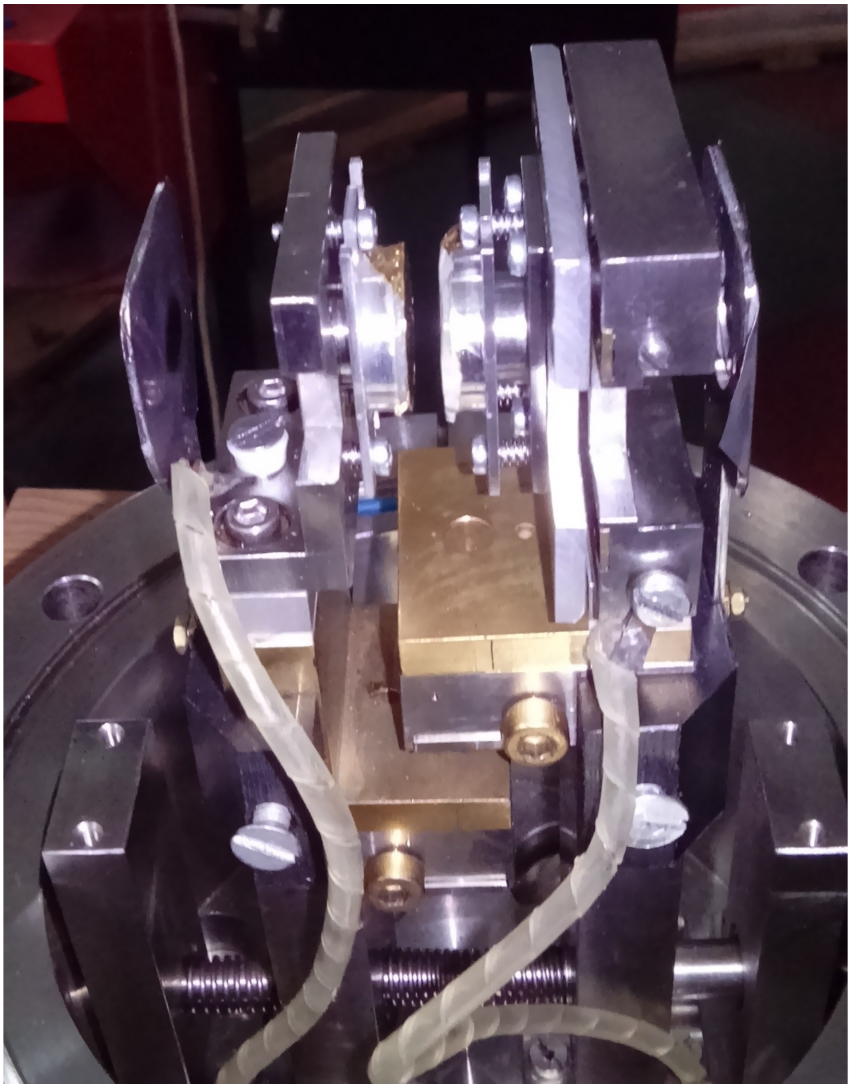


Figure 1: The PLUNGER device.

Two calibration curves of the plunger device can be seen in Fig. 2 and 3. The first figure shows the capacity measured in picofarads over a large range of distances between the target and the stopper and in Fig. 3 a precise measure of the offset is shown (1/C versus distances). The array of 16 Ge detectors was placed mainly in the front half of EAGLE to cover the range 0 to 90°. Three detectors were also placed at 143° to cover backward angles in the case of ambiguity of overlapping $\gamma - ray$ lines.

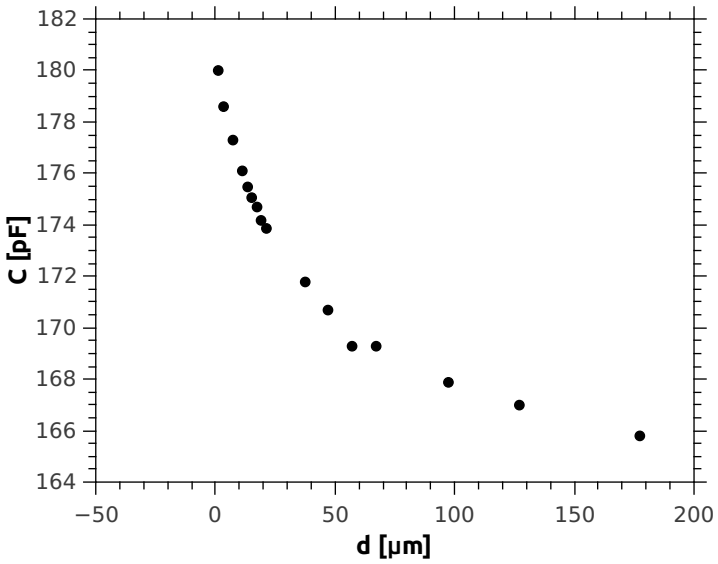


Figure 2: Calibration curve C versus target to stopper distance.

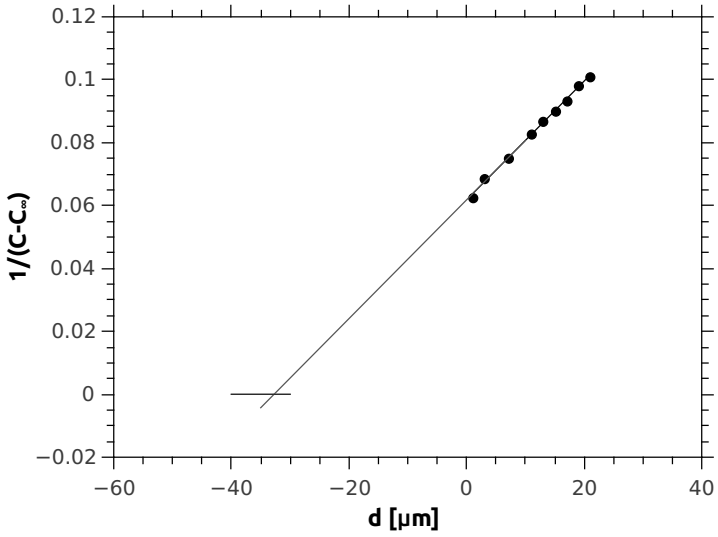


Figure 3: Calibration curve after the experiment 1/C versus distance.

In Fig. 4 one can see a typica of the energy spectrum for the smallest distance between the target and the stopper. Altogether we performed measurements for 13 distances starting from 74 µm up to 5 mm which allowed lifetime measurements from picoseconds to nanoseconds. This means that we were able to recognise and measure isomers with lifetimes not exceeding a couple of nanoseconds. We could theoretically go to more than

1 cm distance between the target and the stopper but then the efficiency loss due to geometrical reasons would be large and special corrections would have to be applied to the efficiency and also to the angular measurements and their precision.

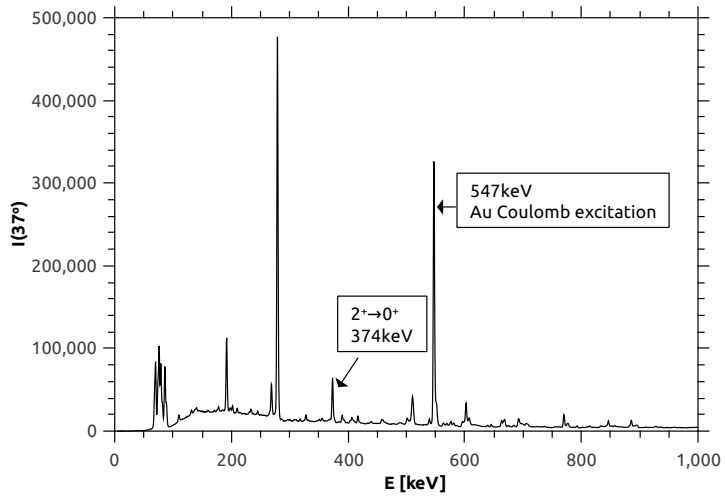


Figure 4: Energy spectrum for the smallest distance between target and stopper.

The first results were lifetime measurements of the 2^+ and 12^+ states of the yrast band. The 12^+ state was already measured in Ref. [1], and the 2^+ state by [2], so we could compare these measurements with our results. In Fig. 5 one can see the lifetime of the 2^+ state of the yrast band and in Fig. 6 the lifetime of the 12^+ state.

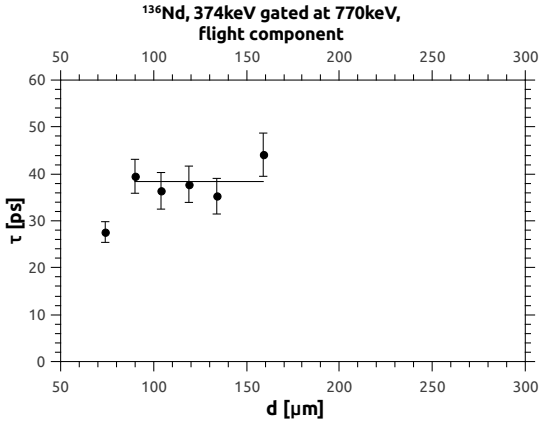


Figure 5: Lifetime of the 2^+ state in ^{136}Nd, $\tau = 38.4(15)$ ps.

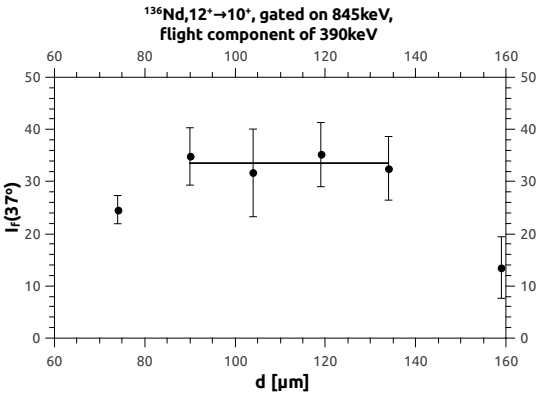


Figure 6: Lifetime of the 12^+ state in ^{136}Na, $\tau = 29.3(3.4)$.

Bibliography

[1] J. Billowes *et al.*, Phys. Rev. **C36** (1987) 974

[2] T.R. Saito *et al.*, Phys. Lett. **B669** (2008) 19

C.4 Attempt to assign the delayed γ rays to the respective masses of fission fragments produced in the ^{16}O + ^{208}Pb induced fission reaction

T. Abraham[1], J. Andrzejewski[2], W. Czarnacki[3], Ch. Droste[4], Ł. Janiak[2], M. Kisieliński[1], A. Kordyasz[1], A. Korman[3], M. Kowalczyk[1], J. Kownacki[1], M. Moszyński[3], P. Napiorkowski[1], M. Palacz[1], J. Perkowski[2], P. Sibczyński[3], J. Srebrny[1], A. Stolarz[1], T. Szczęśniak[3], M. Wolińska-Cichocka[1], D. Wolski[3]

1) Heavy Ion Laboratory, University of Warsaw, Warszawa, Poland
2) Faculty of Physics and Applied Computer Science, University of Lodz, Łódź, Poland
3) National Centre for Nuclear Research, Świerk, Poland
4) Faculty of Physics, University of Warsaw, Warszawa, Poland

The fission products of the ^{16}O (85 and 90 MeV) + ^{208}Pb reaction were studied in order to establish the properties of the excited states especially associated with isomeric behaviour. The detector arrays equipped with 12–16 Compton suppressed HPGe detectors, located at the Heavy Ion Laboratory of the University of Warsaw were employed (Osiris-II & Eagle).

The region of the neutron rich nuclei with $A \approx 80$–130 is often expected to possess isomerism due to the simultaneous existence of high and low j-orbitals in the low energy structure, i.e. $2p_{1/2}$, $1g_{9/2}$ for protons and $1g_{7/2}$, $3s_{1/2}$, $2d_{3/2}$, $1h_{11/2}$ for neutrons. The collective nuclear structure aspects also favour isomerism in this region [1].

Fig. 1 displays an example of the low energy part of the γ-γ coincidence spectra measured at the beginning and at the end of the beam-off period showing the existence of isomers in the time region of several tens of μsec. Inspecting Fig. 1 one can see many delayed γ rays (shown in red), however many of them are not assigned as yet to any of particular fragment mass.

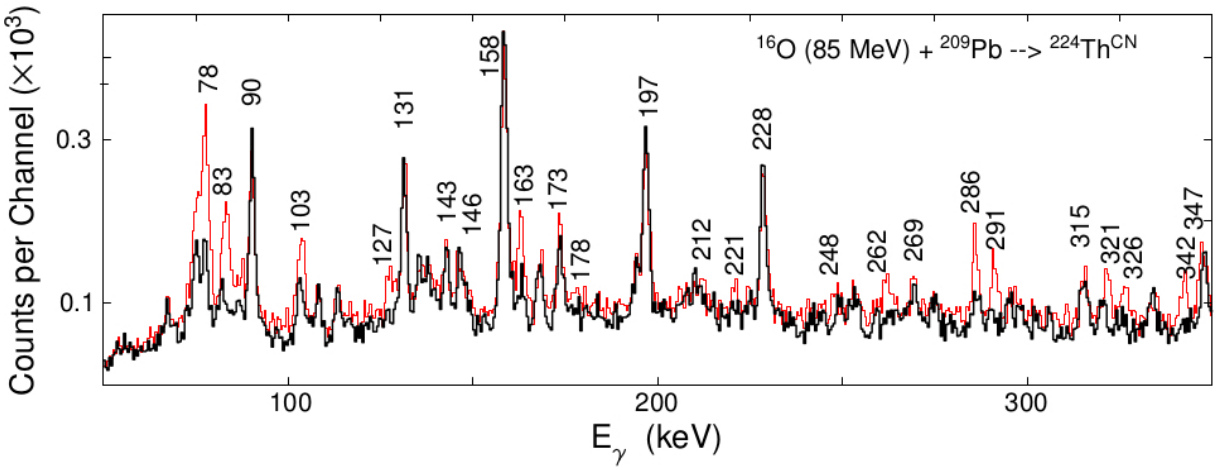


Figure 1: Example of partial two γ-ray spectra collected for a time of 300 µsec at the beginning (red line) and at the end (black line), 3.5 ms later, of the beam-off period respectively. The red lines are possible candidates to be connected to isomeric decays.

The main aim of the present investigation is to identify unknown isomers in the region of neutron-rich nuclei. Table 1 gives a few of the γ-ray lines shown in Fig. 1 γ-lines with half-lives estimated in the present experiments.

Table 1: A few examples of γ-rays suspected as being connected to isomeric decays.

E_γ (keV)	$T_{1/2}$ (µsec)	Comments
78	73.5 ± 1.5	complex line
82	79.4 ± 2.2	
248	42.4 ± 5.0	in coincidence with 291 keV
261	104.3 ± 2.5	^{125}Cd or ^{103}Tc ?
269	63.3 ± 1.2	^{106}Ru ?
286	89.5 ± 2.2	perhaps ^{121}Sb
291	33.0 ± 2.0	in coincidence with 248 keV
342	112.4 ± 1.5	perhaps ^{206}Pb

An identification of fission fragment (FF) masses and energies has been and still is a major concern in spectroscopy of FF research. There are several known studies concerning the mass resolution like [2] where a mass of less then 1 amu for fission fragments is achievable, the other example is Ref. [3] (and the list of references therein), which shows the determination of FF masses by measuring velocities and kinetic energies using specially adapted TOF detectors (Si barrier detectors). The pulse-shape technique with reversed n-type Si detectors for discrimination of protons and alphas produced in fusion-evaporation reactions was tested at the VICKSI cyclotron in Berlin [4].

The authors apply a zero-crossing technique which does not need any external time reference. A consequence of the rear-side injection mode is a strong variation of the charge-collection time with energy, charge, and mass number of the detected ion in case of reversed n-type Si-detectors, and is advantageous for optimum particle discrimination.

Concerning the present work, successful trials to obtain spectra (counts vs. zero crossing time (ns) with a ^{252}Cf source (Fig. 2) using a reversed n-type Si detector as a preparation for the planned in-beam experiment were already performed using NCBJ facilities.

Further experiments with a ^{252}Cf source and in-beam at HIL with the above mentioned reaction (^{16}O+^{208}Pb), with the aim of identifying FF masses are in progress. A comparison of pulse-shape technique based on reversed n-type Si detectors with classical TOF and energy measurements is also being considered.

Bibliography

[1] J. Ăystö *et al.*, Preprint JYFL 18/1989, University of Jyväskylä, Department of Physics, Finland

[2] A. Oed *et al.*, Nucl. Inst. and Meth. **219** (1984) 569

[3] C. Guet, M. Asghar, P. Perrin, C. Signarbieux, Nucl. Inst. and Meth. **150** (1978) 189

[4] G. Pausch *et al.*, Nucl. Inst. and Meth. **365** (1995) 176

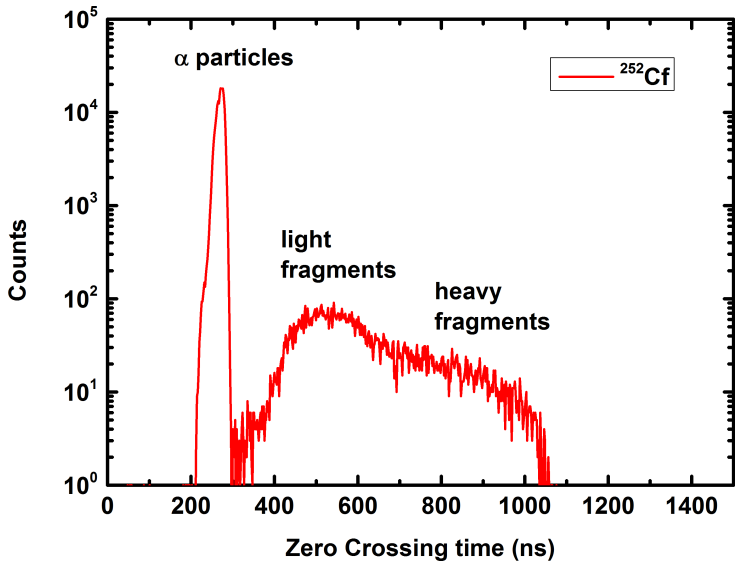


Figure 2: Test of the zero-crossing technique with a reversed n-type Si detector using a ^{252}Cf source, allowing fission fragment discrimination. The start signal of the TAC is the zero position, while in the next channels the stop signals from the TAC give the zero-crossing time.

C.5 The barrier height distributions of the ^{24}Mg + ^{90,92}Zr systems

E. Piasecki[1], A. Trzcińska[1], M. Kowalczyk[1], L. Acosta[2,3], L. Auditore[4], G. Cardella[2], E. De Filippo[2], D. Dell'Aquila[5], S. De Luca[4], L. Francalanza[5], B. Gnoffo[2], G. Lanzalone[6,5], I. Lombardo[7], C. Maiolino[6], N. Martorana[6], S. Norella[4], A. Pagano[2]

1) Heavy Ion Laboratory, University of Warsaw, Warszawa, Poland
2) INFN Sezione di Catania, Catania, Italy
3) Instituto de Física, Universidad Nacional Autónoma de México, Mexico
4) INFN Gr. Coll. Messina and Dip. di fisica Università Messina, Italy
5) Kore University of Enna, Enna, Italy
6) INFN Laboratori Nazionali del Sud, Catania, Italy
7) Università di Napoli Federico II, and INFN Sezione di Napoli, Napoli, Italy

For many systems the fusion cross section at sub-barrier energies is strongly enhanced in comparison with the simple model of the Coulomb barrier transmission. Within the framework of the Coupled Channels (CC) method this enhancement can be understood as a result of coupling of the relative motion of the two nuclei to their collective excitations, connected with their static or dynamic deformations. As a result, the single static interaction barrier is replaced by many barriers: a barrier height distribution is generated [1, 2]. It has been shown both theoretically and experimentally that the barrier distribution can be determined by (difficult) fusion measurements, but also by (much simpler) quasielastic (qe) scattering measurements at backward angles, giving rise to the barrier distribution D_{qe}. The latter method consists in determining the excitation function the quasielastic scattering at large angles, this being the sum of the elastic, inelastic and transfer cross sections, with no need to identify individually the particular channels involved.

According to calculations performed using the CC method, the ^{20}Ne projectile, incident on any medium or heavy nucleus, should give rise to a structured (i.e. possessing more than one maximum) barrier distribution, giving a fingerprint of the couplings involved. We have determined the Dqe distributions for many targets (from Ni to Pb) and noted that while for the ^{58,60}Ni and ^{90}Zr ones the distributions (in agreement with the CC predictions) are indeed structured, for other, apparently very similar systems, the measurements yielded smooth distributions, in strong disagreement with theory [3–6]. This disagreement does not depend on the Optical Model parameters used and the approach did not involve any parameter fitting.

To explain the effect, we put forward the hypothesis that the smoothing is caused by the influence of weak, but numerous, non-collective excitations of the system.

Up to now the only feasible approach for treating the problem is including statistical methods in Quantum Mechanics by utilising the very general Random Matrix Model (RMT). The model was applied to our experimental data and the results [7] demonstrated that coupling to the many non-collective levels in ^{92}Zr visibly smoothed the barrier distribution, while not that ^{90}Zr was almost unchanged by a similar procedure.

In order to progress our understanding of the phenomenon, we decided to change the projectile to ^{24}Mg, which in some respects is similar to ^{20}Ne: it is also strongly clustered (consisting not of 5, but 6 α particles) and is also strongly deformed. Thus the aim of the experiment was to accomplish a more stringent test of theoretical predictions by measurements of the quasielastic barrier distributions for the ^{24}Mg + ^{90,92}Zr systems.

Using the tandem beam of the LNS, Catania and a large number of the Chimera [8] silicon detectors enabled us to perform a more precise determination of barrier distribution in comparison with our previous ones.

The experiment consisted of measurement of the energy of backscattered ions by an array of semiconductor detectors. Different angles (rings) in the Θ_{lab} range from 122° to 170°, correspond to different "effective energies" (E_{eff}), taking into account the angle dependent centrifugal energy. In total 150 detectors were used. Four forward detectors (at an average angle of 34°) were used to measure the Ruthorford scattering and to monitor the beam energy and asymmetry on the target. The energy calibration was be performed using α sources and a precise pulse generator. The ^{24}Mg beam of the intensity of about 2 pnA bombarded the 100μg/cm^2 ^{90,92}Zr targets placed in the CHIMERA multidetector system. The beam energy was changed in steps of about 0.5 MeV over the range of 65–90 MeV.

Sample preliminary results are given in Fig. 1. It is seen that the distribution structure observed for the ^{90}Zr target is smoothed out in the case of ^{92}Zr. Due to the good energy resolution of the tandem beam the effect is even more clearly seen than in the case of the ^{20}Ne projectile. Further data analysis and theoretical calculations are in progress.

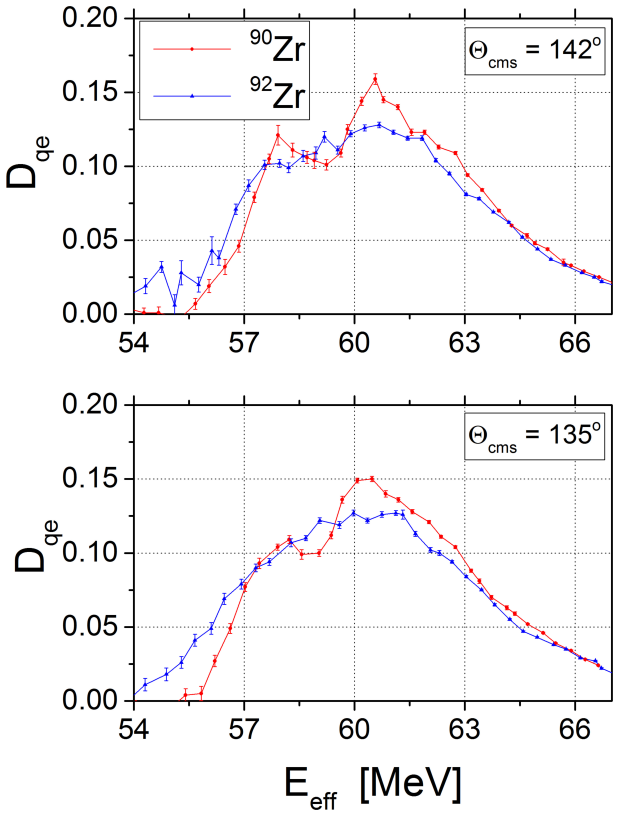


Figure 1: Comparison of the barrier height distributions for the ^{24}Mg + ^{90,92}Zrsystems for two scattering angles (preliminary results).

Bibliography

[1] M. Dasgupta, D.J. Hinde, N. Rowley, and A.M. Stefanini, Ann. Rev. Nucl. Part. Sci. **48** (1998) 401

[2] B. Back, H. Esbensen, C. Jiang and K. E. Rehm, Rev. Mod. Phys. **86** (2014) 317

[3] E. Piasecki *et al.*, Phys. Rev. **C80** (2009) 054613

[4] E. Piasecki *et al.*, Phys. Rev. **C85** (2012) 054604

[5] E. Piasecki *et al.*, Phys. Rev. **C85** (2012) 054608

[6] A. Trzcińska *et al.*, Phys. Rev. **C92** (2015) 034619

[7] S. Yusa, K. Hagino, and N. Rowley, Phys. Rev. **C88** (2013) 054621

[8] A. Pagano, Nucl. Phys. News **22** (2012) 25

C.6 Influence of non-collective excitations on barrier distributions

E. Piasecki[1], A. Trzcińska[1], M. Kowalczyk[1], S. Yusa[2]

1) Heavy Ion Laboratory, University of Warsaw, Warszawa, Poland
2) Faculty of Physics, Tohoku University, Japan

It is known that there is a connection between the reaction mechanism and the internal degrees of freedom of the interacting nuclei. This can manifest itself as a strong enhancement of the fusion cross section at sub-barrier energies in comparison with the simple model of Coulomb barrier transmission. Within the framework of the Coupled Channels (CC) method, this can be understood as a result of the interplay between various reaction channels. The coupling of the relative motion of two nuclei to their collective (rotational and/or vibrational) excitations, connected with the static or dynamic deformations, is particularly important. As a result of the couplings the single interaction barrier is replaced by many barriers: a barrier height distribution is generated [1, 2]. Part of this distribution, corresponding to the heights below the mean barrier value, is responsible for the fusion cross section enhancement, sometimes by many orders of magnitude. In some cases the distribution turns out to be markedly structured giving a fingerprint of the couplings involved.

It has been shown both theoretically and experimentally that the barrier height distribution D_{qe} can be experimentally determined by quasielastic (qe) scattering measurements at backward angles [1, 2].

A few years ago we noticed a quite unexpected effect: a strong difference between the shapes of the barrier distributions for the ^{20}Ne + ^{90,92}Zr systems. Namely, for the ^{90}Zr target D_{qe} is structured, in fair agreement with the CC predictions, while for ^{92}Zr the distribution is smooth, although according to calculations, due to the dominant effect of the large ^{20}Ne deformation, it should have the same (structured) shape [3]. The natural hypothesis was that the smoothing is due to coupling to transfer channels, which for these systems is up to now impossible to calculate in a proper way. However, measurements [3] have shown that the total transfer probability for these 2 targets is almost the same, thus in this case the transfer is probably not responsible for the barrier distribution smoothing observed for the ^{20}Ne + ^{92}Zr system.

Our present hypothesis is that the D_{qe} for this target is smoothed by kinetic energy dissipation, i.e. scattering into a large number of weak (non-collective) excitations. This is due to the fact that, in contrast to ^{90}Zr with a magic number of neutrons, ^{92}Zr has much higher non-collective level density due to the 2 additional neutrons. This hypothesis seems to be confirmed by our experimental studies of barrier distributions for the ^{20}Ne + ^{58,60,61}Ni [4, 5] and ^{24}Mg + ^{90,92}Zr [6] systems.

On the theoretical side the situation is difficult, as up to now the role of the weak channels (transfers and non-collective excitations) is unclear, because their inclusion in the CC scheme is usually difficult or impossible owing to their large number and the complexity of the couplings involved. However, the authors of Ref. [7] quite recently proposed an approach which consists of merging Statistical Physics with Quantum Mechanics by extending the CC method using the very general Random Matrix Theory (RMT). The method was applied to the ^{20}Ne + ^{90,92}Zr systems [7], and it was demonstrated that cou-

pling to the many non-collective levels in the ^{20}Ne + ^{92}Zr system visibly smoothes the barrier distribution.

We utilised the code developed by these authors modifying it to some extent. The most important modification consists in replacing the experimental excitation energy dependence of the target level density by a theoretical one, calculated using the Hartree-Fock-Bogolubov method [8]. The reason was the unavoidable overlapping of energy levels for higher energies, giving rise to missing anever increasing part of them (caused by the experimental resolution)

In our CC+RMT calculations we did not fit any parameters (such as Optical Model potentials and deformations), taking them from available external sources. The calculations were computationally very demanding, as in addition to 5–7 collective levels we took into account 150 non-collective ones. To handle the problem we performed parallel calculations on 50 nodes using the PL-GRID Infrastructure.

An example of a comparison of the experimental and calculated barrier distributions for the ^{20}Ne + ^{58,60,61}Ni systems is shown in Fig. 1.

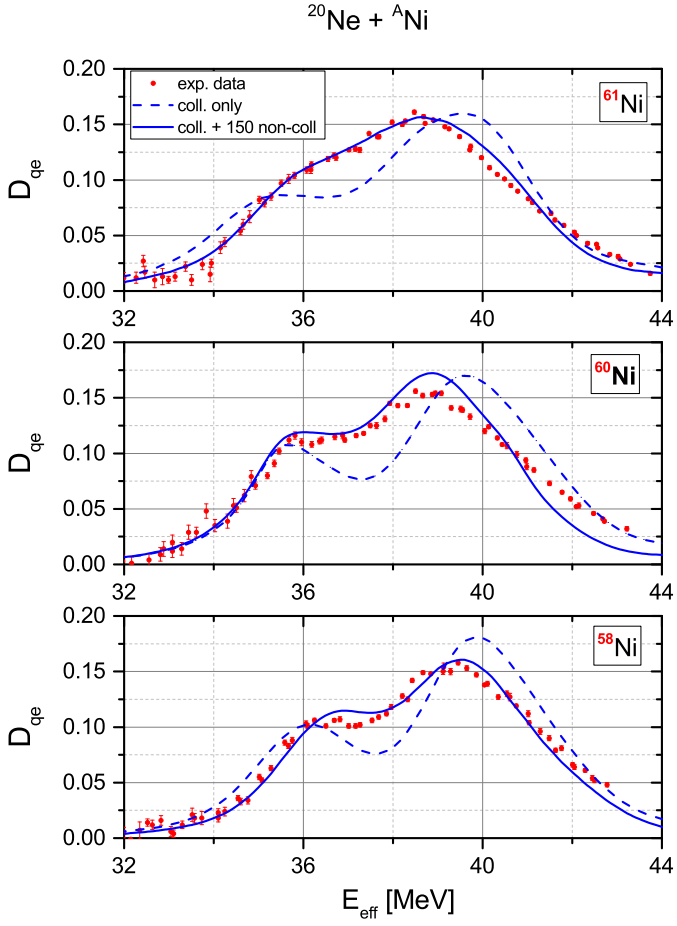


Figure 1: Comparison of experimental and calculated barrier height distributions for the ^{20}Ne + ^{58,60,61}Ni systems. The dashed lines are the results of conventional CC calculations, taking into account collective excitations of projectile and target only. The solid lines denote the result of including 150 non-collective excitations. In both cases the experimental resolution (similar for all targets) was taken into account. No normalisation of the calculated distributions was applied.

The conclusion is that the applied model confirms the strong influence of coupling to the non-collective excitations on the barrier distributions observed in ref. [7], smoothing the distribution for targets of high level density.

Acknowledgements: We wish to thank Kouichi Hagino for many valuable suggestions. This research was supported by the PL-GRID Infrastructure.

Bibliography

[1] M. Dasgupta, D. J. Hinde, N. Rowley, and A. M. Stefanini, Ann. Rev. Nucl. Part. Sci. **48** (1998) 401

[2] B. Back, H. Esbensen, C. Jiang and K. E. Rehm, Rev. Mod. Phys. 86, 317 (2014)

[3] E. Piasecki *et al.*, Phys. Rev. **C80** (2009) 054613

[4] A. Trzcińska *et al.*, Phys. Rev. **C92** (2015) 034619

[5] A. Trzcińska *et al.*, Phys. Rev. **C93** (2016) 054604

[6] A. Trzcińska, to be published

[7] S. Yusa, K. Hagino, and N. Rowley, Phys. Rev. **C88** (2013) 054621

[8] S. Goriely, `http://www-nds.iaea.org/RIPL-3` and `http://www.talys.eu/`

C.7 Coulomb excitation of ^{45}Sc

M. Matejska-Minda[1], P.J. Napiorkowski[1], T. Abraham[1], P. Bednarczyk[2], A. Bezbakh[7], D. Doherty[10], K. Hadyńska-Klęk[3], J. Iwanicki[1], G. Kamiński[7], M. Kisieliński[1], M. Komorowska[1], M. Kowalczyk[1], R. Kumar[9], A. Maj[2], T. Marchlewski[1], P. Matuszczak[1], V. Nanal[6], A. Nannini[5], M. Palacz[1],L. Próchniak[1], M. Rocchini[5,11], M. Saxena[1], M. Siciliano[3,4], J. Srebrny[1], A. Stolarz[1], J. Styczeń[2], B. Wasilewska[2], K. Wrzosek-Lipska[1], M. Zielińska[8]

1) Heavy Ion Laboratory, University of Warsaw, Warszawa, Poland
2) The H. Niewodniczański Institute of Nuclear Physics, Kraków, Poland
3) INFN, Laboratori Nationali di Legnaro, Legnaro, Italy
4) Università degli Studi di Padova, Padova, Italy
5) INFN Sezione di Firenze, Firenze, Italy
6) TIFR, Mumbai, India
7) Joint Institute for Nuclear Research, Dubna, Russia
8) IRFU/SPhN, CEA Saclay, Gif-sur-Yvette, France
9) Inter University Accelerator Centre, New Delhi, India
10) Department of Physics, University of Surrey, Guildford, UK
11) Università degli Studi di Firenze, Dipartimento di Fisica e Astronomia, Firenze, Italy

The medium-light ^{45}Sc nucleus, situated in the nuclear chart above the doubly-magic ^{40}Ca, has an additional 1 proton and 4 neutrons beyond the $Z = N = 20$ shell closure. The number of active particles and the $p_{3/2}f_{7/2}$ configuration space are big enough to allow for collective motion of nucleons. The negative-parity states built on the $7/2^-$ ground state exhibit a spherical structure, while a well deformed rotational-like band is formed upon the $I^\pi = 3/2^+$ intruder level at 12.4 keV [1–4]. Our attention is addressed to the positive parity band built on the low-lying, $T_{1/2} = 318$ ms isomeric state at an energy of 12.4 keV and spin of $3/2^+$.

The Coulomb excitation measurement of ^{45}Sc was performed in November 2016 using a 70 MeV ^{32}S beam from the U-200P cyclotron at the Heavy Ion Laboratory. The ^{32}S beam particles were scattered from a 1 mg/cm^2 ^{45}Sc target. The γ rays depopulating Coulomb excited states in ^{45}Sc were detected by the EAGLE array [5] in coincidence with forward scattered ions. In the present experiment, the EAGLE γ-ray spectrometer was composed of 16 Compton-suppressed HPGe detectors, and the total photo-peak efficiency was 0.9% at 1112 keV. A compact scattering chamber [6], equipped with 48 0.5×0.5 cm^2 PIN-diodes, was used for the detection of the forward scattered particles. The PIN-diode detectors were placed at angles from 49 to 69 degrees in the laboratory frame, with respect to the beam direction. This particle detection array was set at forward angles for the very first time. Detectors were exposed to radiation damage, so only 16 hours of data taking was possible. Nevertheless, the 364, 377, 720 and 1237 keV γ-ray lines from ^{45}Sc were clearly observed.

In the second part of the measurement, a thick (15 mg/cm^2) ^{45}Sc target was mounted and only γ-ray single spectra were collected. The γ-ray energy spectrum summed over 16 HPGe detectors is shown in Fig. 1. Several lines from the Coulomb excited ^{45}Sc nuclei are marked, as well as the most intense γ-ray lines originating from the reaction products on the target oxidation. In the 70 MeV ^{32}S+^{16}O fusion-evaporation reaction the ^{46}Ti, ^{46}V, ^{43}Sc isotopes were produced. With a very small cross section (well below 1 mb) the isotope of interest, ^{45}Sc, could also be produced, hence the registered intensities of

the ^{45}Sc γ-ray lines might not originate exclusively from the Coulomb excitation process. When the observed intensities of the ^{45}Sc γ-ray lines are compared to the population of the ^{46}Ti states (being the most intense fusion-evaporation reaction product) and taking into account the calculated cross sections, the upper limit for the number of counts not derived from the Coulomb excitation of ^{45}Sc can be obtained. In this measurement up to 5% of the registered γ-ray line intensity in ^{45}Sc may originate from the fusion-evaporation reaction. This experimental uncertainty will be included in the further analysis of the data.

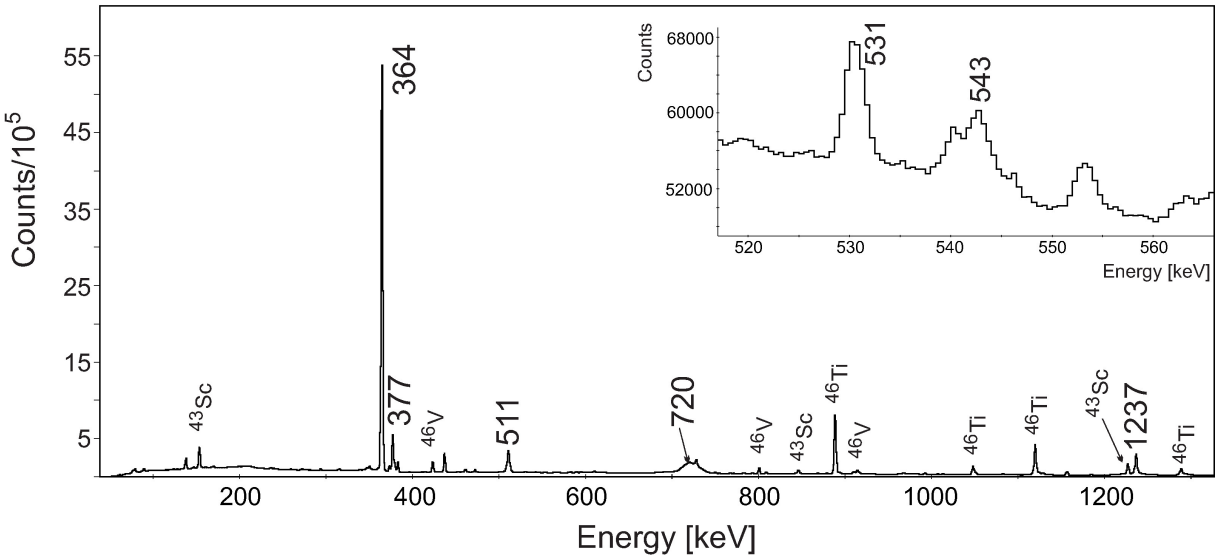


Figure 1: γ-ray energy spectrum following Coulomb excitation of ^{45}Sc by a 70 MeV ^{32}S beam, detected by the EAGLE array. The most intense γ-ray lines originating from the reaction products on the target oxidation are also marked.

The low-lying Coulomb excited states in ^{45}Sc populated in the present measurement are shown in Fig. 2. Observation of the 531 and 543 keV lines confirmed that the positive parity band built on the low-lying 12.4 keV isomeric state was populated in the present projectile–target combination via the Coulomb excitation process. Moreover, the observed branching ratio for these lines confirms the identification.

Further detailed analysis aims to determine the electromagnetic properties of the ^{45}Sc isotope. Using the least square fitting code GOSIA [7], the measured γ-ray intensities will enable us to determine the B(E3) transition probabilities, mainly: B(E3, $7/2^- \rightarrow 3/2^+$) so far only an upper limit is known [8], while the B(E3, $7/2^- \rightarrow 5/2^+$) in unknown.

This work is supported by the Polish National Science Centre under the FUGA3 postdoctoral fellowship grant No. DEC - 2014/12/S/ST2/00483 and under the Harmonia Programme grant No. DEC - 2013/10/M/ST2/00427. This project has received funding from the European Union's Horizon 2020 ENSAR2 research and innovation programme under grant agreement no. 654002.

Bibliography

[1] M. Avgoulea *et al.*,J. Phys. G: Nucl. and Part. Phys. **2011** 025104

[2] P. Bednarczyk *et al.*,Eur. Phys. J. **A 2** (1998) 157

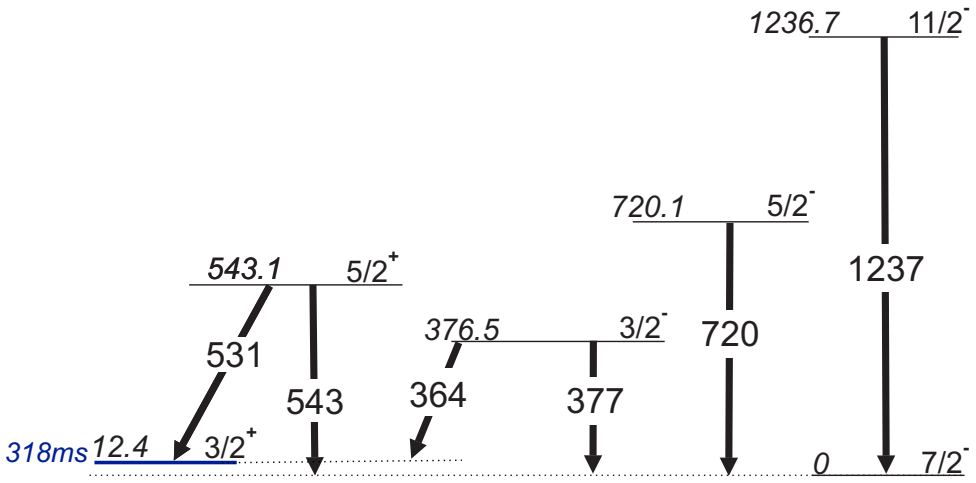


Figure 2: The level scheme of ^{45}Sc observed in the present Coulomb excitation experiment.

[3] P. Bednarczyk *et al.*, Acta Phys. Pol. **B 32** (2001) 747

[4] M.D. Goldberg and B.W. Hooton, Nucl. Phys. **A132** (1969) 369

[5] J. Mierzejewski *et al.*, Nucl. Inst. and Meth. **A659** (2011) 84

[6] M. Würkner *et al.*, Nucl. Phys. **A725** (2003) 3

[7] T. Czosnyka, D. Cline, and C. Y. Wu, Bull. Amer. Phys. Soc. **28** (1983) 745, `http://slcj.uw.edu.pl/en/gosia-code/`.

[8] A.E. Blaugrund, R.E. Holland and F.J. Lynch, Phys. Rev. **159** (1967) 926

C.8 Momentum distribution of the spectator α observed in the ^{16}O(^{20}Ne,αα)^{28}Si reaction for a study of the ^{16}O-burning process

S. Hayakawa[1,2], C. Spitaleri[1,3], N. Burtebayev[4], A. Aimaganbetov[5], G.L. Guardo[1], S. Igamov[6], I. Indelicato[1], G. Kiss[7], S. Kliczewski[8], M. La Cognata[1], M. Lattuada[1], E. Piasecki[9], G.G. Rapisarda[1], S.B. Sakuta[10], R. Siudak[8], A. Trzcińska[9], A. Tumino[1,11], A. Urkinbayev[5],

1) INFN Laboratori Nazionali del Sud, Catania, Italy
2) Center for Nuclear Study, University of Tokyo, Wako, Japan
3) Department of Physics and Astronomy, University of Catania, Catania, Italy
4) Institute of Nuclear Physics of the National Nuclear Center, Almaty, Kazakhstan
5) L.N. Gumilyov Eurasian National University, Astana, Kazakhstan
6) Uzbekistan Academy of Sciences, Institute of Nuclear Physics, Tashkent, Uzbekistan
7) Institute of Nuclear Research (ATOMKI), Debrecen, Hungary
8) The H. Niewodniczański Institute of Nuclear Physics, Kraków, Poland
9) Heavy Ion Laboratory, University of Warsaw, Warszawa, Poland
10) National Research Center "Kurchatov Institute", Moscow, Russia
11) Kore University of Enna, Enna, Italy

This is a continued report of work presented in the previous HIL Annual Report [1]. See the introduction and the methodology section therein for details. The aim of this study is to determine the excitation functions of the main products of the ^{16}O+^{16}O burning reactions, α+ ^{28}Si and p + ^{31}P, at stellar energies. We performed Trojan Horse method (THM) [2] measurements using the ^{16}O(^{20}Ne,αα)^{28}Si and ^{16}O(^{20}Ne, pα)^{31}P reactions.

As mentioned in the previous report [1], we clearly identified protons and α particles by the ΔE-E method. We reconstructed the Q-value spectrum from selected α-α coincidence data by three-body kinematics, which was found to correspond well with the excitation energies of the ^{28}Si nucleus as presented in Fig. 1, which shows the ^{16}O(^{20}Ne, $\alpha\alpha$)^{28}Si reaction. The Q-value spectrum of the ^{16}O(^{20}Ne, pα)^{31}P reaction is also consistent with the known excitation energies, but is more like a continuous spectrum and thus difficult to use for the data analysis at present. To confirm the applicability of the THM to these reactions, one needs to prove that the momentum distribution of the spectator (α, in this case) has a maximum at $p_s = 0$ and is equivalent to that of the inter-cluster motion (α-^{16}O) of the TH nucleus (^{20}Ne), which accordingly guarantees that the quasi-free mechanism is dominant in the observed reaction process. The present work is the first application of the THM to such a heavy nuclear system, and ^{20}Ne is used as the TH nucleus for the first time. The momentum distribution $|\phi(p_s)|^2$ can be determined by the following relations [2]:

$$|\phi(p_s)|^2 \frac{d\sigma}{d\Omega}^{\mathrm{HOES}} \propto \frac{d^3\sigma}{d\Omega_\alpha d\Omega_{\mathrm{Si}} dE_{\mathrm{c.m.}}} / [KF] \propto Y_{\mathrm{exp.}} / Y_{\mathrm{sim.}} \ , \quad (1)$$

where $d\sigma/d\Omega^{\mathrm{HOES}}$ is the half-off-energy-shell differential cross section for the ^{16}O(^{16}O, α)^{28}Si reaction, $d^3\sigma/d\Omega_\alpha/d\Omega_{\mathrm{Si}}/dE_{\mathrm{c.m.}}$ is the triple differential cross section of the ^{16}O(^{20}Ne, $\alpha\alpha$)^{28}Si reaction, $[KF]$ is the kinematic factor, $Y_{\mathrm{exp.}}$ is the experimental yield of the ^{16}O(^{20}Ne, $\alpha\alpha$)^{28}Si reaction, and $Y_{\mathrm{sim.}}$ is that of the Monte Carlo simulation performed in the phase space. Since we had to observe the spectator α itself, the kinematic E-vs.-p_s space could not be covered widely, as shown in Fig. 2. This makes the determination of the momentum distribution very difficult since it depends on the two-

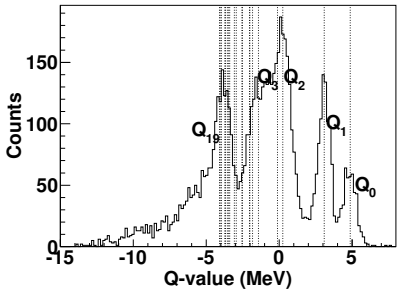


Figure 1: Q-value spectrum of the ^{16}O(^{20}Ne, $\alpha\alpha$)^{28}Si channel. The dotted lines corresponds to the excited states of ^{28}Si.

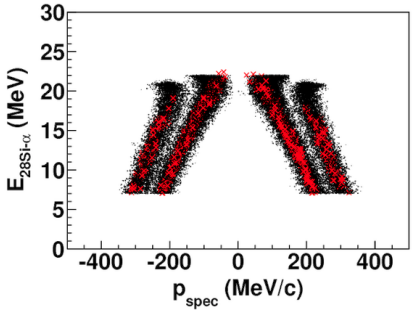


Figure 2: ^{28}Si-α relative energy vs. spectator momentum of the Monte Carlo simulation (black) and the experimental data (red).

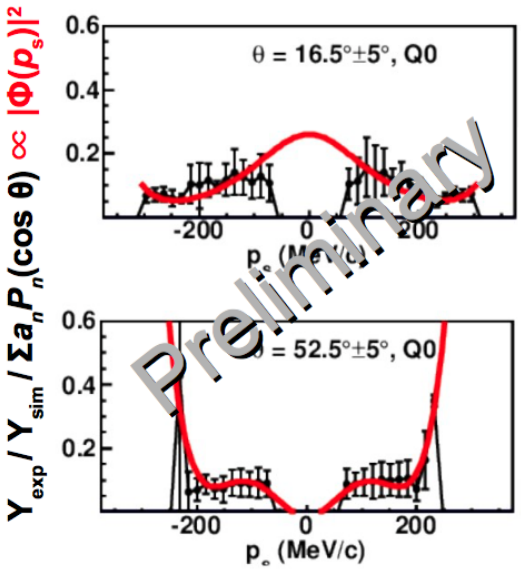


Figure 3: Preliminary momentum distribution of α in ^{20}Ne at $\theta_{\mathrm{c.m.}} = 16.5°$ and $\theta_{\mathrm{c.m.}} = 52.5°$. The red curves are theoretically predicted momentum distributions involving both a one-step virtual decay from the ^{20}Ne ground state and a multi-step virtual decay from the ^{20}Ne first-excited state [3].

body cross section as in Eq. 1, which is an unknown function of the centre-of-mass energy and angle. Firstly, we approximately obtained the linear relation between momentum and energy from Fig. 2. Then we checked the angular distribution of $Y_{\mathrm{exp.}}/Y_{\mathrm{sim.}}$, which enables us to determine $|\phi(p_s)|^2$ at each angle despite the unknown $d\sigma/d\Omega^{\mathrm{HOES}}$. Examples of the preliminary momentum distributions at different angles are shown in Fig. 3. In either case, the momentum distributions do not look to have peaks around $p_s = 0$ and show some complicated structures. The red curves are theoretically predicted momentum distributions involving both a one-step virtual decay from the ^{20}Ne ground state and a multi-step virtual decay from the ^{20}Ne first-excited state [3]. This suggests that the three-body reactions ^{16}O(^{20}Ne, $\alpha\alpha$)^{28}Si and ^{16}O(^{20}Ne, $p\alpha$)^{31}P might not dominantly proceed through the 0^+ ground state of ^{20}Ne but by a multi-step breakup.

In summary, we showed preliminary momentum distributions of the spectator α for the first time, which required a proper understanding of the virtual decay mechanism of the α-^{16}O cluster from the ^{20}Ne nucleus. Further data analysis to determine the definitive momentum distributions, and also a theoretical investigation are needed to describe the behaviour of the current data.

Bibliography

[1] S. Hayakawa *et al.*, HIL Annual Report 2013, page 65.

[2] C. Spitaleri *et al.*, Physics of Atomic Nuclei **74** (2011) 1725.

[3] R. Yarmukhamedov, private communication.

C.9 Asymptotic normalisation coefficient for the 6.356 MeV subthreshold state in ^{17}O from α-transfer studies

A.T. Rudchik[1], N. Keeley[2] and K.W. Kemper[3,4], K. Rusek[4]

1) Institute for Nuclear Research, Ukrainian National Academy of Sciences, Kyiv, Ukraine
2) National Centre for Nuclear Research, Świerk, Poland
3) Physics Department, Florida State University, Tallahassee, USA
4) Heavy Ion Laboratory, University of Warsaw, Warszawa, Poland

Recently, Guo *et al.* [1] explored the use of the ^{13}C(^{11}B,^{7}Li)^{17}O reaction to extract both the spectroscopic factor and asymptotic normalisation coefficient (ANC) for the subthreshold 6.356 MeV $1/2^+$ state in ^{17}O, known to be important for the production of neutrons in the stellar environment through the ^{13}C(α,n) reaction. The present work reports new data for this reaction taken at a ^{11}B beam energy of 45 MeV. The experiment was performed at the Heavy Ion Laboratory of the University of Warsaw. Elastic and inelastic scattering data were published in Ref. [2] where information on the experimental setup may be found.

The experimental data for the α-transfer reaction leading to the 6.356 MeV excited state of ^{17}O are presented in Fig. 1. They were analysed by means of coupled-channels Born-approximation (CCBA) calculations that included coupling to the first excited state of ^{11}B at 2.12 MeV (computer code FRESCO [3]). It was assumed that this state is a member of a K=1/2 rotational band with a quadrupole deformation length of 1.2 fm [2].

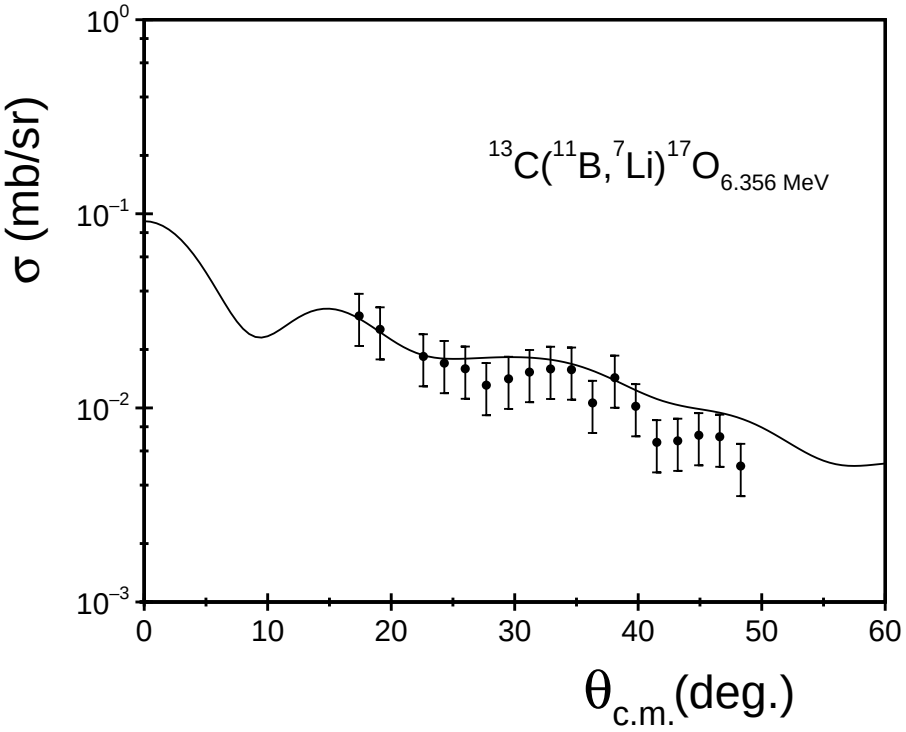


Figure 1: Comparison of the experimental and theoretical results for the 6.356 MeV excited state of ^{17}O.

The results of the calculations for the α-transfer reaction were normalised to the experimental data at the most forward angles (see Fig. 1). Since the spectroscopic amplitudes for the projectile, ^{11}B=^{7}Li+α, are known from shell model calculations [4, 5], the spectroscopic factor for the ^{17}O*=^{13}C + α subthreshold state at 6.356 MeV was extracted. A value of $S = 0.72 \pm 0.22$ was obtained, larger than in the previous studies [1, 6, 7]. From the spectroscopic factor the value of the squared Coulomb modified ANC, $\widetilde{C}^2$, can be extracted using the following relation:

$$\widetilde{C}^2 = S\frac{\psi^2(R)}{W^2(R)}, \quad for\ R >> R_n, \tag{1}$$

where R_n is the range of the nuclear potential, $\psi(R)$ is the wave function of the 6.356 MeV state normalised to unity and $W(R)$ is the Coulomb modified Whittaker function.

The value $\widetilde{C}^2 = 5.1 \pm 1.5$ fm^{-1} was obtained, in good agreement with the results of the previous work summarised in Ref. [8].

Bibliography

[1] B. Guo *et. al.* The Astrophysical Journal. **756** (2012) 193

[2] S.Yu. Mezhevych *et al.* Nucl. Phys. **A724** (2003) 29

[3] I.J. Thompson, Comput. Phys. Rep. **7** (1988) 167

[4] Yu.F. Smirnov and Yu.M. Tchuvilsky, Phys. Rev. **C15** (1977) 84

[5] A.T. Rudchik, Yu.M. Tchuvilgsky, code DESNA, Report KIYAI-82-12, Kiev Institute of Nuclear Research (1982)

[6] E. Liatard *et al.*, Europhys. Lett. **13** (1990) 401

[7] M.G. Pellegriti *et al.*, Phys. Rev. **C77** (2008) 042801

[8] M.L. Avila *et al.*, Phys. Rev. **C91** (2015) 048801

C.10 O_h invariant intrinsic coordinate frame for the octupole collective Hamiltonian

L. Próchniak[1], S.G. Rohoziński[2]

1) Heavy Ion Laboratory, University of Warsaw, Warszawa, Poland
2) Faculty of Physics, University of Warsaw, Warszawa, Poland

Studies of octupole collective excitations of even-even nuclei in the spirit of the General Bohr Hamiltonian (GBH) model need a detailed analysis of the appropriate tensor space and an analysis of the properties of the physically relevant operators defined in this space. In the case of quadrupole excitations the concept of an intrinsic frame (also called a principal axes frame) proved to be extremely useful. In the octupole case there is no self-evident definition of an intrinsic frame, from either the mathematical or physical point of view. We propose to define such a coordinate frame based on the properties of the octupole tensors against transformations of the cubic holohedral group O_h (a group of all the symmetries of a cube), see [1], [2]. The seven dimensional representation (multipolarity $\lambda = 3$) of the O(3) group can be decomposed into the sum $A_2^{-1} \oplus F_1^- \oplus F_2^-$ of irreducible representations of O_h, with dimensions $1, 3, 3$, respectively [3]. Using standard spherical tensor coordinates $\alpha_{3\mu}, \mu = -3, ..., 3$ (with the condition $\alpha^*_{3\mu} = (-)^\mu \alpha_{3-\mu}$) such a decomposition can be given explicitly:

$$A_2^- : \; b = b_{32}, \tag{1}$$

$$F_1^- \begin{cases} f_x = \sqrt{\frac{3}{8}} a_{31} - \sqrt{\frac{5}{8}} a_{33}, \\ f_y = \sqrt{\frac{3}{8}} b_{31} + \sqrt{\frac{5}{8}} b_{33}, \\ f_z = a_{30}, \end{cases} \tag{2}$$

$$F_2^- \begin{cases} g_x = \sqrt{\frac{5}{8}} a_{31} + \sqrt{\frac{3}{8}} a_{33}, \\ g_y = -\sqrt{\frac{5}{8}} b_{31} + \sqrt{\frac{3}{8}} b_{33}, \\ g_z = a_{32}. \end{cases} \tag{3}$$

where $a_{30}{=}\alpha_{30}, a_{3\mu}{=}\sqrt{2}\mathrm{Re}\,\alpha_{3\mu}, b_{3\mu}{=}\sqrt{2}\mathrm{Im}\,\alpha_{3\mu}, \mu{=}1, 2, 3$. We define an intrinsic frame as such that all $g_s, s{=}x, y, z$ components are zero. Hence, instead of seven variables $\alpha_{3\mu}$ one can use four "deformations": $b, f_s, s{=}x, y, z$ and three Euler angles describing the orientation of the intrinsic frame with respect to the laboratory frame.

The definition of the intrinsic frame given above is general and can be applied to any implementation of the octupole tensors. To give some idea of the meaning of the variables b, f_s we show in Fig. 1 plots of surfaces given by the formula

$$r(\theta, \phi) = R_0(1 + \sum \alpha_{3\mu} Y^*_{3\mu}) = R_0\big[1 - A_0(\phi, \theta, 0)b + \textstyle\sum_{s=x,y,z}(1{-}2\delta_{sx}) F_{0s}(\phi, \theta, 0) f_s\big] \tag{4}$$

where A_0 and F_{0s} are appropriate combinations of the Wigner functions (rotation matrices D^3), see [1].

According to the general theory there are four elementary scalars built from octupole variables, namely $\boldsymbol{t}_0^{(2)}, \boldsymbol{t}_0^{(4)}, \boldsymbol{t}_0^{(6)}, \boldsymbol{t}_0^{(10)}$, where $\boldsymbol{t}_l^{(n)}$ denotes the result of coupling n tensors $\boldsymbol{\alpha}_3$ to the angular momentum value l. These quantities are important in a study of the functions and operators defined over the octupole tensor space. Below we give explicit

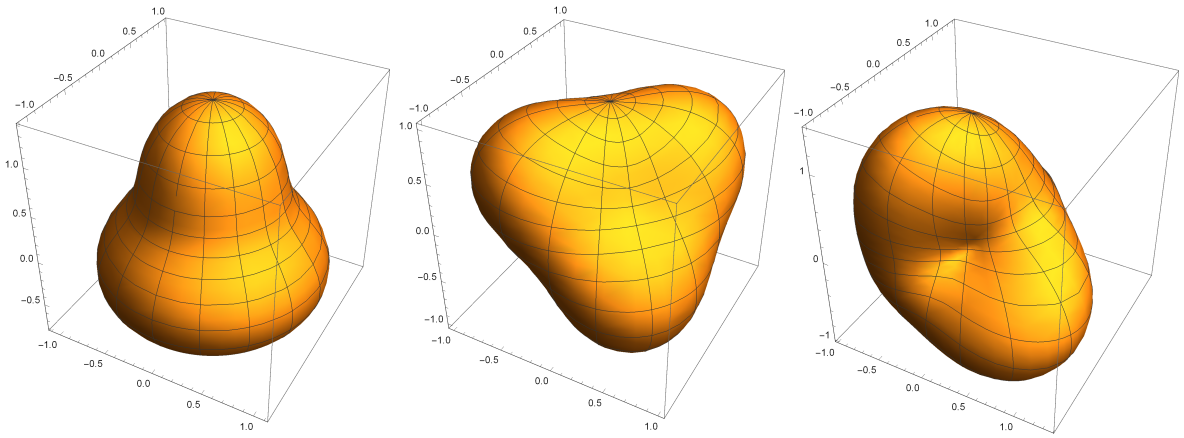


Figure 1: Surfaces given by eq. 4 with specific values of deformations b, f_s. Left panel: f_z=0.5, b=f_x=f_y=0, middle panel: b=0.5, f_x=f_y=f_z=0, right panel: b=0.5, f_z=0.5, f_x=0.3, f_y=0.4.

formulae for $\boldsymbol{t}_0^{(2)}, \boldsymbol{t}_0^{(4)}, \boldsymbol{t}_0^{(6)}$ in the intrinsic frame. The formula for $\boldsymbol{t}_0^{(10)}$ is a bit too long to be included here. Let us recall that in the quadrupole case the elementary scalars are the well known β^2 and $\beta^3 \cos 3\gamma$ invariants.

$$\boldsymbol{t}_0^{(2)} = -\frac{1}{\sqrt{7}}(b^2 + \sigma_2) \tag{5}$$

$$\boldsymbol{t}_0^{(4)} = \frac{1}{84\sqrt{5}}\big(16\sigma_4 - 13\sigma_{42} + 80b^2\sigma_2 + 24\sqrt{15}b\sigma_3\big) \tag{6}$$

$$\boldsymbol{t}_0^{(6)} = \frac{\sqrt{3}}{196}\left((11\sigma_2\sigma_{42} - 15\sigma_3^2) - \frac{16}{5}\sigma_2^3\right) - \frac{1}{7\sqrt{5}}b\sigma_3\sigma_2 + \frac{1}{196\sqrt{3}}b^2(32\sigma_2^2 - 129\sigma_{42}) + \\ + \frac{2\sqrt{5}}{7}b^3\sigma_3 - \frac{20}{147\sqrt{3}}b^4\sigma_2 \tag{7}$$

where

$$\sigma_2 = f_x^2 + f_y^2 + f_z^2, \quad \sigma_4 = f_x^4 + f_y^4 + f_z^4, \quad \sigma_6 = f_x^6 + f_y^6 + f_z^6 \tag{8}$$

$$\sigma_3 = f_x f_y f_z \tag{9}$$

$$\sigma_{42} = f_x^2 f_y^2 + f_y^2 f_z^2 + f_x^2 f_z^2 \tag{10}$$

One should remember that the elementary scalars are not uniquely defined. Firstly, they can be multiplied by real numbers. Secondly, adding e.g. the product $\boldsymbol{t}_0^{(2)}\boldsymbol{t}_0^{(4)}$ (as polynomials) to $\boldsymbol{t}_0^{(6)}$ we obtain again a sixth order (in $\boldsymbol{\alpha}_3$) scalar (with respect to rotations).

Bibliography

[1] S.G. Rohoziński and L. Próchniak, Acta Phys. Pol. Proc. Suppl. **B10** (2017) 191

[2] S.G. Rohoziński and L. Próchniak, to be published.

[3] M. Hamermesh, *Group Theory and its Application to Physical Problems* (Addison-Wesley, Reading, 1964) Chapt. 9, Sect. 4

C.11 Ultra-thin silicon epitaxial strip detectors with very narrow strips produced by a low-temperature technique.

A.J. Kordyasz[1], M. Gerlach[2], Ł. Kordyasz[2], A. Bednarek[1], M. Kowalczyk[1,3], J. Tarasiuk[3], M. Kisieliński[1], T. Kozik[4], J. Sarnecki[5], D. Lipiński[5], H. Wodzińska[5], M. Teodorczyk[5], M. Gajewski[5], A. Zagojski[5], K. Krzyżak[5]

1) Heavy Ion Laboratory, University of Warsaw, Warszawa, Poland
2) SonicTech, Łomianki, Poland
3) Faculty of Physics, University of Warsaw, Warszawa, Poland
4) M. Smoluchowski Institute of Physics, Jagiellonian Univ., Kraków, Poland
4) Institutge of Electronic Materials Technology, Warszawa, Poland

By analogy to high energy applications, silicon vertex detectors consisting of very thin and very narrow strips were proposed for measurements of multi-particle events of low-energy light charged particles, heavy ions and fission fragments [1]. A recently developed low-temperature technique for thin transmission detectors [2] and thin strip detectors [3] gives the possibility to produce a vertex detector for the registration of low-energy multi-particle events.

The aim of this work is to test how narrow detector strips can be achieved for thin epitaxial layers using the low-temperature technique [3]. For tests we used n–n^+ silicon epitaxial structures of resistivity and thickness epitaxial layer of about 30 Ωcm and 5 µm, respectively, produced in the Institute of Electronic Materials Technology in Warsaw. The 5 µm thick epitaxial wafer after B^+ implantation followed by Al metalisation is transparent to light, see Fig. 1

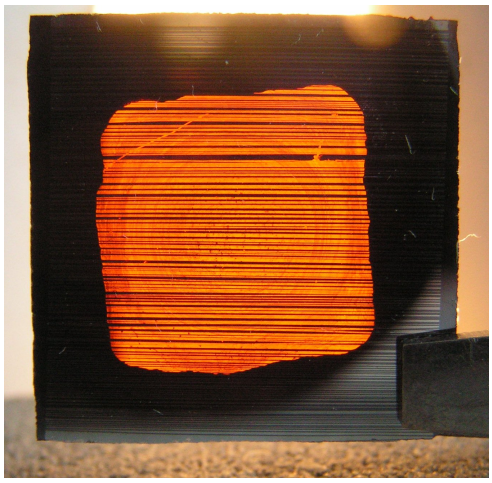


Figure 1: Silicon wafer 21.5×21.5 mm^2 with an epitaxial layer of thickness 5 µm transparent to light. Black lines are detector strips.

A 21.5×21.5 mm^2 5 µm thick strip detector stuck with conductive glue into a PCB board is presented in Fig. 2. A microscope photo of some strips ultrasonically bounded using 25 µm Al wires to make strip contacts with the PCB track is presented in Fig. 3.

The width of the detector strips in Fig. 3 varies from about 100 µm (right most unbounded strip) to about 10 µm. For narrow strips (about 10 µm) the diameters of the bonding Al wires are greater than the widths of the strips. In this case short circuits

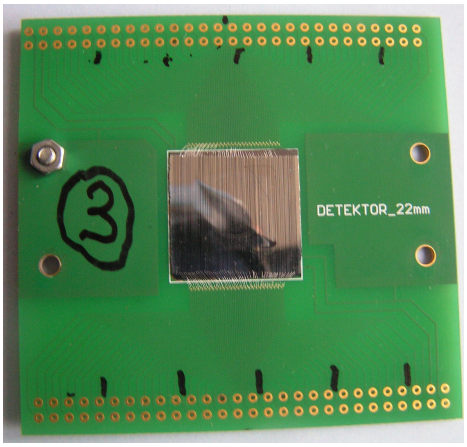


Figure 2: PCB with glued strip detector.

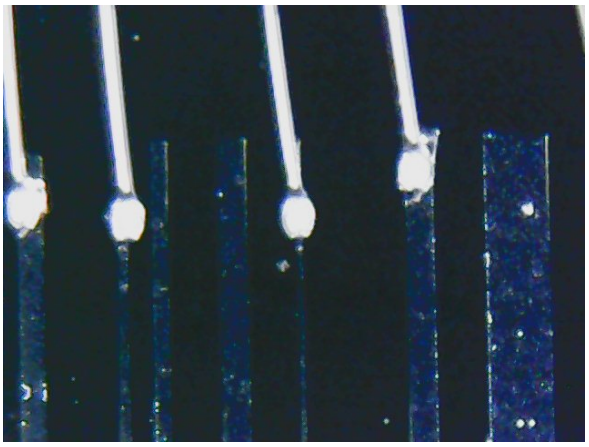


Figure 3: Detector strips bonded using 25 µm Al wires.

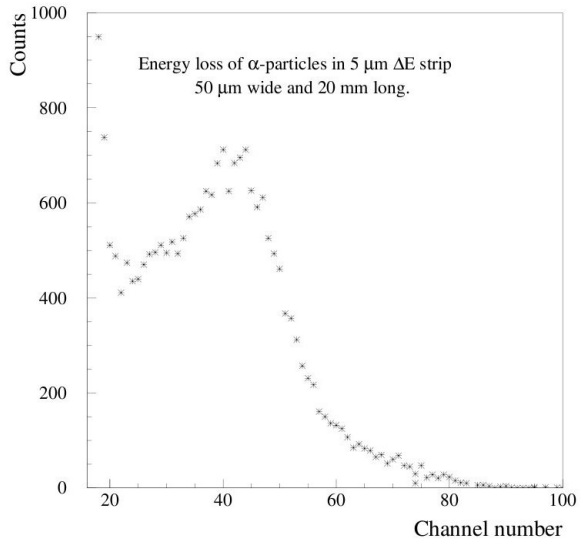


Figure 4: Energy loss of α particles in a single strip.

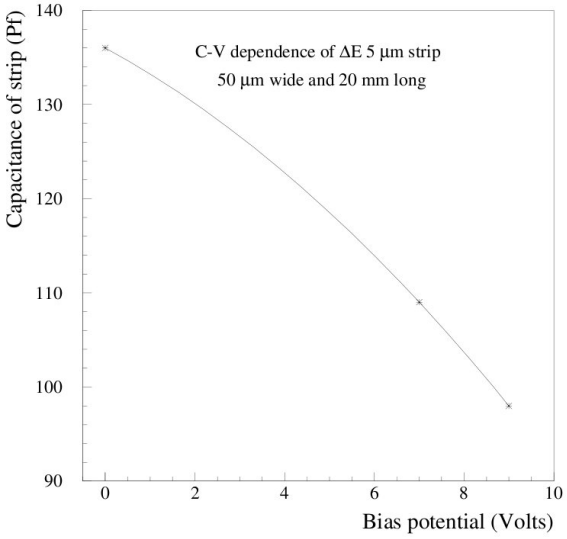


Figure 5: C-V characteristic of a single strip.

(direct connections between Al and Si) prevent the strips from functioning. Test measurements were performed with a 50 µm strip (first bonded strip from the right side of Fig. 3 collimated to a diameter of about 2 mm. In Fig. 4 the energy loss (about 700 keV) of α particles from ^{241}Am is shown. The strip of the detector operated using an internal built-in potential with external bias potential equal to zero. The strip capacitance versus bias potential in the range from 0 to 9 Volts (C-V characteristic) is presented in Fig. 5 The strip capacitance is a decreasing function of the bias potential.

Bibliography

[1] A.J. Kordyasz *et al.*, Proceedings of the IWM2011 International Workshop on Multifragmentation and related topics, Caen (France), 2-5 November 2011 p. 301

[2] A.J. Kordyasz *et al.*, Eur. Phys. J. **A51** (2015) 15

[3] A.J. Kordyasz *et al.*, Acta Phys. Pol. **B47** (2016) 207

C.12 Preparations for the investigations of proton-rich nuclei using the AGATA-NEDA setup at GANIL

M. Palacz[1], for the N=Z Collaboration

1) Heavy Ion Laboratory, University of Warsaw, Warszawa, Poland

A group from HIL has been since long involved in in-beam γ-ray spectroscopy studies of proton-rich nuclei located in the nuclidic chart close to the $N = Z$ line, and in particular in studies of nuclei in the vicinity of the doubly magic ^{100}Sn. In 2016 we concentrated on the preparation of experiments which we plan to run using a new neutron detection array NEDA [1, 2] in connection with the AGATA γ-ray spectrometer [3], located at GANIL, Caen, France. We also contributed to the construction of NEDA.

NEDA is a collection of liquid scintillator neutron detectors, presently under construction by a broad international collaboration. NEDA will ultimately consist of 355 identical detectors containing liquid scintillator (each single detector of approx. 3 litres volume) located in the front half of the solid angle around the target, at a distance of about 1 m from it. Photons generated in the scintillator will be collected and multiplied by the photomultiplier tubes. The resulting output of photomultiplier signals will be analysed using digital electronics. Each detector will provide information about the time of the radiation detection, the intensity of the generated light and the shape of the resultant electronic pulse. The scintillator used in NEDA has a light response which depends on the type of the registered radiation, which leads to different pulse shapes for neutrons and gamma rays. Thus, pulse shape analysis, in combination with a measurement of the time of flight of the detected radiation, enables a precise distinction between neutrons and gamma rays. Otherwise gamma rays detected in the neutron detectors form a disturbing background, significantly limiting the neutron detection capabilities. For studies of proton-rich nuclei, NEDA will be used at GANIL in 2018 for the first time, together with the AGATA array, in a configuration consisting of 54 detectors, amended by the older detectors of the Neutron Wall [4–6].

In spring 2016 a call for proposals of experiments to be run using the AGATA-NEDA array was announced. As part of the preparations for the submission of the proposal a two-day meeting of an informal "N=Z Collaboration" was organised at HIL. The main aim of the meeting was to discuss proposals in which the use of NEDA was anticipated. The status of the preparations of NEDA for the experiments was also evaluated. More than 20 physicists from 13 institutions in 8 countries took part in the meeting. Twelve talks were presented.

The meeting of the Programme Advisory Committee of GANIL was held in June 2016. Six experiments with AGATA-NEDA were accepted, which means that altogether 8 such experiments should be run in 2018 (two experiments were accepted a year earlier). We plan to contribute to all these experiments, and we are co-spokepersons in two of them. Preparations for the experiments are in progress.

Bibliography

[1] G. Jaworski, *et al.*, Nucl. Inst. and Meth. **A673** (2012) 64

[2] T. Huyuk, *et al.*, Eur. Phys. J. **52** (2016) 55

[3] S. Akkoyun *et al.*, Nucl. Inst. and Meth. **A668** (2012) 26

[4] O. Skeppstedt, *et al.*, Nucl. Inst. and Meth. **A421**(1999) 531

[5] J. Ljungvall, M. Palacz, and J. Nyberg Nucl. Inst. and Meth. **A528** (2004) 741

[6] The Neutron Wall web page, `nsg.physics.uu.se/nwall`.

C.13 Sn targets for lifetime measurements

A. Stolarz, J. Kowalska

Heavy Ion Laboratory, University of Warsaw, Warszawa, Poland

Measurements of the picoseconds lifetimes of excited levels in ^{136}Nd were performed by Recoil Distance Method using a precise device called plunger (Fig. 1 and Ref. [1]). The plunger set-up consists of a reaction target and a recoil stopper mounted at a distance of a few to tenths of micrometres. This necessitates a high smoothness and flatness of the surface of both target and stopper. The final tuning of the foil smoothness is completed by stretching the foil over the dome of the foil holder.



Figure 1: The plunger device: left showing the inside dome, right with stretched test foil.

The investigated nucleus was produced in the ^{120}Sn(^{20}Ne,4n)^{136}Nd reaction. The requested thickness of the Sn layer (about 500 µg/cm^2) needed for populating the studied nucleus can be completed only by high vacuum evaporation. The layer prepared this way had to be supported by a backing foil to sustain the stretching forces. The ^{120}Sn layer was supported by a Au backing. The cost of the isotopically enriched material and the demand of high thickness homogeneity were challenges in completing the task with costs as low as possible. Since the collection efficiency of the evaporated material increases with decreasing vapour source-substrate distance (consumption increase proportional to the square root of the distance) it was desirable to set the target backing, i.e. the Au foil, as close to the Sn vapour source as possible without losing too much of the thickness homogeneity. The set-up of the evaporating device allowed the substrate to be brought as close as about 2 cm to the vapour source. The re-evaporation of the already deposited Sn (which has a low melting point) was avoided by clipping the Au backing to a water cooled copper block. This cooling not only prevents the deposited material from re-evaporating but also enhances the efficiency of vapour condensation. To minimise the loss of the evaporated material, due to the 2π distribution from a standard open vapour source, a new type of crucible (Fig. 2) with a conical shape was used for the Sn evaporation.

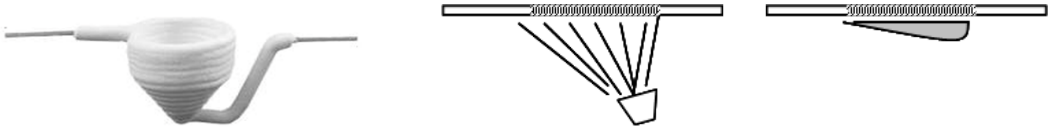


Figure 2: Conical crucible used for the Sn evaporation.

The vertical positioning of the crucible orifice was of high concern as a small twisting of the crucible from its vertical position would result in an angle/twisted vapour distribution

causing inhomogeneity in the deposited layer (Fig. 2). Similar precision is needed in setting the backing foil parallelism in relation to the crucible top. This was controlled using a mini spirit-level

The Au backing foil mounted in the mask was placed above the crucible orifice (dia. 6 mm) taking care to ensure central alignment of the crucible orifice and the foil. The alignment was controlled using a home made device (Fig. 3, right) controlling the axial position of the crucible and mask apertures. High smoothness of the deposited layer was achieved by carrying out the evaporation/deposition very slowly, with an evaporation rate of approximately 30 to 33 ng/(cm$^2 \cdot$ s), otherwise the Sn vesicles appeared on the surface of the deposited Sn layer (Fig. 4).



Figure 3: Evaporation set-up (left). The axial position of the crucible and backing foil was controlled with the tool shown on the right.

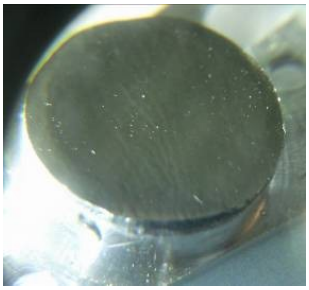


Figure 4: The test deposit of nat Sn on Al backing, the small droplets of Sn are visible on the surface (magnification: 40 times)

With the listed modifications of the evaporation procedure and the precautions taken during the deposition process such as:

- close geometry of the evaporation set-up (distance between the vapour source (crucible) and substrate of 22 mm,
- application of water cooling of the substrate and carrying out the evaporation with a very low evaporation rate ($\approx$ 30 ng/(cm$^2 \cdot$ s)).

the requested targets with a thickness of $\approx$ 0.5 mg/cm^2 and an area of 3.14 cm^2 (deposit $\phi \approx$ 2 cm) were produced with approximatelyplaced on the target holder was mounted and tightly fixed to the holder as described earlier.

35% deposition efficiency (using 4.5 to 4.8 mg of ^{120}Sn per target), with a thickness inhomogeneity in the range of 10% across the 10 mm diameter of the deposited area

(Fig. 5). The thickness of the Sn layer was measured with an α energy loss method using ^{241}Am as the α source.

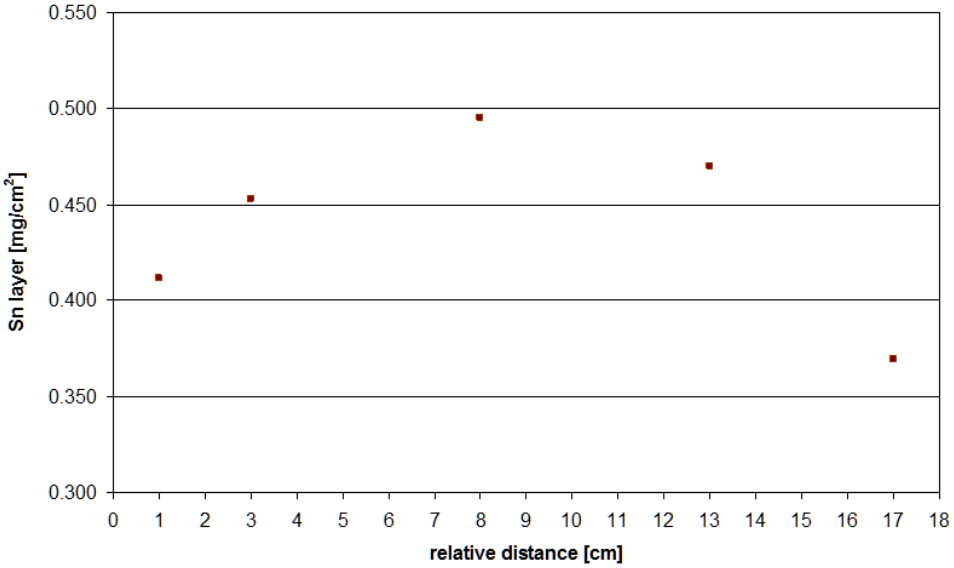


Figure 5: The thickness distribution of the ^{120}Sn deposit on the Au backing; thickness inhomogeneity of the deposit in the area needed to cover the aperture of the plunger dome (dia. 8 mm) is about 5%.

This work completed within project no. DEC 8211/2013/10/M/ST2/00427 funded by the National Science Center of Poland under the Harmonia Programme grant.

Bibliography

[1] A. Tucholski *et al.* this Report, page 56

C.14 ^{132}Ba targets for nuclear shell structure studies

A. Stolarz[1], J.A. Kowalska[1], P. Napiorkowski[1], S. Dutt[2], R. Kumar[3], M. Saxena[4], H.-J. Wollersheim[5]

1) Heavy Ion Laboratory, University of Warsaw, Warszawa, Poland
2) Department of Physics, Aligarh Muslim University, Aligarh, India
3) Inter University Accelerator Centre, New Delhi, India
4) Department of Physics and Astrophysics, University of Delhi, New Delhi, India
5) GSI Helmholtzzentrum für Schwerionenforschung GmbH, Darmstadt, Germany

Studies of the shell structure of nuclei with mass $A \approx 130$ were carried using highly enriched ^{132}Ba targets and a 100 MeV ^{32}S beam provided by the U-200P cyclotron, and a 175 MeV ^{58}Ni beam provided by the Inter University Accelerator Center in New Delhi, India. The targets for these studies had to be as thick as about 500 µg/cm^2, and if necessary supported by a thin backing (20 µg/cm^2) composed of light nuclei. Due to the chemical properties of barium (very high affinity to oxygen) work with the metallic form, although there are some advantages to work with the elemental form, would cause difficulties in transferring the target to the experimental area and with completing the measurements. In addition the requested thickness can only be achieved by evaporation of the target material, which means higher consumption, ten to twenty times greater than the target thickness, of the deposited material. Taking into account the high price of the enriched ^{132}Ba isotope, a method economising the usage of the target material was highly desirable. In the first approach the target was prepared by sedimentation of $BaCO_3$ powder from a solution of epoxy glue as binder (powder sedimented without binder is mechanically unstable — it easily peels off). However, the target beam test showed that epoxy glue as a component of the target is not acceptable as it burns when exposed to the 100 MeV ^{32}S ions (Fig. 1), most probably due to the very low melting temperature of polyepoxides).

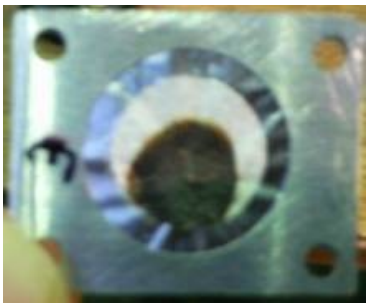


Figure 1: $^{nat}BaCO_3$ sedimented with the addition of epoxy glue after irradiation with 100 MeV ^{32}S.

Therefore, for the experiment performed at HIL the ^{132}Ba targets were prepared in form of barium chloride (melting temperature 962 °C). The appropriate amount of barium carbonate was first dissolved in 10 µl of 36% HCl and 40 µl of H_2O and dried under a lamp taking care to make a quantified collection of the crystallising $BaCl_2$ which in practise meant "knocking" the vessel nearly all the time during the drying process to force the appearing crystals to fall to the bottom of the crystallizer. The dry residue was then dissolved in 10 µl of H_2O, to which 20 µl of acetone was added as surfactant (other surfactants can not be used due to the target purity requirements) and transferred

with a micropipette to the surface of a carbon foil stretched over 15 mm aperture of the supporting frame. The deposited drop of barium chloride solution was left for spontaneous drying. This procedure resulted in $^{132}BaCl_2$ targets (with a thickness of 631 µg/cm^2 which corresponds to 410 µg/cm^2 of Ba) on ≈ 30 µg/cm^2 carbon foils with ≈ 20% higher target thickness on the edge of the deposit (Fig. 2). The thickness of the deposit was checked by weighing and with alpha particle energy loss measurements.



Figure 2: $BaCl_2$ target mounted at a target holder.

A similar procedure was applied to the preparation of the targets for the experiment carried out in India, but due to the high hygroscopicity of $BaCl_2$ it was decided to produce the target layer in the form of an organic compound of barium that has lower hygroscopicity. This also gave a compound where the barium is accompanied by lighter elements than in chloride. Two different compounds (barium acetate and barium oxalate) and two different backings (Mylar and carbon foil) were tested to accomplish the task. The barium acetate $Ba(COO)_2$ (melting temp. 450 ° C) was produced by direct dissolution of $BaCO_3$ in acetate acid while oxalate $Ba(COO)_2$ (melting temperature 400° C) was obtained in a two step process: conversion of the carbonate into $BaCl_2$ or acetate and then converting the inter-product into the oxalate by dissolving in a solution of oxalate acid. Taking into account the needle type structure of Ba oxalate crystals (Fig. 3 left) it was decided to prepare the targets from Ba acetate (Fig. 3 middle). In this case acetone was not added to the solution as its influence on the wettability of carbon foil was not noticed. The Mylar backing was rejected. Although it had much better wettability (the drop of acetate was distributed over nearly the whole aperture of the frame (Fig. 3 right) but had low mechanical resistance to stress appearing after the deposit dried. The five day irradiation with ^{58}Ni beam was performed with a single target of about 650 µg/cm^2 (relating to ^{132}Ba) on about 30 µg/cm^2 C foil. The spare targets were not used.



Figure 3: Crystals of Ba oxalate (left), solution of Ba-acetate on C foil (middle) and solution of Ba-acetate on Mylar (right)

The work was completed within the Erasmus Mundus students project.

Part D

Appendices

D.1 List of experiments performed at HIL in 2016

A list of the experiments performed in 2016 is presented in the following pages. The following acronyms of institution names are used in the list:

- HIL — Heavy Ion Laboratory, University of Warsaw, Warszawa, Poland;
- CEA Saclay — IRFU/SPhN, CEA Saclay, Gif-sur-Yvette, France;
- HCCC Kielce — Holycross Cancer Center, Kielce, Poland;
- IEP UW — Institute of Experimental Physics, University of Warsaw, Warszawa, Poland;
- INFN Florence — INFN e Università di Firenze, Firenze, Italy;
- INFN LNL — INFN, Laboratori Nationali di Legnaro, Legnaro, Italy;
- INP Kraków — The H. Niewodniczański Institute of Nuclear Physics, Kraków, Poland;
- IUAC New Delhi — Inter University Accelerator Centre, New Delhi, India;
- JINR — Joint Institute for Nuclear Research, Dubna, Russia;
- NCNR Świerk — National Centre for Nuclear Research, Świerk, Poland;
- TIFR Mumbai — Tata Institute of Fundamental Research, Mumbai, Indie;
- UB — University of Białystok, Białystok, Poland;
- U.Florence — University of Florence, INFN Sezione di Firenze, Italy;
- US Katowice — Institute of Physics, University of Silesia, Katowice, Poland;
- U.Sofia — Sofia University "St. Kliment Ohridski", Sofia, Bulgaria;
- U.Surray — University of Surrey, Guildford, Surrey, United Kingdom;

For each experiment the following information is provided: ion, energy, setup/beam line information, date, proposal number, subject, spokespersons and institutions.

04–07, 11, 12, 26, 27, 29, 30.01

HIL000 — Test of the amplifiers (P. Gmaj)
HIL

$^{24}Mg^{+5}$ 08.02–09.02
HIL000 — Test of the cyclotron (P. Gmaj)
HIL

$^{24}Mg^{+4}$ 11.02–12.02
HIL000 — Test of the cyclotron (P. Gmaj)
HIL

$^{12}C^{+3}$ 16–18, 22, 23.03
HIL000 — Test of the cyclotron (P. Gmaj)
HIL

$^{20}Ne^{+4}$ — 97.5 MeV — EAGLE 04.04–08.04
HIL061 — Test experiment of lifetime measurement of ^{136}Nd (A. Tucholski)
HIL, IEP UW

$^{4}He^{+1}$ – 30 MeV — Internal beam 10.04–15.04
HIL058 — Production of the Targeted Alpha Therapy (TAT) isotope ^{211}At with He^{+} beams from the Warsaw Heavy Ion Cyclotron (J. Jastrzębski)
HIL, US Katowice

$^{10}B^{+2}$ 12, 13, 17.05
HIL000 — Test of the cyclotron (P. Gmaj)
HIL

14–16, 20–22.06
HIL000 — Test of the amplifiers (P. Gmaj)
HIL

$^{14}N^{+3}$ 12.07
HIL000 — Test of the chopper (P. Gmaj)
HIL

$^{4}He^{+1}$ 29.09
HIL000 — Test of the cyclotron (P. Gmaj)
HIL

$^{12}C^{+3}$ – 90 MeV 03.10–07.10
HIL062 — Particle track structure for Carbon ions (PTSCI) (M. Pietrzak, A. Bancer, S. Pszona)
NCNR Świerk, HIL

$^{4}He^{+1}$ – 30 MeV — Internal beam 10.10–14.10
HIL058 — Production of the Targeted Alpha Therapy (TAT) isotope ^{211}At with He+ beams from the Warsaw Heavy Ion Cyclotron (J. Jastrzębski)
HIL, US Katowice

$^{12}C^{+3}$, $^{16}O^{+4}$ — 90 MeV, 118 MeV — Radiobiology 17.10–21.10
HIL057 — Survival of CHO-K1 cells after double-ions irradiation (Z. Szefliński, J. Czub)
HCCC Kielce, HIL

$^{20}Ne^{+4}$ — 54 MeV EAGLE, ICARE 24.10–26.10
HIL001 — Students' workshop
HIL

$^{32}S^{+5}$ 28.10
HIL000–Test of the cyclotron (P. Gmaj)
HIL

$^{32}S^{+4}$ 02.11
HIL000–Test of the cyclotron (P. Gmaj)
HIL

$^{32}S^{+5}$ 03.11
HIL000–Test of the cyclotron (P. Gmaj)
HIL

$^{12}C^{+3}$ – 90 MeV 07.11–10.11
HIL062 — Particle track structure for Carbon ions (PTSCI)
(M. Pietrzak, A. Bancer, S. Pszona)
NCNR Świerk, HIL

$^{32}S^{+5}$ – 90 MeV — EAGLE 14.11–25.11
HIL060 — Coulomb excitation of ^{45}Sc
(M. Matejska-Minda, K. Hadyńska-Klęk)
HIL, INFN LNL, CEA Saclay, University of Surray, JINR, INP Kraków, IUAC New Delhi, TIFR Mumbai, University of Firenze, INFN Firenze, UB

$^{20}Ne^{+4}$ — 97 MeV — EAGLE 28.11–12.12
HIL061 — Study of low lying states of ^{136}Nd (A. Tucholski, C. Petrache)
HIL, CEA Orsay, IEP UW, U.Sofia

$^{12}C^{+3}$ – 90 MeV 12.12–16.12
HIL062 — Particle track structure for Carbon ions (PTSCI) (M. Pietrzak, A. Bancer, S. Pszona)
NCNR Świerk, HIL

$^{24}Mg^{+4}$ 20.12–21.12
HIL000 — Test of the cyclotron (P. Gmaj)
HIL

D.2 Degrees and theses completed in 2016 or in progress

D.2.1 PhD theses of students affiliated to HIL, of HIL staff members, and supervised by HIL staff

Tomasz Marchlewski, Faculty of Physics, University of Warsaw
Measurement of nuclear excited state lifetimes in ^{124}Cs; study of the mechanism of spontaneous chiral symmetry breaking
Supervisors: prof. dr hab. K. Rusek, dr E. Grodner. Expected completion time: 2017.

Łukasz Standyło, National Centre for Nuclear Research, Świerk
Badanie oddziaływania ^{6}He z jądrami ^{206}Pb przy energiach blisko bariery kulombowskiej
Study of the interaction of ^{6}He with ^{206}Pb nuclei at energies close to the Coulomb barrier
Supervisor: prof. dr hab. K. Rusek. Expected completion time: 2017.

Michalina Komorowska, Faculty of Physics, University of Warsaw
Pear-shaped Nuclei in the $N \sim 88$ mass region
Supervisors: dr hab. L. Próchniak, dr P. Napiorkowski, dr W. Korten, dr M. Zielińska.
Expected completion time: 2018.

Mateusz Pęgier, Faculty of Chemistry, University of Warsaw
Synteza i kontrola jakości radiofarmaceutyków znakowanych izotopem ^{44}Sc
Synthesis and quality control of radiopharmaceuticals labelled with ^{44}Sc
Supervisor: prof. dr hab. K. Pyrzyńska. Expected completion time: 2018.

Olga Saeed Mohamed Nassar, Faculty of Physics, Warsaw University of Technology
Optyka jonowa w centrum cyklotronu U-200P
Ion trajectories in the central region of the U-200P cyclotron
Supervisors: dr hab. Marcin Palacz, dr Ivan Ivanenko. Expected completion time: 2018.

Mateusz Sitarz, Faculty of Physics, University of Warsaw
Supervisors: prof. dr hab. T. Matulewicz, dr A. Trzcińska.
Expected completion time: 2019.

D.2.2 Other PhD theses based on experiments performed at HIL

Katarzyna Szkliniarz, Silesian University
Supervisor: prof. dr hab. W. Zipper. Defended in May 2017.

Frank Leonel Bello Garrote, University of Oslo
Supervisor: prof. A. Görgen. Expected completion time: 2017.

Malin Klientefjord, University of Oslo
Supervisor: prof. A. Görgen. Expected completion time: 2017.

Sunil Dutt, Aligarh Muslim University, Aligarh, (U.P.) India
Supervisor: prof. A. Rizvi. Expected completion time: 2018.

D.2.3 MSc and BSc theses supervised by HIL staff members

Roman Szenborn, Faculty of Physics, University of Warsaw
Analysis of random γ-γ coincidences in DSA experiments with the EAGLE array
Supervisors: dr E. Grodner, dr J. Srebrny. MSc thesis, expected completion time: 2017.

Agnieszka Strzeżek, Faculty of Physics, University of Warsaw
Analiza wykrywalności guzów o podwyższonej aktywności na rzeczywistych i symulowanych obrazach w tomografii pojedynczych fotonów (SPECT).
Analysis of detection of tumors with increased activity in real and simulated images in single photon tomography (SPECT).
Supervisor: dr hab. Z. Szefliński. MSc thesis, expected completion time: 2017.

Mateusz Filipek, Faculty of Physics, University of Warsaw
Badanie wydajności detekcji jonów w nanodozymetrze Jet Counter
Study of ion detection efficiency in the Jet Counter nanodosimeter
Supervisor: dr hab. Z. Szefliński. MSc thesis, expected completion time: 2017.

Norbert Suchojad, Faculty of Physics, University of Warsaw
Kalibracja Gamma Kamery i dozymetria przy przygotowaniu fantomów
Gamma Camera calibration and dosimetry in phantom preparation
Supervisor: dr hab. Z. Szefliński. BSc thesis completed in February 2016.

Zofia Biały, Faculty of Physics, University of Warsaw
Określenie granic wykrywania patologii w obrazowaniu medycznym z użyciem fantomu Jaszczaka.
Determination of pathology detection limits in medical imaging using a Jaszczak phantom.
Supervisor: dr hab. Z. Szefliński. BSc thesis completed in September 2016.

Łukasz Celejewski, Faculty of Physics, University of Warsaw
Porównanie systemów dozymetrycznych stosowanych w Pracowni Obrazowania Medycznego ŚLCJ.
Comparison of dosimetry systems used in the Laboratory of Medical Imaging at HIL.
Supervisor: dr hab. Z. Szefliński. BSc thesis completed in December 2016.

Kamila Żujewska, Faculty of Physics, University of Warsaw
Badanie struktury trajektorii cząstki alfa oddziaływującej w rozrzedzonym molekularnym azocie.
Examination of the structure of the trajectory of alpha particles interacting in rarefied molecular nitrogen.
Supervisor: dr hab. Z. Szefliński. BSc thesis, expected completion time: 2017.

D.3 Publications

D.3.1 Publications in journals of the Journal Citation Reports (JCR) list

M. F. Alshudifat, R. Grzywacz, M. Madurga, C. J. Gross, K. P. Rykaczewski, J. C. Batchelder, C. Bingham, I. N. Borzov, N. T. Brewer, L. Cartegni, A. Fijalkowska, J. H. Hamilton, J. K. Hwang, S. V. Ilyushkin, C. Jost, M. Karny, A. Korgul, W. Krolas, S. H. Liu, C. Mazzocchi, A. J. Mendez, K. Miernik, D. Miller, S. W. Padgett, S. V. Paulauskas, A. V. Ramayya, D. W. Stracener, R. Surman, J. A. Winger, M. Wolinska-Cichocka, and E. F. Zganjar. *Reexamining Gamow-Teller decays near ^{78}Ni.* Phys. Rev. C **93**, 044325 (2016).

J. C. Batchelder, N. T. Brewer, C. J. Gross, R. Grzywacz, J. H. Hamilton, M. Karny, A. Fijalkowska, S. H. Liu, K. Miernik, S. W. Padgett, S. V. Paulauskas, K. P. Rykaczewski, A. V. Ramayya, D. W. Stracener, and M. Wolinska-Cichocka. *^{124}In levels populated in the β decay of ^{124}Cd.* Phys. Rev. C **94**, 024317 (2016).

N. Burtebayev, A. Duisebayev, B. A. Duisebayev, M. Nassurlla, S. K. Sakhiev, B. M. Sadykov, S. B. Sakuta, T. K. Zholdybayev, S. Kliczewski, R. Siudak, and M. Wolińska-Cichocka. *Refraction Effects in the alpha and (3) He Scattering on (14) N Nuclei at Energies About 50 MeV.* Acta Phys. Pol. B **47**, 2017 (2016).

T. Cap, K. Siwek-Wilczynska, J. Wilczynski, F. Amorini, L. Auditore, G. Cardella, E. D. Filippo, E. Geraci, L. Grassi, A. Grzeszczuk, E. L. Guidara, J. Han, T. Kozik, G. Lanzalone, I. Lombardo, R. Najman, N. G. Nicolis, A. Pagano, M. Papa, E. Piasecki, S. Pirrone, R. Planeta, G. Politi, F. Rizzo, P. Russotto, I. Skwira-Chalot, A. Trifiro, M. Trimarchi, G. Verde, and W. Zipper. *Determination of Impact Parameters in Aligned Breakup of Projectile-like Fragments in ^{197}Au ^{197}Au Collisions at 23A MeV.* Acta Phys. Pol. B **47**, 983 (2016).

E. Cedrowska, M. Lyczko, A. Piotrowska, A. Bilewicz, A. Stolarz, A. Trzcinska, K. Szkliniarz, and B. Was. *Silver impregnated nanoparticles of titanium dioxide as carriers for At-211.* Radiochim. Acta. **104**, 267 (2016).

E. Clement, M. Zielinska, A. Gorgen, W. Korten, S. Peru, J. Libert, H. Goutte, S. Hilaire, B. Bastin, C. Bauer, A. Blazhev, N. Bree, B. Bruyneel, P. A. Butler, J. Butterworth, P. Delahaye, A. Dijon, D. T. Doherty, A. Ekstrom, C. Fitzpatrick, C. Fransen, G. Georgiev, R. Gernhauser, H. Hess, J. Iwanicki, D. G. Jenkins, A. C. Larsen, J. Ljungvall, R. Lutter, P. Marley, K. Moschner, P. J. Napiorkowski, J. Pakarinen, A. Petts, P. Reiter, T. Renstrom, M. Seidlitz, B. Siebeck, S. Siem, C. Sotty, J. Srebrny, I. Stefanescu, G. M. Tveten, J. V. de Walle, M. Vermeulen, D. Voulot, N. Warr, F. Wenander, A. Wiens, H. D. Witte, and K. Wrzosek-Lipska. *Spectroscopic Quadrupole Moments in ^{96,98}Sr: Evidence for Shape Coexistence in Neutron-Rich Strontium Isotopes at N=60.* Phys. Rev. Lett. **116**, 022701 (2016).

E. Clement, M. Zielinska, S. Peru, H. Goutte, S. Hilaire, A. Gorgen, W. Korten, D. T. Doherty, B. Bastin, C. Bauer, A. Blazhev, N. Bree, B. Bruyneel, P. A. Butler, J. Butterworth, J. Cederkall, P. Delahaye, A. Dijon, A. Ekstrom, C. Fitzpatrick,

C. Fransen, G. Georgiev, R. Gernhauser, H. Hess, J. Iwanicki, D. G. Jenkins, A. C. Larsen, J. Ljungvall, R. Lutter, P. Marley, K. Moschner, P. J. Napiorkowski, J. Pakarinen, A. Petts, P. Reiter, T. Renstrom, M. Seidlitz, B. Siebeck, S. Siem, C. Sotty, J. Srebrny, I. Stefanescu, G. M. Tveten, J. V. de Walle, M. Vermeulen, D. Voulot, N. Warr, F. Wenander, A. Wiens, H. D. Witte, and K. Wrzosek-Lipska. *Low-energy Coulomb excitation of ^{96,98}Sr beams.* Phys. Rev. C **94**, 054326 (2016).

F. Consoli, R. De Angelis, A. Bonasera, J. Sura, P. Andreoli, G. Cristofari, M. Cipriani, G. Di Giorgio, F. Ingenito, M. Barbarino, C. Labaune, C. Baccou, S. Depierreux, C. Goyon, and V. Yahia. *Study on a compact and adaptable Thomson Spectrometer for laser-initiated ^{11}B(p,α)^{8}Be reactions and low-medium energy particle detection.* J. Instrum. **11**, C05010 (2016).

P. Delahaye, A. Galatà, J. Angot, J. F. Cam, E. Traykov, G. Ban, L. Celona, J. Choinski, P. Gmaj, P. Jardin, H. Koivisto, V. Kolhinen, T. Lamy, L. Maunoury, G. Patti, T. Thuillier, O. Tarvainen, R. Vondrasek, and F. Wenander. *Optimizing charge breeding techniques for ISOL facilities in Europe: Conclusions from the EMILIE project.* Rev. Sci. Instrum. **87**, 02B510 (2016).

S. Dutt, P. J. Napiorkowski, T. Abraham, L. Janiak, M. Kisielinski, M. Komorowska, M. Kowalczyk, R. Kumar, T. Marchlewski, M. Matejska-Minda, M. Palacz, W. Piatek, L. Prochniak, I. A. Rizvi, J. Samorajczyk, M. Saxena, J. Srebrny, A. T. W. Wroblewski, K. Wrzosek-Lipska, and M. Zielinska. *Nuclear Structure Study of ^{104}Pd by Coulomb Excitation at the Warsaw Heavy Ion Laboratory.* Acta Phys. Pol. B **47**, 917 (2016).

C. Ghosh, V. Nanal, R. G. Pillay, K. V. Anoop, N. Dokania, S. Pal, M. S. Pose, G. Mishra, P. C. Rout, S. Kumar, D. Pandit, D. Mondal, S. Pal, S. R. Banerjee, P. J. Napiorkowski, O. Dorvaux, S. Kihel, C. Mathieu, and A. Maj. *Characterization of PARIS $LaBr_3$(Ce)-NaI(Tl) phoswich detectors up to E_{gamma} ~ 22 MeV.* J. Instrum. **11**, P05023 (2016).

T. Grahn, J. Pakarinen, L. Jokiniemi, M. Albers, K. Auranen, C. Bauer, C. Bernards, A. Blazhev, P. A. Butler, S. Bonig, A. Damyanova, T. D. Coster, H. D. Witte, J. Elseviers, L. P. Gaffney, M. Huyse, A. Herzan, U. Jakobsson, R. Julin, N. Kesteloot, J. Konki, T. Kroll, L. Lewandowski, K. Moschner, P. Peura, M. Pfeiffer, D. Radeck, P. Rahkila, E. Rapisarda, P. Reiter, K. Reynders, M. Rudiger, M.-D. Salsac, S. Sambi, M. Scheck, M. Seidlitz, B. Siebeck, T. Steinbach, S. Stolze, J. Suhonen, P. Thoele, M. Thurauf, N. Warr, P. V. Duppen, M. Venhart, M. J. Vermeulen, V. Werner, M. Veselsky, A. Vogt, K. Wrzosek-Lipska, and M. Zielinska. *Collective 2^+_1 excitations in ^{206}Po and ^{208,210}Rn.* Eur. Phys. J. A **52**, 340 (2016).

K. Hadynska-Klek, P. J. Napiorkowski, M. Zielinska, J. Srebrny, A. Maj, F. Azaiez, J. J. V. Dobon, M. Kicinska-Habior, F. Nowacki, H. Naidja, B. Bounthong, T. R. Rodriguez, G. de Angelis, T. Abraham, G. A. Kumar, D. Bazzacco, M. Bellato, D. Bortolato, P. Bednarczyk, G. Benzoni, L. Berti, B. Birkenbach, B. Bruyneel, S. Brambilla, F. Camera, J. Chavas, B. Cederwall, L. Charles, M. Ciemala, P. Cocconi, P. Coleman-Smith, A. Colombo, A. Corsi, F. C. L. Crespi, D. M. Cullen, A. Czermak, P. Desesquelles, D. T. Doherty, B. Dulny, J. Eberth, E. Farnea, B. Fornal, S. Franchoo, A. Gadea, A. Giaz, A. Gottardo, X. Grave, J. Grebosz, A. Gorgen, M. Gulmini,

T. Habermann, H. Hess, R. Isocrate, J. Iwanicki, G. Jaworski, D. S. Judson, A. Jungclaus, N. Karkour, M. Kmiecik, D. Karpinski, M. Kisielinski, N. Kondratyev, A. Korichi, M. Komorowska, M. Kowalczyk, W. Korten, M. Krzysiek, G. Lehaut, S. Leoni, J. Ljungvall, A. Lopez-Martens, S. Lunardi, G. Maron, K. Mazurek, R. Menegazzo, D. Mengoni, E. Merchan, W. Meczynski, C. Michelagnoli, J. Mierzejewski, B. Million, S. Myalski, D. R. Napoli, R. Nicolini, M. Niikura, A. Obertelli, S. F. Ozmen, M. Palacz, L. Prochniak, A. Pullia, B. Quintana, G. Rampazzo, F. Recchia, N. Redon, P. Reiter, D. Rosso, K. Rusek, E. Sahin, M.-D. Salsac, P.-A. Soderstrom, I. Stefan, O. Stezowski, J. Styczen, C. Theisen, N. Toniolo, C. A. Ur, V. Vandone, R. Wadsworth, B. Wasilewska, A. Wiens, J. L. Wood, K. Wrzosek-Lipska, and M. Zieblinski. *Superdeformed and Triaxial States in ^{42}Ca.* Phys. Rev. Lett. **117**, 062501 (2016).

T. Huyuk, A. D. Nitto, G. Jaworski, A. Gadea, J. J. Valiente-Dobon, J. Nyberg, M. Palacz, P. A. Soderstrom, R. J. Aliaga-Varea, G. de Angelis, A. Atac, J. Collado, C. Domingo-Pardo, F. J. Egea, N. Erduran, S. Erturk, G. de France, R. Gadea, V. Gonzalez, V. Herrero-Bosch, A. Kaskas, V. Modamio, M. Moszynski, E. Sanchis, A. Triossi, and R. Wadsworth. *Conceptual design of the early implementation of the NEutron Detector Array (NEDA) with AGATA.* Eur. Phys. J. A **52**, 55 (2016).

M. Karny, K. P. Rykaczewski, A. Fijałkowska, B. C. Rasco, M. Wolińska-Cichocka, R. K. Grzywacz, K. C. Goetz, D. Miller, and E. F. Zganjar. *Modular total absorption spectrometer.* Nucl. Instrum. Methods Phys. Res. A **836**, 83 (2016).

K. Kilian, M. Pęgier, and K. Pyrzyńska. *The fast method of Cu-porphyrin complex synthesis for potential use in positron emission tomography imaging.* Spectrochim. Acta A-Molecular and Biomolecular Spectr. **159**, 123 (2016).

K. Kilian, M. Pegier, A. Pekal, and K. Pyrzynska. *Distribution and separation of metallic and radionuclidic impurities in the production of F-18-fluorodeoxyglucose.* J. Radioanal. Nucl. Chem. **307**, 1037 (2016).

K. Kilian, A. Pekal, and J. Juszczyk. *Synthesis of C-11-methionine through gas phase iodination using Synthra MeIPlus synthesis module.* Nukleonika **61**, 29 (2016).

K. Kilian, Z. Rogulski, L. Cheda, A. Drzal, M. Gerszewska, M. Cudny, and M. Elas. *Imaging of hypoxia in small animals with F-18 fluoromisonidasole.* Nukleonika **61**, 219 (2016). International Conference on Research and Applications of Plasmas (PLASMA), Warsaw, POLAND, SEP 07-11, 2015.

M. Klintefjord, K. Hadynska-Klek, A. Gorgen, C. Bauer, F. L. B. Garrote, S. Bonig, B. Bounthong, A. Damyanova, J.-P. Delaroche, V. Fedosseev, D. A. Fink, F. Giacoppo, M. Girod, P. Hoff, N. Imai, W. Korten, A.-C. Larsen, J. Libert, R. Lutter, B. A. Marsh, P. L. Molkanov, H. Naidja, P. Napiorkowski, F. Nowacki, J. Pakarinen, E. Rapisarda, P. Reiter, T. Renstrom, S. Rothe, M. D. Seliverstov, B. Siebeck, S. Siem, J. Srebrny, T. Stora, P. Thole, T. G. Tornyi, G. M. Tveten, P. V. Duppen, M. J. Vermeulen, D. Voulot, N. Warr, F. Wenander, H. D. Witte, and M. Zielinska. *Structure of low-lying states in ^{140}Sm studied by Coulomb excitation.* Phys. Rev. C **93**, 054303 (2016).

M. Komorowska, M. Zielinska, P. Napiorkowski, D. T. Doherty, K. Wrzosek-Lipska, P. A. Butler, L. Prochniak, W. Korten, R. Briselet, H. D. Witte, L. P. Gaffney, G. Georgiev,

A. Goasduff, A. Gorgen, A. Gottardo, E. T. Gregor, K. Hadynska-Klek, H. Hess, M. Klintefjord, T. Konstantinopoulos, J. Ljungvall, R. Lutter, , I. Matea, P. Matuszczak, G. G. O'Neill, W. Piatek, P. Reiter, D. Rosiak, M. Scheck, M. Seidlitz, B. Siebeck, M. Thurauf, and N. Warr. *Study of Octupole Collectivity in ^{146}Nd and ^{148}Sm Using the New Coulomb Excitation Set-up at ALTO.* Acta Phys. Pol. B **47**, 923 (2016).

A. J. Kordyasz, J. Kownacki, Ł. Kordyasz, M. Konop, A. Bednarek, M. Kowalczyk, J. Tarasiuk, M. Kisieliński, T. Kozik, E. Piasecki, P. Sibczyński, A. Stolarz, J. Kowalska, A. Tucholski, J. Srebrny, M. Wolińska-Cichocka, P. Napiorkowski, J. Sarnecki, D. Lipiński, H. Wodzińska, M. Teodorczyk, M. Gajewski, A. Zagojski, and K. Krzyżak. *First Tests of Superthin, Ion-implanted Silicon Strip Detectors Produced by Low-temperature Technique.* Acta Phys. Pol. B **47**, 797 (2016).

A. Korgul, K. P. Rykaczewski, R. K. Grzywacz, C. R. Bingham, N. T. Brewer, C. J. Gross, A. A. Ciemny, C. Jost, M. Karny, M. Madurga, C. Mazzocchi, A. J. Mendez, K. Miernik, D. Miller, S. Padgett, S. V. Paulauskas, M. Piersa, D. W. Stracener, M. Stryjczyk, M. Wolinska-Cichocka, and E. F. Zganjar. *β and β - n decay of the neutron-rich ^{84}Ge nucleus.* Phys. Rev. C **93**, 064324 (2016).

J. Kownacki, M. Kisielinski, A. Kordyasz, M. Kowalczyk, P. Napiorkowski, J. Srebrny, A. Stolarz, S. Lalkovski, C. Droste, E. Ruchowska, W. Czarnacki, A. Korman, P. Sibczynski, J. Andrzejewski, J. Perkowski, L. Janiak, and J. Samorajczyk. *Investigation of γ-ray Emission in Heavy Ion Induced Fission During the Cyclotron Beam-on Periods.* Acta Phys. Pol. B **47**, 723 (2016).

M. Madurga, S. V. Paulauskas, R. Grzywacz, D. Miller, D. W. Bardayan, J. C. Batchelder, N. T. Brewer, J. A. Cizewski, A. Fijalkowska, C. J. Gross, M. E. Howard, S. V. Ilyushkin, B. Manning, M. Matos, A. J. Mendez, II, K. Miernik, S. W. Padgett, W. A. Peters, B. C. Rasco, A. Ratkiewicz, K. P. Rykaczewski, D. W. Stracener, E. H. Wang, M. Wolinska-Cichocka, and E. F. Zganjar. *Evidence for Gamow-Teller Decay of ^{78}Ni Core from Beta-Delayed Neutron Emission Studies.* Phys. Rev. Lett. **117**, 092502 (2016).

G. Marquinez-Duran, I. Martel, A. M. Sanchez-Benitez, L. Acosta, R. Berjillos, J. Duenas, K. Rusek, N. Keeley, M. A. G. Alvarez, M. J. G. Borge, A. Chbihi, C. Cruz, M. Cubero, J. P. Fernandez-Garcia, B. Fernandez-Martinez, J. L. Flores, J. Gomez-Camacho, K. W. Kemper, J. A. Labrador, M. Marques, A. M. Moro, M. Mazzocco, A. Pakou, V. V. Parkar, N. Patronis, V. Pesudo, D. Pierroutsakou, R. Raabe, R. Silvestri, N. Soic, L. Standylo, I. Strojek, O. Tengblad, R. Wolski, and Z. Abou-Haidar. *Precise measurement of near-barrier ^{8}He+ ^{208}Pb elastic scattering: Comparison with ^{6}He.* Phys. Rev. C **94**, 064618 (2016).

G. Marquinez-Duran, A. M. Sanchez-Benitez, I. Martel, L. Acosta, K. Rusek, M. A. G. Alvarez, R. Berjillos, M. J. G. Borge, A. Chbihi, C. Cruz, M. Cubero, J. A. Duenas, J. P. Fernandez-Garcia, B. Fernandez-Martinez, J. L. Flores, J. Gomez-Camacho, N. Keeley, J. A. Labrador, M. Marques, A. M. Moro, M. Mazzocco, A. Pakou, V. V. Parkar, N. Patronis, V. Pesudo, D. Pierroutsakou, R. Raabe, R. Silvestri, N. Soic, L. Standylo, I. Strojek, O. Tengblad, R. Wolski, and A. H. Zia. *Study of the Near-barrier Scattering of ^{8}He on ^{208}Pb.* Acta Phys. Pol. B **47**, 841 (2016).

K. Miernik, K. P. Rykaczewski, R. Grzywacz, C. J. Gross, M. Madurga, D. Miller, D. W. Stracener, J. C. Batchelder, N. T. Brewer, L. Cartegni, A. Fijalkowska, M. Karny, A. Korgul, W. Krolas, C. Mazzocchi, A. J. Mendez II, S. W. Padgett, S. V. Paulauskas, J. A. Winger, M. Wolinska-Cichocka, and E. F. Zganjar. *β-decay study of ^{94}Kr.* Phys. Rev. C **94**, 024305 (2016).

R. Najman, R. Płaneta, A. Sochocka, F. Amorini, L. Auditore, T. Cap, G. Cardella, E. De Filippo, E. Geraci, A. Grzeszczuk, S. Kowalski, T. Kozik, G. Lanzalone, I. Lombardo, Z. Majka, N. G. Nicolis, A. Pagano, E. Piasecki, S. Pirrone, G. Politi, F. Rizzo, P. Russotto, K. Siwek-Wilczyńska, I. Skwira-Chalot, A. Trifiro, M. Trimarchi, J. Wilczyński, and W. Zipper. *Investigation of the Freeze-out Configuration in the (197) Au + (197) Au Reaction at 23 A MeV.* Acta Phys. Pol. B **47**, 975 (2016).

K. Nowak, K. Wimmer, S. Hellgartner, D. Mucher, V. Bildstein, J. Diriken, J. Elseviers, L. P. Gaffney, R. Gernhauser, J. Iwanicki, J. G. Johansen, M. Huyse, J. Konki, T. Kroll, R. Krucken, R. Lutter, R. Orlandi, J. Pakarinen, R. Raabe, P. Reiter, T. Roger, G. Schrieder, M. Seidlitz, O. Sorlin, P. V. Duppen, N. Warr, H. D. Witte, and M. Zielinska. *Spectroscopy of ^{46}Ar by the (t, p) two-neutron transfer reaction.* Phys. Rev. C **93**, 044335 (2016).

A. Pakou, V. Soukeras, F. Cappuzzello, L. Acosta, C. Agodi, X. Aslanoglou, S. Calabrese, D. Carbone, M. Cavallaro, A. Foti, N. Keeley, G. Marquinez-Duran, I. Martel, M. Mazzocco, C. Parascandolo, D. Pierroutsakou, K. Rusek, O. Sgouros, E. Strano, and V. A. B. Zagatto. *Probing the cluster structure of ^{7}Li via elastic scattering on protons and deuterons in inverse kinematics.* Phys. Rev. C **94**, 014604 (2016).

B. C. Rasco, M. Wolinska-Cichocka, A. Fijalkowska, K. P. Rykaczewski, M. Karny, R. K. Grzywacz, K. C. Goetz, C. J. Gross, D. W. Stracener, E. F. Zganjar, J. C. Batchelder, J. C. Blackmon, N. T. Brewer, S. Go, B. Heffron, T. King, J. T. Matta, K. Miernik, C. D. Nesaraja, S. V. Paulauskas, M. M. Rajabali, E. H. Wang, J. A. Winger, Y. Xiao, and C. J. Zachary. *Decays of the Three Top Contributors to the Reactor $\nu(bar)_e$ High-Energy Spectrum, ^{92}Rb, ^{96gs}Y, and ^{142}Cs, Studied with Total Absorption Spectroscopy.* Phys. Rev. Lett. **117**, 092501 (2016).

A. T. Rudchik, K. A. Chercas, K. W. Kemper, K. Rusek, A. A. Rudchik, O. V. Herashchenko, E. I. Koshchy, V. M. Pirnak, E. Piasecki, A. Trzcinska, S. B. Sakuta, R. Siudak, I. Strojek, A. Stolarz, A. P. Ilyin, O. A. Ponkratenko, Y. M. Stepanenko, Y. O. Shyrma, A. Szczurek, and V. V. Uleshchenko. *Elastic and inelastic scattering of ^{15}N ions by ^{9}Be at 84 MeV.* Nucl. Phys. A **947**, 161 (2016).

F. Salomon, P. Edelbruck, G. Brulin, B. Borderie, A. Richard, M. F. Rivet, G. Verde, E. Wanlin, A. Boiano, G. Tortone, G. Poggi, M. Bini, G. Casini, S. Barlini, G. Pasquali, S. Valdré, M. Petcu, R. Bougault, N. Le Neindre, R. Alba, E. Bonnet, M. Bruno, A. Chbihi, M. Cinausero, D. Dell'Aquila, H. De Préaumont, J. A. Duenas, Q. Fable, D. Fabris, L. Francalanza, J. D. Frankland, E. Galichet, F. Gramegna, D. Gruyer, M. Guerzoni, A. Kordyasz, T. Kozik, R. La Torre, I. Lombardo, O. Lopez, J. Mabiala, C. Maiolino, T. Marchi, P. Maurenzig, A. Meoli, Y. Merrer, L. Morelli, A. Nannini, A. Olmi, A. Ordine, M. Pârlog, G. Pastore, S. Piantelli, E. Rosato, D. Santonocito,

E. Scarlini, G. Spadacini, A. Stefaninni, E. Vient, and M. Vigilante. *Front-end electronics for the FAZIA experiment.* J. Instrum. **11**, C01064 (2016).

O. Sgouros, A. Pakou, D. Pierroutsakou, M. Mazzocco, L. Acosta, X. Aslanoglou, C. Betsou, A. Boiano, C. Boiano, D. Carbone, M. Cavallaro, J. Grebosz, N. Keeley, M. L. Commara, C. Manea, G. Marquinez-Duran, I. Martel, N. G. Nicolis, C. Parascandolo, K. Rusek, A. M. Sanchez-Benitez, C. Signorini, F. Soramel, V. Soukeras, C. Stefanini, E. Stiliaris, E. Strano, I. Strojek, and D. Torresi. *α and ^{3}He production in the ^{7}Be+^{28}Si reaction at near-barrier energies: Direct versus compound-nucleus mechanisms.* Phys. Rev. C **94**, 044623 (2016).

E. Strano, D. Torresi, M. Mazzocco, N. Keeley, A. Boiano, C. Boiano, P. D. Meo, A. Guglielmetti, M. la Commara, P. Molini, C. Manea, C. Parascandolo, D. Pierroutsakou, C. Signorini, F. Soramel, D. Filipescu, A. Gheorghe, T. Glodariu, J. Grebosz, S. Jeong, Y. H. Kim, J. A. Lay, H. Miyatake, M. Nicoletto, A. Pakou, K. Rusek, O. Sgouros, V. Soukeras, L. Stroe, N. Toniolo, A. Vitturi, Y. Watanabe, and K. Zerva. *^{17}O ^{58}Ni scattering and reaction dynamics around the Coulomb barrier.* Phys. Rev. C **94**, 024622 (2016).

K. Szkliniarz, M. Sitarz, R. Walczak, J. Jastrzebski, A. Bilewicz, J. Choinski, A. Jakubowski, A. Majkowska, A. Stolarz, A. Trzcinska, and W. Zipper. *Production of medical Sc radioisotopes with an alpha particle beam.* Appl. Radiat. Isot. **118**, 182 (2016).

A. Trzcinska, E. Piasecki, A. Amar, W. Czarnacki, N. Keeley, M. Kisielinski, S. Kliczewski, M. Kowalczyk, B. Lommel, M. Mutterer, R. Siudak, A. Stolarz, I. Strojek, G. Tiourin, and W. H. Trzaska. *Examination of the influence of transfer channels on the barrier height distribution: Scattering of ^{20}Ne on ^{58}Ni, ^{60}Ni, and ^{61}Ni at near-barrier energies.* Phys. Rev. C **93**, 054604 (2016).

S. Valdre, S. Piantelli, G. Casini, S. Barlini, S. Carboni, M. Ciemala, M. Kmiecik, A. Maj, K. Mazurek, M. Cinausero, F. Gramegna, V. L. Kravchuk, L. Morelli, T. Marchi, G. Baiocco, L. Bardelli, P. Bednarczyk, G. Benzoni, M. Bini, N. Blasi, A. Bracco, S. Brambilla, M. Bruno, F. Camera, A. Chbihi, A. Corsi, F. C. L. Crespi, M. D'Agostino, M. Degerlier, D. Fabris, B. Fornal, A. Giaz, M. Krzysiek, S. Leoni, M. Matejska-Minda, I. Mazumdar, W. Meczynski, B. Million, D. Montanari, S. Myalski, R. Nicolini, A. Olmi, G. Pasquali, G. Prete, O. J. Roberts, J. Styczen, B. Szpak, B. Wasilewska, O. Wieland, J. P. Wieleczko, and M. Zieblinski. *Charged particle decay of hot and rotating ^{88}Mo nuclei in fusion-evaporation reactions.* Phys. Rev. C **93**, 034617 (2016).

K. Wrzosek-Lipska and L. P. Gaffney. *Unique and complementary information on shape coexistence in the neutron-deficient Pb region derived from Coulomb excitation.* J. Phys. G (London) **43**, 024012 (2016).

M. Zielinska, L. P. Gaffney, K. Wrzosek-Lipska, E. Clement, T. Grahn, N. Kesteloot, P. Napiorkowski, J. Pakarinen, P. V. Duppen, and N. Warr. *Analysis methods of safe Coulomb-excitation experiments with radioactive ion beams using the GOSIA code.* Eur. Phys. J. A **52**, 99 (2016).

D.3.2 Other publications in journals and conference proceedings not included in the JCR list

J. C. Batchelder, N. T. Brewer, C. J. Gross, R. Grzywacz, J. H. Hamilton, M. Karny, A. Fijalkowska, S. H. Liu, K. Miernik, S. W. Padgett, S. V. Paulauskas, K. P. Rykaczewski, A. V. Ramayya, D. W. Stracener, and M. Wolińska-Cichocka. *^{124}In Levels Populated in the β-decay of ^{124}Cd.* In *APS Division of Nuclear Physics Meeting Abstracts* (2016).

A. Bilewicz, L. Dziawer, P. Kozminski, M. Pruszynski, A. Majkowska-Pilip, A. Stolarz, K. Szkliniarz, J. Jastrzebski, G. Celichowski, J. Grobelny, and E. Tomaszewska. *Gold nanoparticles labelled with At-211 conjugated to substance P and trastuzumab - new radiopharmaceuticals for alpha particle therapy.* European J. Nucl. Med. Molec. Imaging **43**, S198 (2016). Annual Congress of the European-Association-of-Nuclear-Medicine (EANM), Barcelona, SPAIN, OCT 15-19, 2016.

A. Bilewicz, R. Walczak, A. Majkowska, R. Misiak, J. Choinski, M. Sitarz, A. Stolarz, and J. Jastrzebski. *Cyclotron production of theranostic pair Sc-43-Sc-47 on calcium targets.* European J. Nucl. Med. Molec. Imaging **43**, S135 (2016). Annual Congress of the European-Association-of-Nuclear-Medicine (EANM), Barcelona, SPAIN, OCT 15-19, 2016.

N. Burtebayev, J. T. Burtebayeva, A. Duisebayev, T. Zholdybayev, M. Nassurlla, C. Spitaleri, S. B. Sakuta, E. Piasecki, K. Rusek, A. Trzcinska, M. Wolińska-Cichocka, and S. V. Artemov. *Scattering of 13C ions by 12C nuclei at energies close to the Coulomb barrier.* Int. J. of Mathematics and Physics **7**, 107 (2016).

E. De Filippo, A. Pagano, P. Russotto, L. Acosta, L. Auditore, V. Baran, T. Cap, G. Cardella, M. Colonna, L. Francalanza, B. Gnoffo, G. Lanzalone, I. Lombardo, G. Marquínez-Durán, C. Maiolino, T. Minniti, S. Norella, E. V. Pagano, M. Papa, E. Piasecki, S. Pirrone, G. Politi, F. Porto, L. Quattrocchi, F. Rizzo, E. Rosato, A. Trifirò, M. Trimarchi, G. Verde, M. Vigilante, K. Siwek-Wilczyńska, and J. Wilczyński. *Sensitivity of N/Z ratio in projectile break-up of isobaric systems.* EPJ Web of Conf. **117**, 07017 (2016).

B. Gnoffo, S. Pirrone, G. Politi, M. La Commara, J. P. Wieleczko, E. De Filippo, P. Russotto, M. Trimarchi, M. Vigilante, G. Ademard, F. Amorini, L. Auditore, C. Beck, I. Bercenau, E. Bonnet, B. Borderie, G. Cardella, A. Chibihi, M. Colonna, A. D'Onofrio, J. D. Frankland, E. Geraci, E. Henry, E. La Guidara, G. Lanzalone, P. Lautesse, D. Lebhertz, N. LeNeidre, I. Lombardo, K. Mazurek, S. Norella, A. Pagano, E. V. Pagano, M. Papa, E. Piasecki, F. Porto, L. Quattrocchi, M. Quinlann, F. Rizzo, U. Shoroeder, G. Spadaccini, A. Trifirò, J. Toke, and G. Verde. *Isospin influence on the decay modes of the systems produced in the ^{78,86}Kr +^{40,48}Ca reactions at 10 AMeV.* EPJ Web of Conf. **117**, 08012 (2016).

S. Hayakawa, C. Spitaleri, N. Burtebayev, A. Aimaganbetov, P. Figuera, M. Fisichella, G. L. Guardo, S. Igamov, I. Indelicato, G. Kiss, S. Kliczewski, M. La Cognata, L. Lamia, M. Lattuada, E. Piasecki, G. G. Rapisarda, S. Romano, S. B. Sakuta, R. Siudak, A. Trzcińska, A. Tumino, and A. Urkinbayev. *Indirect Study of the ^{16}O+^{16}O Fusion Reaction Toward Stellar Energies by the Trojan Horse Method.* EPJ Web of Conf. **117**, 09013 (2016).

J. Jastrzębski, J. Choiński, A. Jakubowski, M. Sitarz, A. Stolarz, K. Szkliniarz, A. Trzcińska, and W. Zipper. *Production of and research on medical radioisotopes at the heavy ion laboratory, University of Warsaw.* Radiotherapy and Oncology **118**, S52 (2016).

J. Jastrzębski, K. Szkliniarz, M. Sitarz, R. Walczak, A. Bilewicz, J. Choiński, A. Jakubowski, A. Majkowska, and A. Stolarz. *Comparison of the various paths of 44Sc isomeric pair production.* Radiotherapy and Oncology **118**, S53 (2016).

M. Mazzocco, A. Boiano, C. Boiano, M. La Commara, C. Manea, C. Parascandolo, D. Pierroutsakou, C. Signorini, E. Strano, D. Torresi, H. Yamaguchi, D. Kahl, L. Acosta, P. Di Meo, J. P. Fernandez-Garcia, T. Glodariu, J. Grebosz, A. Guglielmetti, N. Imai, Y. Hirayama, H. Ishiyama, N. Iwasa, S. C. Jeong, H. M. Jia, N. Keeley, Y. H. Kim, S. Kimura, S. Kubono, J. A. Lay, C. J. Lin, G. Marquinez-Duran, I. Martel, H. Miyatake, M. Mukai, T. Nakao, M. Nicoletto, A. Pakou, K. Rusek, Y. Sakaguchi, A. M. Sánchez-Benítez, T. Sava, O. Sgouros, C. Stefanini, F. Soramel, V. Soukeras, E. Stiliaris, L. Stroe, T. Teranishi, N. Toniolo, Y. Wakabayashi, Y. X. Watanabe, L. Yang, and Y. Y. Yang. *^{7}Be- and ^{8}B-reaction dynamics at Coulomb barrier energies.* EPJ Web of Conf. **117**, 06006 (2016).

M. Nassurlla, N. Burtebayev, A. Duisebayev, J. Burtebayeva, C. Spitaleri, A. Urkinbayev, K. Rusek, E. Piasecki, S. Kliczewski, A. Trzcinska, S. B. Sakuta, I. Boztosun, S. V. Artemov, and L. I. Galanina. *Complex analysis of scattering 1p-shell nuclei in the framework of coupled channel method.* J. Phys.: Conf. Ser. **703**, 012022 (2016).

S. Piantelli, G. Casini, P. R. Maurenzig, A. Olmi, S. Barlini, M. Bini, G. Pasquali, G. Pastore, G. Poggi, A. A. Stefanini, S. Valdrè, G. Ademard, L. Auger, R. Bougault, E. Bonnet, B. Borderie, A. Chbihi, J. D. Frankland, D. Gruyer, O. Lopez, N. LeNeindre, M. Parlog, M. F. Rivet, E. Vient, E. Rosato, G. Spadaccini, M. Vigilante, M. Bruno, T. Marchi, L. Morelli, M. Cinausero, M. Degerlier, F. Gramegna, A. Kordyasz, T. Kozik, T. Twarog, R. Alba, C. Maiolino, D. Santonocito, and E. Galichet. *FAZIA applications.* EPJ Web of Conf. **117**, 10005 (2016).

S. Pirrone, G. Politi, J. P. Wieleczko, E. De Filippo, B. Gnoffo, P. Russotto, M. Trimarchi, M. La Commara, M. Vigilante, G. Ademard, F. Amorini, L. Auditore, C. Beck, I. Berceanu, E. Bonnet, B. Borderie, G. Cardella, A. Chibihi, M. Colonna, A. D'Onofrio, J. D. Frankland, E. Geraci, E. Henry, E. La Guidara, G. Lanzalone, P. Lautesse, D. Lebhertz, N. Le Neindre, I. Lombardo, K. Mazurek, S. Norella, A. Pagano, E. V. Pagano, M. Papa, E. Piasecki, F. Porto, L. Quattrocchi, M. Quinlann, F. Rizzo, W. U. Schroeder, G. Spadaccini, A. Trifirò, J. Toke, and G. Verde. *Isospin influence on the decay modes of compound systems produced in the ^{78,86}Kr + ^{40,48}Ca at 10 AMeV.* EPJ Web of Conf. **122**, 13001 (2016).

M. Sitarz, K. Szkliniarz, R. Walczak, J. Jastrzebski, J. Choinski, A. Majkowska, A. Stolarz, A. Trzcinska, W. Zipper, and A. Bilewicz. *Production yield and isotopic purity of medical Sc radioisotopes formed by proton, deuteron and alpha particle beams.* European J. Nucl. Med. Molec. Imaging **43**, S200 (2016). Annual Congress of

the European-Association-of-Nuclear-Medicine (EANM), Barcelona, SPAIN, OCT 15-19, 2016.

V. Werner, C. Santamaria, C. Louchart, A. Obertelli, P. Doornenbal, F. Nowacki, G. Authelet, H. Baba, D. Calvet, F. Château, A. Corsi, A. Delbart, J.-M. Gheller, A. Gillibert, T. Isobe, V. Lapoux, M. Matsushita, S. Momiyama, T. Motobayashi, M. Niikura, H. Otsu, C. Péron, A. Peyaud, E. C. Pollacco, J.-Y. Roussé, H. Sakurai, M. Sasano, Y. Shiga, S. Takeuchi, R. Taniuchi, T. Uesaka, H. Wang, K. Yoneda, F. Browne, L. X. Chung, Z. Dombradi, S. Franchoo, F. Giacoppo, A. Gottardo, K. Hadynska-Klek, Z. Korkulu, S. Koyama, Y. Kubota, J. Lee, M. Lettmann, R. Lozeva, K. Matsui, T. Miyazaki, S. Nishimura, L. Olivier, S. Ota, Z. Patel, N. Pietralla, E. Sahin, C. Shand, P.-A. Söderström, I. Stefan, D. Steppenbeck, T. Sumikama, D. Suzuki, Z. Vajta, J. Wu, and Z. Xu. *Collectivity of neutron-rich Cr and Fe toward N=50.* EPJ Web of Conf. **107**, 03007 (2016).

D.4 Seminars

D.4.1 Seminars co-organised by HIL

Nuclear Physics Seminars

Seminars organised jointly by the divisions of Nuclear Physics, Nuclear Spectroscopy and Nuclear Structure Theory of the Faculty of Physics, University of Warsaw, and the Heavy Ion Laboratory, University of Warsaw

Z. Marcinkowska — National Centre for Nuclear Research 7 January 2016
Reaktor Badawczy MARIA
The MARIA Research Reactor

J. Marton — Stefan Meyer Institute, Vienna, Austria 14 January 2016
Selected experiments on exotic, forbidden and antimatter atoms

R. Ryblewski — The H. Niewodniczański Institute of Nuclear Physics, Kraków, Poland 21 January 2016
Jak najlepiej opisać plazmę kwarkowo-gluonową
What is the best description of the quark-gluon plasma

M. Skurzok — Jagiellonian Univ., Kraków, Poland 25 February 2016
Poszukiwanie jąder etowych w eksperymencie WASA-at-COSY
The search for eta-mesic nuclei with WASA-at-COSY

M. Kowal — National Centre for Nuclear Research 3 March 2016
Kandydaci na długo żyjące jądra superciężkie
Candidates for long lived superheavy nuclei

M. Konieczka — Inst. of Theoretical Physics, Univ. of Warsaw 10 March 2016
Mieszanie konfiguracji w modelu funkcjonału gętości w rachunkach dotyczących rozpadów beta
Configuration mixing in the density functional model in beta decay calculations

J. Ciborowski — Inst. of Exp. Physics, University of Warsaw, Warszawa, Poland 17 March 2016
Study of quantum spin correlations of relativistic electron pairs

M. Krzysiek — The H. Niewodniczański Institute of Nuclear Physics, Kraków, Poland 7 April 2016
Badanie pigmejskiego rezonansu dipolowego przy użyciu spektroskopii gamma wyskokiej rozdzielczości
Study of pygmy dipole resonances using high-resolution gamma spectroscopy

W. Wiślicki — National Centre for Nuclear Research 14 April 2016
Discovery of pentaquark states by the LHCb at CERN

V. Begun — Institute of Physics, Jan Kochanowski University, Kielce, Poland — 21 April 2016
Fizyka statystyczna w wysokoenergetycznych zderzeniach jądrowych
Stastistical Physics in high-energy nuclear collisions

T. Matulewicz — Inst. of Exp. Physics, University of Warsaw, Warszawa, Poland — 5 May 2016
International Fusion Materials Irradiation Facility - DEMO-Oriented Neutron Source (IFMIF-DONES) w Rzeszowie?
International Fusion Materials Irradiation Facility - DEMO-Oriented Neutron Source (IFMIF-DONES) in Rzeszów?

A. Tucholski — Heavy Ion Laboratory, University of Warsaw, Warszawa, Poland — 12 May 2016
Czasy życia oraz momenty magnetyczne wzbudzonych stanów jądrowych
Lifetimes and magnetic moments of excited nuclear states

A. Trzcińska — Heavy Ion Laboratory, University of Warsaw, Warszawa, Poland — 19 May 2016
Siła "słabych" kanałów reakcji — badania rozkładów barier na fuzję
The strength of "weak" reaction channels; a study of fusion barrier distribution

Z. Tymiński — Institute of Atomic Energy POLATOM, Otwock-Świerk, Poland — 2 June 2016
Meteoryty i zawarte w nich izotopy
Meteorites and their isotopic content

M. Kortelainen — Department of Physics, University of Jyväskylä, Finland — 9 June 2016
Model building and nuclear EDFs

A. Afanasjev — Mississipi State University, USA — 3 October 2016
Relativistic description of finite nuclei: successes and challenges

K. Rykaczewski — Oak Ridge National Laboratory, Oak Ridge, TN, USA — 6 October 2016
Ostatnie wyniki i plany badań jąder superciężkich
Recent results and plans for the studies of super-heavy nuclei

J. Andrzejewski — Faculty of Physics and Applied Computer Science, University of Lodz, Łódź, Poland — 13 October 2016
Nowe wyniki w badaniach przekroju czynnego rekacji ^{7}Be(n,α) i ^{7}Be(n,p) przy urządzeniu n_{TOF} w CERN
New results for the ^{7}Be(n,a) and ^{7}Be(n,p) reaction cross sections studied with n_{TOF} at CERN

P. Napiorkowski — Heavy Ion Laboratory, University of Warsaw, Warszawa, Poland — 20 October 2016
Superdeformacja i trójosiowość w jądrze ^{42}Ca badana metodą wzbudzeń kulombowskich
Superdeformation and triaxiality in ^{42}Ca studied with Coulomb excitation

K. Pomorski — Inst. of Physics, Maria Curie-Sklodowska Univ., Lublin, Poland — 27 October 2016
Opis rozpadów ciężkich jąder atomowych poprzez emisję klastrów, lekkich cząstek naładowanych i rozszczepienie
Description of the heavy nuclei decay trough emission of clusters and light charged particles and trough fission

W. Wiślicki — National Centre for Nuclear Research — 11 November 2016
Pentaquarks and other multiquark exotic states at LHCb

K. Sekizawa — Warsaw University of Technology, Warszawa, Poland — 17 November 2016
Time-Dependent Density Functional Theory for Low-Energy Nuclear Reactions

P. Bączyk — Inst. of Theoretical Physics, Univ. of Warsaw — 24 November 2016
Naruszenie symetrii izospinowej przez oddziaływanie silne w jądrach o $N \sim Z$
Isospin symmetry violation through strong interactions in $N \sim Z$ nuclei

K. Miernik — Inst. of Exp. Physics, University of Warsaw, Warszawa, Poland — 1 December 2016
Spektroskopia jąder neutrononadmiarowych od kuchni
Backstage of neutron-rich nuclei spectroscopy

Ch. Mazzocchi — Inst. of Exp. Physics, University of Warsaw, Warszawa, Poland — 8 December 2016
Studies of astrophysically-relevant nuclei around ^{78}Ni

Ł. Świderski — National Centre for Nuclear Research — 15 December 2016
Metody eksperymentalne badania podstawowych właśności scyntylatorów
Experimental methods to study basic properities of scintilators

D.4.2 Other seminars organised at HIL

Internal semi-formal HIL seminars

K. Szkliniarz — Inst. of Physics, University of Silesia, Katowice, Poland — 15 June 2016
Optymalizacja wytwarzania radioizotopów medycznych z wykorzystaniem warszawskich cyklotronów
Medical radioisotope production optimisation using Warsaw cyclotrons

V. Loginov — Joint Institute for Nuclear Research, Dubna, Russia — 29 June 2016
Recent developments of ECR ion sources at FLNR

V. Nanal — Tata Institute of Fundamental Research, Mumbai, India — 23 November 2016
Search for neutrinoless double beta decay

D.4.3 External seminars given by the HIL staff

K. Wrzosek-Lipska — 27–29 January 2016
Normalisation in Coulex experiments
Isolde Coulex School, CERN, Geneve

K. Wrzosek-Lipska — 27–29 January 2016
Shape coexistance studies with Coulex. The role of complementary data
Isolde Coulex School, CERN, Geneve

J. Choiński — February 2016
Production of and research into medical radioisotops at the Heavy Ion Laboratory, University of Warsaw
ICTR–PHE, CERN, Geneve

J. Jastrzębski — February 2016
Comparison of various paths of ^{44}Sc isomeric pair production
ICTR–PHE, Cern, Geneve

M. Komorowska — 22–28 February 2016
Study of octupole collectivity in ^{146}Nd and ^{148}Sn using Coulomb excitation
IIIrd Topical Workshop on Modern Aspects in Nuclear Structure, Bormio, Italy

Ł. Standyło — 22 March 2016
Recycling of sediments of ECR chamber wall by the electron escape paths changing in the magnetic trap
Emilie Workshop 2016, Cean (GANIL), France

K. Kilian — 17–20 April 2016
Opracowanie metody radiometrycznego oznaczania aktywności enzymatycznej dehydrogenazy 11-beta-hydroksysteroidowej w próbkach tkanki łożyska
Development of the method of radiometric determination of enzymatic activity of 11-beta-hydroxysteroid dehydrogenase in placenta samples
VII Konferencja Radiochemii i Chemii Jądrowej, Lublin, Polska

K. Kilian — 17–20 April 2016
Wykorzystanie 18FDG w procesie znakowania komórek macierzystych
Application of 18FDG in steam cells labeling
VII Konferencja Radiochemii i Chemii Jądrowej, Lublin, Polska

A. Trzcińska 26–29 April 2016
Quasielastic barrier distribution studies — the influence of weak channels
COPIGAL and POLITA Workshop, Joint LIA COLL-AGAIN, Catania, Italy

K. Kilian 11–13 May 2016
Zastosowanie kompleksów metali z flawonoidami w chemii analitycznej oraz ich potencjał w medycynie
Application of flavonoid metalocomplexes in analytical chemistry and medicine
IX Konferencja "Flawonoidy i ich zastosowania", Łańcut, Polska

M. Pęgier 11–13 May 2016
Zastosowanie kompleksów metali z flawonoidami w chemii analitycznej
Application of flavonoids in analytical chemistry
IX Konferencja "Flawonoidy i ich zastosowania", Łańcut, Polska

A. Sentkowska 11–13 May 2016
Analiza chromatograficzna flawonoidów - porównanie trybów HILIC i RP
Chromatographic analysis of flavonoids - comparison of HILIC and RP
IX Konferencja "Flawonoidy i ich zastosowania", Łańcut, Polska

J. Choiński 19 May 2016
Production of innovative radioisotopes at the Heavy Ion Laboratory, University of Warsaw
Warsaw, Poland

Z. Szefliński 19 May 2016
Bystander effect in radiobiological studies at HIL
Radio-Warsaw meeting, Warsaw, Poland

J. Choiński 23 June 2016
Production of and research into medical radioisotopes at the Heavy Ion Laboratory, University of Warsaw
2nd Bern Cyclotron Symposium

M. Sitarz 23 June 2016
Production of and research into medical radioisotopes at the Heavy Ion Laboratory, University of Warsaw
2nd Bern Cyclotron Symposium

J. Choiński 12 July 2016
Presentation of the PET cyclotron facility at HIL
HIL, Warsaw, Poland

M. Pęgier 6–15 July 2016
Identification of radionuclidic impurities and determination of metal content along the synthesis path of ^{18}F–fluorodeoxyglucose
16th CEEPUS Symposium and Summer School on Bioanalysis, Warsaw, Poland

A. Sentkowska 6–15 July 2016
Bioactive components and antioxidant properties of green coffee brews
16th CEEPUS Symposium and Summer School on Bioanalysis, Warsaw, Poland

A. Stolarz 11–16 September 2016
Production of medical radioisotopes with p/d medical and heavy ion cyclotrons at the Heavy Ion Laboratory of University of Warsaw
Nuclear Data for Science and technology (ND2016), Bruges, Belgium

M. Wolińska-Cichocka 11–16 September 2016
β-strength and anti-neutrino spectra from Total Absorption Spectroscopy of the decay chain $^{142}Cs \rightarrow {}^{142}Ba \rightarrow {}^{142}La$
Nuclear Data for Science and technology (ND2016), Bruges, Belgium

K. Kilian 11–15 September 2016
Identification and distribution of metallic and radionuclidic contaminants in the production of ^{18}F–fluorodeoxyglucose
6th EuCheMS, Sevila, Spain

M. Pęgier 11–15 September 2016
Identification and distribution of metallic and radionuclidic contaminants in the production of ^{18}F–fluorodeoxyglucose
6th EuCheMS, Sevila, Spain

A. Sentkowska 11–15 September 2016
Synergistic and antagonistic interactions between bioactive compounds
6th EuCheMS, Seviila, Spain

Z. Szefliński 11–16 September 2016
Relative biological effectiveness of a double ion beam containing carbon and oxygen ions
HCI 2016, 18th International Conference on the Physics of Highly Charged Ions, Kielce, Poland

L. Próchniak 30 September 2016
Properties of octupole variables
23th Nuclear Physics Workshop, Kazimierz Dolny, Poland

K. Rusek 6 October 2016
Status of HIL 2016
ENSAR2 Facility Coordination Group Meeting, Vienna, Austria

J. Choiński 9–13 October 2016
Production of and research into medical radioisotopes at the Heavy Ion Laboratory, University of Warsaw
The European Nuclear Conference, Warsaw, Poland

M. Sitarz 15–19 October 2016
Production yield and isotopic purity of medical Sc radioisotopes formed by proton, deuteron and alpha particle beams
29th Annual Congress of the European Association of Nuclear Medicine, Barcelona, Spain

K. Rusek 18–21 October 2016
Nuclear reactions with exotic nuclei; the role of the continuum
EURISOL DF, KU Leuven, Belgium

A. Stolarz 13–18 Novermber 2016
Targets for production of research quantities of the medical radioisotops with a and p/d beams
28th World INTDS conference, Cape Town, South Africa

P.J. Napiorkowski 28–30 Novermber 2016
Numerical methods in COULEX analysis
3rd COULEX School, INFN Laboratori Nazionali di Legniaro, Legnaro, Italy

D.4.4 Poster presentations

J. Jastrzębski 15–19 February 2016
Production of and research into medical radioisotopes at the Heavy Ion Laboratory, University of Warsaw
International Conference on Translational Research in Radio-Oncology - Physics for Health (ICTR-PHE), Geneve, Switzerland

K. Kilian 17–20 April 2016
Synteza 18Fmiso do obrazowania stanów niedotlenienia w badaniu nowotworów z wykorzystaniem modeli zwierzęcych
Synthesis of 18FMiso for hypoxia imaging in animal models
VII Konferencja Radiochemii i Chemii Jądrowej, Lublin, Polska

K. Kilian 11–13 May 2016
Związek kompleksowy Ga(III) z moryną na potrzeby diagnostyki medycznej
Ga(III) complex with morin for medical imaging
IX Konferencja "Flawonoidy i ich zastosowania", Łańcut, Polska

A. Sentkowska 11–13 May 2016
Efekty synergiczne i antagonistyczne flawonoidów z innymi związkami biologicznie aktywnymi
Synergic and anatagonistic interaction of flavonoids with biologically active substances
IX Konferencja "Flawonoidy i ich zastosowania", Łańcut, Polska

M. Pęgier 10 June 2016
Zanieczyszczenia metaliczne i radionuklidów w procesie wytwarzania ^{18}F-fluorodeoksyglukozy
Metalic and radionuclidic impurities in 18FDG manufacturing
XIII Warszawskie Seminarium Doktorantów Chemików ChemSession, Warszawa, Polska

M. Wolińska-Cichocka 24–29 July 2016
$\beta-$ decay Studies of the Decay Chain $^{142}Cs \rightarrow {}^{142}Ba \rightarrow {}^{142}La$ with the Modular Total Absorption Spectrometer
The Nuclear Structure (NS2016), Knoxville, USA

M. Wolińska-Cichocka 29–31 July 2016
$\beta-$ decay Studies of the Decay Chain $^{142}Cs \rightarrow {}^{142}Ba \rightarrow {}^{142}La$ with the Modular Total Absorption Spectrometer
Workshop Neutrinos Physics in Nuclear Physics, Knoxville, USA

D.4.5 Lectures for students and student laboratories

K. Kilian winter semester of the academic year 2016/2017, 90 hours
Pracownia Analizy Środowiska
Environmental Analysis Laboratory
Faculty of Chemistry, University of Warsaw, Warszawa, Poland

K. Kilian winter semester of the academic year 2016 /2017 , 20 hours
Zarzadzanie Środowiskiem
Environmental Management
Faculty of Chemistry, University of Warsaw, Warszawa, Poland

K. Kilian winter semester of the academic year 2016/2017, 30 hours
Metody izotopowe i chemia radiofarmaceutyków
Radiochemistry and radiopharmacy
Faculty of Physics, University of Warsaw, Warszawa, Poland

K. Kilian summer semester of the academic year 2015/2016, 60 hours
Pracownia radiofarmaceutyków
Laboratory of Radiopharmaceuticals
Faculty of Physics, University of Warsaw, Warszawa, Poland

K. Kilian summer semester of the academic year 2015/2016, 15 hours
Radiofarmaceutyki — synteza, wytwarzanie i zastosowania
Radiopharmaceuticals — synthesis, production and applications
Faculty of Chemistry, University of Warsaw, Warszawa, Poland

Z. Szefliński summer semester of the academic year 2015/2016, 30 hours
Energetyka Jądrowa
The nuclear power industry
Faculty of Physics, University of Warsaw, Warszawa, Poland

Z. Szefliński summer semester of the academic year 2015/2016, 30 hours
Techniki jadrowe w diagnostyce i terapii medycznej
Nuclear techniques in Medical Diagnostics and Therapy
Faculty of Physics, University of Warsaw, Warszawa, Poland

Z. Szefliński winter semester of the academic year 2016/2017, 30 hours
Energia w Środowisku — technika ograniczenia i koszty
Energy in the environment — technique limitations and costs
Faculty of Physics, University of Warsaw, Warszawa, Poland

Z. Szefliński winter semester of the academic year 2016/2017, 45 hours
Fizyka I
Physics 1, mechanics, lectures
Faculty of Physics, University of Warsaw, Warszawa, Poland

Z. Szefliński winter semester of the academic year 2016/2017, 15 hours
Fizyka I — ćwiczenia do wykładu
Physics 1, mechanics, plenary classes
Faculty of Physics, University of Warsaw, Warszawa, Poland

D.4.6 Science popularisation lectures

P.J. Napiorkowski lectures for middle school pupils

Fizyka dla bramkarzy (2x60 min)
Physics for goalkeepers

Z. Szefliński lectures for high school pupils and students

Protony i ciężkie jony w terapii nowotworów — dziś czy jutro medycyny (2x45 min)
Protons and heavy ions in cancer therapy

Dawka lokalna i jej rola w biologicznej odpowiedzi linii komórkowej CHO-K1
(Local dose and its role in the biological response of the CHO-K1 cell Line)

Fizyka w biologii i medycynie
Physics in biology and medicine

Promieniowanie jonizujące — radon w naszym otoczeniu (1x45 min)
Ionizing radiation — radon in the environment

Bystander effect in radiobiological studies at HIL

Co fizyka wnosi do leczenia nowotworów (2x45 min)
What physics does to treat cancer

D.5 Honours and Awards

State Awards

The following employees of the Heavy Ion Laboratory received Honours and Awards from the President of Poland:
Jerzy Jastrzębski — Knight's Cross of the Order of Polonia Restituta;
Wanda Wesoły — Gold Medal for Long Service.

The Rector of the University of Warsaw awards

In 2016 the following employees of the Heavy Ion Laboratory received the Rector of the University of Warsaw award:
Mariusz Antczak, Marek Budziszewski, Przemysław Czwarnok, Andrzej Jakubowski, Jerzy Jastrzębski, Wiesław Kalisiewicz, Krzysztof Kilian, Marian Kopka, Ireneusz Mazur, Marcin Palacz, Bogusław Paprzycki, Krzysztof Sosnowski, and Wanda Wesoły

D.6 Laboratory staff

Director: Krzysztof Rusek
Deputy directors: Jarosław Choiński
Paweł Napiorkowski
Financial executive: Agnieszka Maciejewska

Senior scientists:

Jerzy Jastrzębski[a], Andrzej Kordyasz[a], Marcin Palacz, Ernest Piasecki[a], Leszek Próchniak, Krzysztof Rusek, Anna Stolarz, Józef Sura, Zygmunt Szefliński[a]

Scientific staff and engineers:

Tomasz Abraham, Andrzej Bednarek, Jarosław Choiński, Mateusz Filipek[ab], Przemysław Gmaj, Andrzej Jakubowski, Urszula Kaźmierczaka[c], Krzysztof Kilian, Maciej Kisieliński[a], Marian Kopka, Michał Kowalczyk, Magdalena Matejska-Minda, Paweł Matuszczak[a], Ireneusz Mazur, Jan Miszczak, Paweł Napiorkowski, Wojciech Piątek, Bogdan Radomyski, Olga Saeed Mohamed Nassar, Justyna Samorajczyk-Pyśk[c], Mansi Saxena[d], Aleksandra Sentkowska[e], Mateusz Sobolewski[a], Julian Srebrny[a], Łukasz Standyło, Krzysztof Sudlitz[af], Roman Tańczyk, Agnieszka Trzcińska, Andrzej Tucholski, Marzena Wolińska-Cichocka, Katarzyna Wrzosek-Lipska[c], Bogumił Zalewski[g]

Doctoral candidates:

Michalina Komorowska[h], Tomasz Marchlewski[h], Mateusz Pęgier[i], Mateusz Sitarz[h]

Technicians:

Mariusz Antczak, Tomasz Bracha, Andrzej Górecki, Piotr Jasiński, Wiesław Kalisiewicz, Robert Kopik, Wojciech Kozaczka, Zbigniew Kruszyński, Piotr Krysiak, Kamil Makowski, Krzysztof Łabęda, Zygmunt Morozowicz, Bogusław Paprzycki, Andrzej Pietrzak, Krzysztof Pietrzak, Krzysztof Sosnowski, Łukasz Świątek

Administration and support:

Eliza Balcerowska[e], Anna Błaszczyk-Duda, Marek Budziszewski, Przemysław Czwarnok, Barbara Kowalska[a], Joanna Kowalska, Agnieszka Maciejewska, Jolanta Matuszczak, Jolanta Ormaniec[c], Piotr Piegat[j], Ewa Sobańska, Lidia Strzelczyk, Krystyna Szczepaniak, Wanda Wesoły[k], Andrzej Wiechowski, Katarzyna Włodarczyk[a], Magdalena Zawal, Irena Żejmo[a]

Voluntary scientists:

Jędrzej Iwanicki, Jan Kownacki, Andrzej Wojtasiewicz

---

[a] part time
[b] since 1 December
[c] on maternity leave
[d] since 1 November
[e] since 1 April
[f] since 1 June
[g] on leave
[h] PhD student at the Faculty of Physics, University of Warsaw
[i] PhD student at the Faculty of Chemistry, University of Warsaw
[j] until 19 February
[k] until 27 December

D.7 Laboratory Council

1. Prof. dr hab. Józef Andrzejewski
Nuclear Physics Division
University of Łódź
90-236 Łódź, ul. Pomorska 149/153

2. Prof. dr hab. Rajmund Bacewicz
Warsaw University of Technology
00-661 Warszawa, Plac Politechniki 1

3. Prof. dr hab. Janusz Braziewicz
Institute of Physics
Jan Kochanowski University
25-406 Kielce, ul. Świętokrzyska 15

4. Prof. dr hab. Ewa Bulska
Biological and Chemical Research Centre
02-089 Warszawa, ul. Żwirki i Wigury 101

5. Prof. dr hab. Katarzyna Chałasińska-Macukow (**Chairman of the Council**)
Institute of Geophysics
University of Warsaw
02-093 Warszawa, ul. Pasteura 7

6. Prof. dr hab. inż. Andrzej Chmielewski
Institute of Nuclear Chemistry and Technology
03-195 Warszawa, ul. Dorodna 16

7. Przemysław Gmaj
(representative of the HIL staff)
Heavy Ion Laboratory
University of Warsaw
02-093 Warszawa, ul. Pasteura 5A

8. Prof. dr hab. Andrzej Góźdź
Dep. of Theoretical Physics
Maria Curie-Skłodowska University
20-031 Lublin, ul. Radziszewskiego 10

9. Prof. dr hab. Zenon Janas
Inst. of Experimental Physics
University of Warsaw
02-093 Warszawa, ul. Pasteura 7

10. Prof. dr hab. Jerzy Jastrzębski
Heavy Ion Laboratory
University of Warsaw
02-093 Warszawa, ul. Pasteura 5A

11. Prof. dr hab. Marta Kicińska-Habior
Inst. of Experimental Physics,
University of Warsaw
02-093 Warszawa, ul. Pasteura 5

12. Prof. dr hab. Stanisław Kistryn
Jagiellonian University
31-007 Kraków, ul. Gołębia 24

13. Prof. dr hab. Adam Maj
The Henryk Niewodniczański
Institute of Nuclear Physics
Polish Academy of Sciences
31-342 Kraków, ul. Radzikowskiego 152

14. Prof. dr hab. Wojciech Nawrocik
Faculty of Physics
Adam Mickiewicz University
61-614 Poznań, ul. Umultowska 85

15. Prof. dr hab. Sławomir Nazarewski
Medical University of Warsaw
02-091 Warszawa, ul. Żwirki i Wigury 61

16. Prof. dr hab. Paweł Olko
The Henryk Niewodniczański
Institute of Nuclear Physics
Polish Academy of Sciences
31-342 Kraków, ul. Radzikowskiego 152

17. Prof. dr hab. Ernest Piasecki
Heavy Ion Laboratory
University of Warsaw
02-093 Warszawa, ul. Pasteura 5A

18. Dr hab. Ludwik Pieńkowski
AGH University of Science and Technology
30-059 Kraków, ul. Mickiewicza 30

19. Prof. dr hab. Krzysztof Rusek
(Director of HIL)
Heavy Ion Laboratory
University of Warsaw
02-093 Warszawa, ul. Pasteura 5A

20. Prof. dr hab. Teresa Rząca-Urban
Faculty of Physics
University of Warsaw
02-093 Warszawa, ul. Pasteura 5

21. Prof. dr hab. Adam Sobiczewski
The National Centre for Nuclear Research
02-093 Warszawa, ul. Pasteura 5

22. Prof. dr hab. Ryszard Sosnowski
The National Centre for Nuclear Research
05-400 Świerk k/Warszawy

23. Prof. dr hab. Wiktor Zipper
Institute of Physics
University of Silesia
40-007 Katowice, ul. Uniwersytecka 4

D.8 Programme Advisory Committee

PAC members

- Dimiter Balabanski (Sofia University, Sofia, Bulgaria)
- Konrad Czerski (Institute of Physics, University of Szczecin, Szczecin, Poland; Physics Department, Technical University of Berlin, Germany)
- Piotr Bednarczyk (The H. Niewodniczański Institute of Nuclear Physics, Kraków, Poland)
- Gilles de France (GANIL, Caen, France)
- Zenon Janas (Faculty of Physics, University of Warsaw, Warszawa, Poland)
- Nicholas Keeley (National Centre for Nuclear Research, Świerk, Poland)
- Rainer Lieder (RFW, University of Bonn, Germany)
- Piotr Magierski (Faculty of Physics, Warsaw University of Technology, Warszawa, Poland)
- Leszek Próchniak (Heavy Ion Laboratory, University of Warsaw, Warszawa, Poland)
- Brunon Sikora (Faculty of Physics, University of Warsaw, Warszawa, Poland)
- Władysław Trzaska (Department of Physics, University of Jyväskylä, Finland)

The international Programme Advisory Committee of the Heavy Ion Laboratory usually meets twice a year, in spring and autumn. The deadline for submitting proposals is three weeks before a PAC meeting. PAC approved experiments are scheduled at the meetings of the Users' Committee, which also serves as a link between cyclotron users and the Laboratory. The Users' Committee is chaired by Julian Srebrny (the Heavy Ion Laboratory).

D.9 External participants in HIL experiments and HIL guests

A. Abramczuk	Faculty of Physics, University of Warsaw, Warszawa, Poland
M. Adamus	National Centre for Nuclear Research, Świerk, Poland
A. Abramuk	Faculty of Physics, University of Warsaw, Warszawa, Poland
A. Astier	CSNSM, CNRS-IN2P3 and Université Paris-Sud, Orsay, France
H. Azizakram	University of Mohaghegh, Ardabili, Iran
D. Banaś	Institute of Physics, Jan Kochanowski University, Kielce, Poland
A. Bancer	National Centre for Nuclear Research, Świerk, Poland
P. Bednarczyk	The H. Niewodniczański Institute of Nuclear Physics, Kraków, Poland
A.A. Bezbakh	Joint Institute for Nuclear Research, Dubna, Russia
J. Boryc	Poznań University of Technology, Poznań, Poland
J. Braziewicz	Institute of Physics, Jan Kochanowski University, Kielce, Poland
W. Bryliński	Warsaw University of Technology, Warszawa, Poland
J. Ciborowski	Faculty of Physics, University of Warsaw, Warszawa, Poland
J. Czub	Institute of Physics, Jan Kochanowski University, Kielce, Poland
D.T. Doherty	University of Surrey, Guildford, Surrey, United Kingdom
Ch. Droste	Faculty of Physics, University of Warsaw, Warszawa, Poland
A. Dudziński	National Centre for Nuclear Research, Świerk, Poland
E. Dupont	CSNSM, CNRS-IN2P3 and Université Paris-Sud, Orsay, France
A. Ebinger	Faculty of Physics, University of Warsaw, Warszawa, Poland
M. Fila	Faculty of Physics, University of Warsaw, Warszawa, Poland
J. Furtak	Faculty of Physics, University of Warsaw, Warszawa, Poland
T. Hanusek	Poznań University of Technology, Poznań, Poland
Ł. Janiak	Fac. of Phys. and Appl. Comp. Sci., U. of Lodz, Łódź, Poland
E. Jaworska	National Centre for Nuclear Research, Świerk, Poland
M. Jelonek	Institute of Physics, University of Silesia, Katowice, Poland
K. Hadyńska-Klęk	INFN, Laboratori Nationali di Legnaro, Legnaro, Italy
M. Kaja	Warsaw University of Technology, Warszawa, Poland
G. Kamiński	Joint Institute for Nuclear Research, Dubna, Russia
M. Kmiecik	The H. Niewodniczański Institute of Nuclear Physics, Kraków, Poland
K. Krutul	University of Białystok, Białystok, Poland
A.I. Krylov	Joint Institute for Nuclear Research, Dubna, Russia
R. Kumar	Inter University Accelerator Centre, New Delhi, India
S. Lalkovski	Sofia University, Sofia, Bulgaria
V. Loginov	Joint Institute for Nuclear Research, Dubna, Russia
B. Lv	CSNSM, CNRS-IN2P3 and Université Paris-Sud, Orsay, France
A. Maj	The H. Niewodniczański Institute of Nuclear Physics, Kraków, Poland
V. Nanal	Tata Institute of Fundamental Research, Mumbai, Indie
A. Nanini	University of Florence, INFN Sezione di Firenze, Italy
N. Pchelkin	Joint Institute for Nuclear Research, Dubna, Russia
J. Peszka	University of Wrocław, Wrocław, Poland
C. Petrache	CSNSM, CNRS-IN2P3 and Université Paris-Sud, Orsay, France
D. Pietrasz	AGH University of Science and Technology, Kraków, Poland
M. Pietrzak	National Centre for Nuclear Research, Świerk, Poland

S. Pszona	National Centre for Nuclear Research, Świerk, Poland
M. Rocchini	University of Florence, INFN Sezione di Firenze, Italy
M. Rostampour	Department of Physics, Arak University, Arak, Iran
K. Rozwadowska	Faculty of Physics, University of Warsaw, Warszawa, Poland
M. Sadeghi	Nuclear Science and Technology Research Institute, Teheran, Iran
G. Saworska	Faculty of Physics, University of Warsaw, Warszawa, Poland
M. Seniut	Warsaw University of Technology, Warszawa, Poland
M. Siciliano	INFN, Laboratori Nationali di Legnaro, Legnaro, Italy
S. Sidorchuk	Joint Institute for Nuclear Research, Dubna, Russia
I. Stabrawa	Institute of Physics, Jan Kochanowski University, Kielce, Poland
A. Struski	Poznań University of Technology, Poznań, Poland
J. Styczeń	The H. Niewodniczański Institute of Nuclear Physics, Kraków, Poland
K. Szkliniarz	Institute of Physics, University of Silesia, Katowice, Poland
A. Tom	Institute of Physics, University of Silesia, Katowice, Poland
M. Urbaniak	Institute of Physics, University of Silesia, Katowice, Poland
B. Wasilewska	The H. Niewodniczański Institute of Nuclear Physics, Kraków, Poland
W. Wróblewski	Fac. of Phys. and Appl. Comp. Sci., U. of Lodz, Łódź, Poland
V.B. Zager	Joint Institute for Nuclear Research, Dubna, Russia
T. Zawistowski	Faculty of Physics, University of Warsaw, Warszawa, Poland
E. Zbróg	Institute of Physics, Jan Kochanowski University, Kielce, Poland
M. Zielińska	IRFU/SPhN, CEA Saclay, Gif-sur-Yvette, France
W. Zipper	Institute of Physics, University of Silesia, Katowice, Poland